

**DECISION SUPPORT FRAMEWORK FOR TRANSFORMING
URBAN BUILDINGS AT MULTIPLE SCALES**

A Dissertation
Presented to
The Academic Faculty

by

Soowon Chang

In Partial Fulfillment
of the Requirements for the Degree
DOCTORAL OF PHILOSOPHY in the
SCHOOL OF BUILDING CONSTRUCTION

Georgia Institute of Technology
May 2020

COPYRIGHT © 2020 BY SOOWON CHANG

DECISION SUPPORT FRAMEWORK FOR TRANSFORMING URBAN BUILDINGS AT MULTIPLE SCALES

Supervised by:

Dr. Daniel Castro-Lacouture, Advisor
School of Building Construction
Georgia Institute of Technology

Dr. Baabak Ashuri
School of Building Construction
Georgia Institute of Technology

Dr. Perry P.J. Yang
School of City and Regional Planning &
School of Architecture
Georgia Institute of Technology

Dr. James S. Roberts
School of Psychology
Georgia Institute of Technology

Dr. Yoshiki Yamagata
Center for Global Environmental Research
*National Institute of Environmental Studies,
Japan & Global Carbon Project – Tsukuba
International Office*

Date Approved: [March 17, 2020]

[To anyone who ponders the betterment of our community]

ACKNOWLEDGEMENTS

I would like to express my sincere gratitude to my advisor, Prof. Daniel Castro, for the great support of my PhD study, for his immense knowledge and advice, and for his understanding and patience. I would like to thank my minor advisor Prof. Perry Yang, for his comments and guidance during my research. His guidance inspires me to pursue more and better things in my research and teaching. My sincere thanks also go to Prof. Yoshiki Yamagata, the principal researcher of the Center for Global Environmental Research in National Institute for Environmental Studies (NIES) in Japan and the head of the Global Carbon Project Tsukuba International Office. I thank him for sharing his ample expertise and thorough visions for future smart city. I appreciate Prof. Baabak Ashuri, the director of the Economics of Sustainable Built Environment (ESBE) in the school of building construction for sharing his ample knowledge during my PhD study. I also would like to express my gratitude to Prof. James S. Roberts, Associate Professor in the School of Psychology. His patience and earnest advice always give me inspiration.

My PhD journey was made fruitful with broadening perspectives with my colleagues and friends in Georgia Tech and NIES. Many thanks to Yuqing Hu, Dr. Takahiro Yoshida, Robert Brent Binder, Michael Boynton Tobey, Dr. Steven Jige Quan, and Dr. Kanae Matsui. I also appreciate my mentor and dear friend Dr. Jeehee Lee.

Last, but not least of all, I would not have been able to complete this without the love and support given to me by my family. Especially, the support given by my husband, Heung Jin Oh, helped me in more ways than I can count. In addition, I appreciate my parents, and my sister and brother. My sincere gratitude also goes to parents in law, sister

in law, and grandparents in law. I am very fortunate in having wonderful grandparents. Especially, I sincerely appreciate and admire my grandfather, Inhyop Chang. His integrity and righteousness always inspire me to be passionate about earnest values in my life. Last, I thank my grandmother, Chuok Choi, who always finds a positive side of people. Your warm and kind soul will be remembered in my heart. I pray for the warm repose of you.

TABLE OF CONTENTS

ACKNOWLEDGEMENTS	iv
LIST OF TABLES	viii
LIST OF FIGURES	ix
LIST OF SYMBOLS AND ABBREVIATIONS	xii
SUMMARY	xiii
CHAPTER 1. INTRODUCTION	1
1.1 Background	1
1.2 Research Scope	5
1.3 Research Questions, Objectives, and Hypotheses	8
1.4 Research Significance	10
1.5 Organization of the Dissertation	11
CHAPTER 2. LITERATURE REVIEW	13
2.1 Strategies and Objectives of Retrofitting Urban Buildings	13
2.1.1 Building Level	13
2.1.2 Block Level	16
2.1.3 Community Level	18
2.2 Performance Evaluation Methods at Multiple Scales	19
2.3 Summary of Literature Review	23
CHAPTER 3. RESEARCH METHODOLOGY	30
CHAPTER 4. RETROFITTING BUILDING ENVELOPES ON AN INDIVIDUAL BUILDING	33
4.1 Approach for Multi-Objective Optimization Model	34
4.1.1 Multi-criteria for building envelope retrofits	35
4.1.2 Considering uncertainties and constraints	36
4.1.3 Designing a multi-objective optimization model	38
4.2 Case Study of Retrofitting Building Envelopes for Residential Buildings in Kyojima, Japan	50
4.2.1 Input parameters and variables	51
4.2.2 Uncertainty identification	53
4.2.3 Application of multi-objective optimization model	56
4.2.4 Case study results and findings	57
4.3 Chapter Conclusions	61

CHAPTER 5. REORGANIZING BUILDING TOPOLOGICAL AND TYPOLOGICAL PARAMETERS ON A BLOCK	65
5.1 Approach for Supporting Decisions about Building Typology Transformation	66
5.2 Case Study of Transforming Building Typology: Kyojima, Tokyo, Japan	69
5.2.1 Study Area	69
5.2.2 Parametric Modelling Results	70
5.2.3 Relationships between typology and performance	72
5.3 Performance Predictions of Building Typologies	84
5.4 Chapter Conclusions	85
CHAPTER 6. BLOCK BOUNDARIES FOR SHARING ELECTRICITY AMONG BUILDINGS ON A COMMUNITY	87
6.1 Approach for Identifying Electricity Sharing Boundaries	89
6.2 Case Study of Reconfiguring Block Boundaries: Kyojima, Tokyo, Japan	92
6.2.1 Data Acquisition	93
6.2.2 Buildings' Connectivity	96
6.2.3 Block Boundaries to Share Electricity	99
6.3 Chapter Conclusions	101
CHAPTER 7. INTEGRATED DECISION SUPPORT FRAMEWORK FOR URBAN BUILDING TRNASFORMATIONS	103
7.1 Interrelated Parameters	104
7.2 Integrated Decision Support Framework: Top-down and Bottom-up	106
7.1.1 Top-down decision framework	106
7.1.2 Bottom-up decision framework	107
7.3 Performance Comparisons of Integrated Decisions	108
7.4 Chapter Conclusions	110
CHAPTER 8. CONCLUSIONS	112
8.1 Conclusion	112
8.2 Research Implications	114
8.3 Contribution	116
8.4 Limitations	117
8.5 Future Research	118
APPENDIX A. OPTIMIZED ENVELOPE SELECTION OPTIONS FOR RESIDENTIAL BUIDLINGS, KYOJIMA, TOKYO, JAPAN	120
APPENDIX B. BAYESIAN MULTILEVEL MODELS FOR BLOCK-LEVEL PERFORMANCE ESTIMATION BY BUILDING PARAMETERS	127
APPENDIX C. RELATIONSHIPS BETWEEN BUILDING HEIGHTS AND MULTIPLE PERFORMANCE IN BLOCKS	128
REFERENCES	129

LIST OF TABLES

Table 1	– Summary of literature review	25
Table 2	– Lifecycle CO2 emissions by energy sources (Varun et al. 2009a; World Nuclear Association 2011)	44
Table 3	– Envelope options for vertical façades and roofs	48
Table 4	– Overview of Building Information for Sample Buildings	52
Table 5	– Estimated effects on uncertainty estimating thermal energy consumption	56
Table 6	– Generalized collinearity diagnostics	75
Table 7	– Relationships between urban building performance indicators and building topological and typology parameters	78
Table 8	– Methodological inputs and outputs	104
Table 9	– Optimized Envelope Selection Option for Apartment 1	120
Table 10	– Optimized Envelope Selection Option for Apartment 2	122
Table 11	– Optimized Envelope Selection Option for Wooden House 1	123
Table 12	– Optimized Envelope Selection Option for Wooden House 2	125

LIST OF FIGURES

Figure 1.1	– Global emissions pathway (IPCC 2018)	1
Figure 1.2	– Research scope: multiple scales and topological parameters	6
Figure 1.3	– Research scope: performance evaluation at multiple scales	7
Figure 3.1	– Overall research	30
Figure 3.2	– Research Methodology	32
Figure 4.1	– Methodology for selecting building envelopes by using a multi-objective optimization (Chang et al. 2020a)	35
Figure 4.2	– Multi-criteria objectives and their potential relationships	36
Figure 4.3	– Framework considering uncertainties in physical, design, scenario parameters (Chang et al. 2019a; d, 2020a)	37
Figure 4.4	– Framework of designing multi-objective model (Chang et al. 2020a)	38
Figure 4.5	– Samples buildings and context in North Sumida, Tokyo, Japan	52
Figure 4.6	– One set of solutions for the east orientation in the apartment 1 (left) and the apartment 2 (right)	58
Figure 4.7	– One set of solutions for the east orientation in the wooden house 1 (left) and the wooden house 2 (right)	59
Figure 4.8	– Histogram of retrofiting ratio	62
Figure 5.1	– Research methodology for building typology transformation in blocks	67
Figure 5.2	– Diversity of building topological and typological parameters in blocks	69
Figure 5.3	– Predicted annual average energy demands using EnergyPlus (kWh/m ²)	71
Figure 5.4	– Predicted percentage of comfort hours per year (%)	71

Figure 5.5	– Average solar radiation potential on building façades (kWh/m ²): individual buildings (Left) and average on blocks (Right)	72
Figure 5.6	– Sky exposure on blocks	72
Figure 5.7	– Non-linear population effects of coverage ratio (y coordinates: average energy unit intensity (top-left), solar potential (top-right), average percentages of comfort time (bottom-left), and sky exposure (bottom-right))	80
Figure 5.8	– Non-linear population effects of floor area ratio (y coordinates: average energy unit intensity (top-left), solar potential (top-right), average percentages of comfort time (bottom-left), and sky exposure (bottom-right))	81
Figure 5.9	– Density estimations of impacts on intercept of energy demands by land use	82
Figure 5.10	– Density estimations of impacts on intercept of thermal comfort by land use	82
Figure 5.11	– Density estimations of impacts on intercept of sky exposure by land use	83
Figure 5.12	– Density estimations of impacts on intercept of thermal comfort by rise type– Density estimations of impacts on intercept of thermal comfort by rise type	83
Figure 6.1	– Research methodology to identify block boundaries to support for sharing electricity among buildings (Chang et al. 2020b)	89
Figure 6.2	– An example of edge betweenness	91
Figure 6.3	– Study area of a community scale	93
Figure 6.4	– Data acquisition for temporal energy supply and demand of buildings	94
Figure 6.5	– Examples of hourly electricity demand: 12PM (left), and 6PM (right)	95
Figure 6.6	– Solar power generation potential: solar irradiation on rooftop (left), total annual solar irradiation (middle), and hourly averaged solar power (right)	95

Figure 6.7	– Connectivity for sharing electricity among nearest buildings (Left); number of neighboring buildings for sharing energy (Right)	96
Figure 6.8	– Hourly demand and supply during the time of the day	97
Figure 6.9	– Connectivity for sharing electricity among nearest buildings during 11AM ~ 1PM (Left); number of neighboring buildings for sharing electricity 11AM ~ 1PM (Right)	98
Figure 6.10	– Connectivity for sharing electricity among nearest buildings during 5 ~ 7PM (Left); number of neighboring buildings for sharing electricity 5 ~ 7PM (Right)	99
Figure 6.11	– Current administrative block boundaries (Left); Clustering-based Voronoi diagram (Right)	100
Figure 6.12	– Connectivity for sharing electricity among nearest buildings during 11AM ~ 1PM (Left); number of neighboring buildings for sharing electricity 11AM ~ 1PM (Right)	101
Figure 7.1	– Potential interrelationships among variables	105
Figure 7.2	– Top-down decision framework	107
Figure 7.3	– Bottom-up decision framework	108
Figure 7.4	– Comparing changes in average building energy demand on blocks	109
Figure 7.5	– Comparing changes in average building-integrated solar potential on blocks	109
Figure 7.6	– Comparing change in average percentages of thermal comfort on blocks	110
Figure 7.7	– Comparing changes in average visibility on blocks	110
Figure 8.1	– Non-linear patterns of block-level performance by building height (y coordinates: average energy unit intensity (top-left), solar potential (top-right), average percentages of comfort time (bottom-left), and sky exposure (bottom-right))	128

LIST OF SYMBOLS AND ABBREVIATIONS

AAC	Autoclaved aerated concrete
CO ₂	Carbon Dioxide
FAR	Floor Area Ratio
GA	Genetic Algorithm
GIS	Geographic Information System
HVAC	Heating, Ventilation, and Air Conditioning
IoT	Internet of Things
NPV	Net Present Value
PV	Photovoltaic
PCM	Phase Change Materials
MOO	Multi-Objective Optimization

SUMMARY

Due to the increasing population, cities are requiring more energy. Among urban elements, buildings account for about 40% of energy demands and 30% of carbon dioxide emissions globally. To address the increase of energy demands and environmental responsibility, existing buildings should be transformed into highly energy efficient forms.

This research explores how to support decisions that affect performance-driven smart and resilient urban systems focusing on building renovations. The research scope covers the redevelopment of existing built forms at multiple scales. Since urban objects influence urban patterns at other scales, both individual and collective performances of buildings at larger scales should be evaluated to support proper redevelopment decisions. In addition, the transformation of existing buildings will encounter different problems and challenges at different scales in urban areas. On an individual building level, the selection of different envelope options can project the future architectural environment of buildings. On a block level, the performance will be changed along with combinations of building typologies such as land use, height, floor area, etc., and therefore changes to building typologies should be managed collectively to improve the performance. When PV are applied in buildings and hourly electricity demands are recognized, the dynamic energy flows on a community level will become complex to manage.

In this respect, this research is devised to identify and address redevelopment problems at different scales: individual buildings, block, and community. On the individual building level, this research studies how to support decision-making when optimizing the selection of building envelopes by using a Genetic Algorithm (GA). Based on the findings

from optimizing at each scale, an interdependence of building parameters and multiple performance is observed. Therefore, decision frameworks across multiple scales are extrapolated to support community-driven and building-driven decisions. On the block level, this research explores how existing building typologies influence multiple performance indicators in a collective manner to support reconfiguring decisions using a Bayesian Multilevel Modeling. On the community level, this study addresses how the community can optimize block boundaries for resiliently managing the energy demand and supply of groups of buildings by using K-nearest neighbors (KNN) and community clustering algorithms.

This research will contribute to making appropriate decisions for investment, regulations, or guidelines when renovating physical building assets at different scales in urban areas. The research findings will consolidate theoretical understandings about the relationships between building design and construction parameters considering multiple performance indicators at multiple scales in urban areas. Since many cities are at the tipping point trying to become more resilient, increasingly focusing on sustainability, economic feasibility, and human well-being, a better understanding of the impact of built forms at multiple scales will support urban development decisions for the future smart and connected communities.

CHAPTER 1. INTRODUCTION

1.1 Background

The United Nations (UN) announced a vigorous and viable guidance to address global climate change in the 2018 Intergovernmental Panel on Climate Change (IPCC) report. The guidance limits global warming to 1.5°C (2.7 degrees Fahrenheit), and it can be achieved when carbon dioxide (CO₂) emissions become net zero globally around 2050 as shown in Figure 1.1 (IPCC 2018).

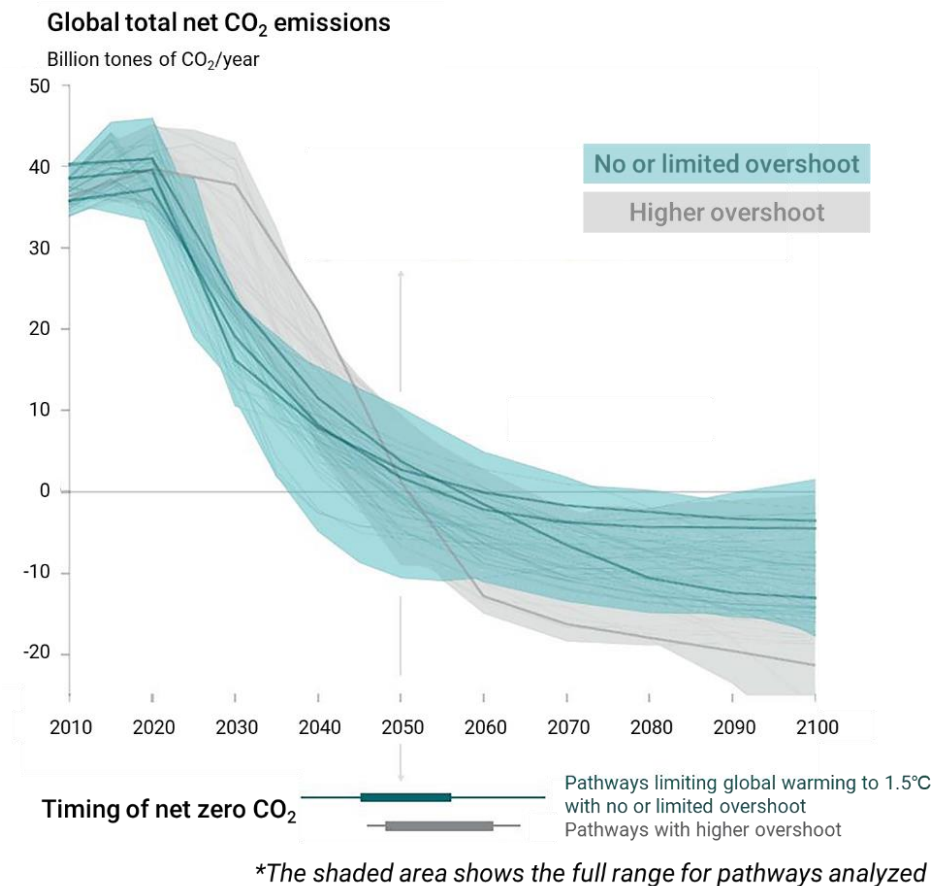


Figure 1.1 – Global emissions pathway (IPCC 2018)

This goal requires transitions in systems of energy, industry, buildings, transport and land use in cities (IPCC 2018). It is expected that 66% of the world population will live in urban areas by 2050, with cities consuming more energy and emitting more CO₂ (UN 2014). The anticipated population growth increases energy demands and environmental responsibility of urban areas, and it will require transitions of urban infrastructure and buildings (Bazaz et al. 2018). Among urban elements, buildings consume about 20-40% of total energy use in developed countries (Pérez-Lombard et al. 2008). Buildings also contribute to more than 30% of carbon dioxide (CO₂) emissions in the U.S. (U.S. EIA 2018a). To come up with the 1.5°C cap, the CO₂ emissions from building stocks should be reduced by 80-90% by 2050 from 2010 levels, building renovation rates should increase from less than 1% in 2015 to 5% by 2020 in developed countries, and all new buildings should achieve fossil-free and near-zero energy by 2020 (Bazaz et al. 2018; Kuramochi et al. 2018). At the same time, in energy systems, electricity supply by renewable sources should increase about 70-80% by 2050 under the 1.5°C pathways (Bazaz et al. 2018; IPCC 2018).

Since existing building stocks influence the urban energy demands and environmental emissions, this research focuses on transformations of existing buildings to increase energy efficiency and potential renewable power generation. Retrofitting existing buildings provides opportunities to save energy, influence economic growth, and reduce environmental impacts. The building energy efficiency retrofit market was valued as a \$279 billion investment opportunity (Herbst et al. 2012) in 2012, meanwhile, the total construction market was about \$850.5 billion (U.S. Census Bureau 2018). This investment for building energy efficient retrofits can save energy valued as more than \$1 trillion over

a decade (Herbst et al. 2012). The increased building retrofits are expected to create more than 3 million job opportunities (Herbst et al. 2012). Moreover, energy savings contribute to reducing greenhouse gas emissions by mitigating about 616 million metric tons of CO₂ per year (U.S. Census Bureau 2018). Total CO₂ emissions in the building sector in 2017 was 1,831 million metric tons (U.S. EIA 2018b). The estimated CO₂ reduction through energy-efficient building retrofits is about one third of the total CO₂ emissions in the building sector in 2017.

Energy-efficient building retrofits can face different issues when considering transformations at different scales. Scales in this research indicate spatial size of measuring performance and the extent of the data resolution (Lloyd 2014). This research addresses building transformation problems at three different scales: individual buildings, block, and community. Community consists of blocks, and block consists of buildings. At different scales, performance indicators related to transforming the built environment will be varied. For example, while thermal energy transfer through wall assemblies can be important on an individual building scale, total energy demands can be more concerned than the heat transfer of wall layers for evaluating a group of buildings in a block. It requires appropriate and applicable methods to evaluate performance on each scale. In addition, scales can impose different possible options of building transformation strategies because of different levels of data resolution. For example, while research about buildings can focus on constituent building elements such as envelopes, HVAC systems, renewable system installations etc., research for block and community levels can focus on building footprints, typology, or land use. While material selections can be important to achieve energy efficiency and CO₂ reduction for individual buildings, a community level more likely

concerns building locations or functions than detailed materials. In this respect, transformation strategies optimized on the individual building scale may not achieve expected performance at different scales such as block and community scales. Therefore, to support existing building transformation decisions along the direction of improving energy efficiency and reducing CO₂ emissions, a research framework should be designed to tailor possible transformation strategies and objectives at different scales. The various performance indicators require separate modeling systems for each scale.

However, the decisions siloed in a certain urban scale can be challenged for transforming existing buildings due to the need to localize decision support systems on a certain urban scale and the lack of communication across different scales. Even if decisions for retrofitting buildings are isolated on each scale because performance indicators vary, buildings will influence urban areas at different scales. Two research questions arise: given the urban settings and requirements for CO₂ and energy reduction, and renewable energy supply increase, what are the suitable transformation strategies that can be applied for buildings at multiple urban scales to achieve sustainable and resilient communities? How does a decision at a certain scale influence on other scales? To answer these questions, this research explores decision support frameworks for retrofitting urban buildings at multiple scales with appropriate modeling systems that can evaluate different performance indicators for each scale. Based on the experiments, key attributes across multiple scales are identified in order to integrate multi-level urban transformation strategies. This research will provide an innovative interdisciplinary approach to address significant national and worldwide needs for appropriate decision-making when investing in aging and degrading buildings to support energy-efficient and sustainable renovations of built forms.

1.2 Research Scope

Urban patterns have a hierarchical structure consisting of city, neighborhood, clusters of buildings, buildings, rooms and construction details (Alexander et al. 1977). An urban pattern is composed with reconciling urban form components such as materials, structures, rooms, buildings, plots, streets, and blocks, and urban tissues (Lozano 1990). The patterns are interdependent on the others connecting to both larger and smaller scales (Ünlü 2018). When defining minor, medium, and major scales in the urban pattern, Ünlü categorized the urban objects as city, neighborhoods, buildings, and households, and their morphological parameters on each scale (Ünlü 2018). This dissertation adapts these different scales to fit three urban patterns focusing on buildings: individual buildings, buildings clustered by blocks, and buildings within a community. Building are constituent elements of blocks (Stephan and Crawford 2014), and their characteristics compose urban forms at block level (Vanderhaegen and Canters 2017). Blocks can be defined as closed urban space that can be accessible from all sides by being linked to street networks (Bürklin and Peterek 2017). In this respect, blocks are considered as clusters of buildings surrounded by pedestrian streets in this research. In that a community can be gridded by street networks (Dumbaugh and Rae 2009), the community is defined as a collection of blocks. The multiple scales are presented in Figure 1.2. Each scale contains topological parameters that form urban patterns and the parameters can be considered as transformation strategies.

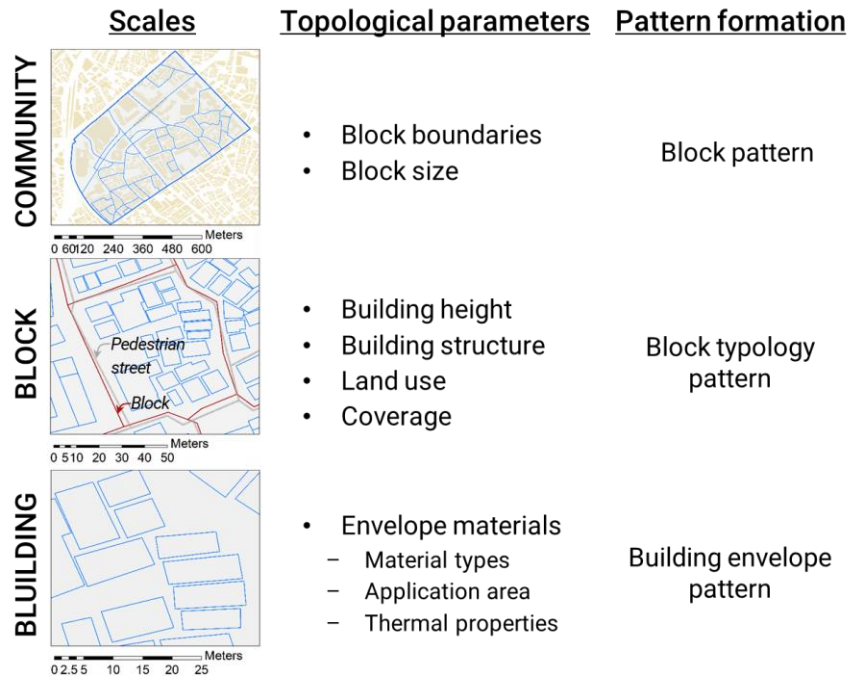


Figure 1.2 – Research scope: multiple scales and topological parameters

To identify suitable transformation strategies, this study devises and tests appropriate modeling methods to evaluate different performance indicators on each scale. On an individual building scale, envelope selections and their performance influence indoor thermal comfort and energy savings (Wang et al. 2007). Environmental and economic criteria should also be evaluated to determine an appropriate envelope decision (Chantrelle et al. 2011). On a block level, energy-efficient transformations should not compromise human thermal comfort (Chang et al. 2019e). Sky view factor can also be considered because it can influence thermal environment by providing shaded areas (He et al. 2015) as well as represent visibility performance indicators in blocks (Chang et al. 2019c). On a community scale, as energy uses and production of buildings become dynamic (Chang et al. 2020b; Yamagata and Seya 2014), multiple micro-grids have been proposed to reduce electricity losses and environmental emissions from the typical distribution grid (Anastasiadis et al. 2010; Bullich-Massagué et al. 2018). Especially, the

boundaries of a micro-grid should be determined to minimize the energy imbalance of urban objects within the boundary (Nunna and Srinivasan 2017). In this respect, the scope of evaluating performance on each scale is shown in Figure 1.3.

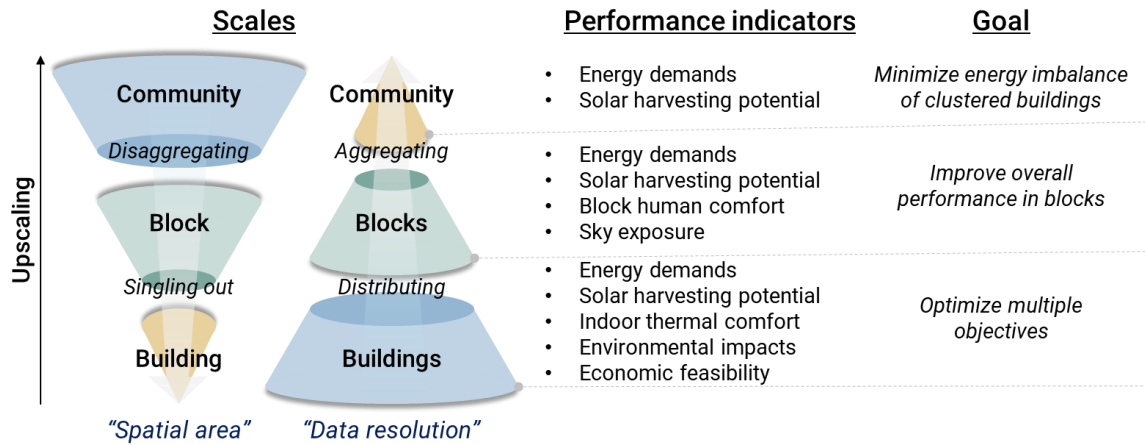


Figure 1.3 – Research scope: performance evaluation at multiple scales

Based on the findings on each scale, interrelationships among topological parameters and performance can be observed to create top-down and bottom-up decision support frameworks of retrofitting buildings at multiple scales. While cities are constructed from the bottom-up (from the components hierarchically), they are also operated from top-down processes at every level (Batty 2013). In the bottom-up perspective, individual buildings’ transformations will deviate types of buildings in a block and the collective performance of the buildings in a block. The changes in building typologies in a block can correspondingly change block size and boundary on a community level. On the other hand, in the top-down perspective, changes in block size and form can influence the number of buildings and combination of building typologies in a block. The overall performance of the block can require renovations of individual buildings.

1.3 Research Questions, Objectives, and Hypotheses

This research explores how to transform urban buildings at multiple scales to support future smart and sustainable communities. The main research questions of this dissertation are what are the appropriate strategies of transforming urban buildings at different scales and how does the renovation strategy at a certain scale influence on multiple scales?

To address the questions, this research receives its motivation from three challenges:

1) gaps of transformable parameters and objectives at building, block, and community scales, 2) lack of appropriate modeling and simulation methods for each scale, and 3) lack of understanding interrelationships among multiple scales. In this study, the transformable building parameters are limited to building envelope materials for individual buildings, building topological and typological parameters on a block scale, and block size and boundaries on a community scale. The performance objectives are limited to four criteria on the individual building scale: building energy use, renewable energy production integrated in building envelopes, indoor thermal comfort hours, and payback period for individual buildings, four criteria on the block scale: sky view factor on a block, building energy uses in a block, potential solar PV energy production on exterior walls and rooftops in buildings within a block, and percentages of thermal comfort time in buildings in a block, and one criterion on the community scale: energy balance based on electricity use and potential solar PV electricity generation on rooftops in buildings within a community. Based on the challenges and research scope, four questions can be developed as follows:

- 1) How can building envelopes be retrofitted by considering multiple objectives and potential options including renewable and disruptive technology?
- 2) How will urban blocks change building topological parameters for multiple performance of energy demands, potential PV supplies, thermal comfort, and sky view factor?
- 3) How can blocks change their size and boundaries to support an energy sharing architecture for the future sharing economy and connected infrastructure? and
- 4) What are the interdependent relationships that can be observed in the multi-level transformations of buildings?

The primary objective of this research is to investigate urban building transformations at multiple scales and to discern interrelationships of the transformations among the scales. Decisions of building transformations should be analyzed at multiple scales such as an individual building, a set of buildings, and the community. Four research objectives are devised to address research questions and achieve the primary research objective as follows:

- 1) To optimize building envelopes including any newly developed envelope options and to support decisions of retrofitting building envelopes,
- 2) To identify relationships between building topological parameters and block performance of energy, thermal comfort, and sky exposure as well as to support decisions of reorganizing building typologies in a block for better performance,
- 3) To establish an appropriate method to identify block boundaries that can share electricity among nearby buildings and to support decisions of reconfiguring blocks, and

- 4) To discern interrelationships of building retrofit decisions at multiple scales in urban areas and to support an integrated decision of changing buildings within a community.

1.4 Research Significance

This study tests models of retrofitting buildings at multiple scales: building envelopes, building typology in blocks, and block boundaries at a community, then devises an integrated decision support framework considering impacts across the scales. The study of decision support for transforming urban buildings at multiple scales is important for several reasons. First, decisions of building envelopes including any newly developed materials can suggest directions of forming building exteriors and developing new envelope options. Second, understanding relationships between building typology and performance in a block can extend previous studies by experimenting existing building typology with multiple performance rather than using virtual building forms. Third, optimization of block boundaries based on buildings' energy can support establishing smart-grid systems by identifying the optimal spatial size when sharing electricity among buildings in a community and address a concern about managing dynamic energy distribution in a community. Above all, top-down and bottom-up decision frameworks based on interrelationships among different scales contributes to broadening perspective for transforming urban buildings by predicting potential ripple effects at different scales. The research findings will be grounded for establishing a scalable decision-making system to redevelop urban patterns focusing on buildings for the future smart and sustainable cities.

1.5 Organization of the Dissertation

This thesis consists of eight chapters, and the chapters are outlined as follows:

1. **Chapter 1 Introduction** presents motivation for transforming existing buildings and challenges in retrofit decisions siloed on each scale, and provides research scope, questions, objectives, hypotheses, and significance.
2. **Chapter 2 Literature Review** describes the background knowledge and foundations related to this research. The literature includes articles addressing possible transformation parameters in urban buildings, and their evaluation. Research scale, parameters and performance evaluation criteria, and study area of previous literature are compared.
3. **Chapter 3 Research Methodology** presents an overview of the methodological framework by summarizing research approaches. The entire research project consists of four tasks. The first three tasks support decisions on each scale: building envelope optimization, performance evaluation of each block with building typology, and optimization of block boundaries. Then, the interrelationships of topological parameters and performance among scales are explored.
4. **Chapter 4 Retrofitting Building Envelopes** optimizes building envelope options including any newly developed materials using an evolutionary algorithm.
5. **Chapter 5 Building Typology Transformations** analyzes relationships between performance and building topological and typological parameters in blocks using the Bayesian multilevel modeling.

6. ***Chapter 6 Block Boundaries for Sharing Electricity among Buildings*** studies establishing an appropriate approach of optimizing block boundaries and size to share electricity among buildings in a community.
7. ***Chapter 7 Integrated Decision Support Model for Urban Building Transformations*** integrates lessons learned from transformation strategies at multiple scales in a community. This chapter summarizes inputs and outputs of each decision support system in Chapter 4 ~ 6 and demonstrates possible interactions among transformation options at multiple scales.
8. ***Chapter 8 Conclusions*** summarizes research findings and contributions and concludes the thesis with suggesting future research.

CHAPTER 2. LITERATURE REVIEW

This chapter reviews previous research related to decisions of urban building transformations. Currently, decisions of retrofitting buildings are usually made at a certain urban scale with considering different parameters and performance criteria. This chapter first outlines transformation strategies of building parameters and performance criteria at multiple scales. Then, current performance evaluation methods are reviewed to discern appropriate modeling and simulation methods. The reviews are elaborated based on study scales in order to recognize current information gaps among different scales.

2.1 Strategies and Objectives of Retrofitting Urban Buildings

Buildings are not only the components of the urban infrastructure system but also deliver points for energy and resources carried by the urban infrastructure systems such as transportation, water, utility, electricity, etc. (Derrible 2017). To reduce and optimize loads of urban infrastructure systems, existing buildings should be retrofitted considering possible transformation options at different scales of the community levels, blocks, and individual buildings. Also, their impacts should be evaluated at each scale where the transformation strategies are established, and their possible impacts should also be projected across the multiple scales.

2.1.1 Building Level

Among building retrofit strategies including building components and systems, envelopes account for most of heating and cooling energy and determine building energy performance. Building envelope retrofits can also provide opportunities for decentralizing

energy resources in individual buildings. Building envelope retrofit options can be categorized into two parts: 1) reducing energy demands, and 2) decentralizing energy supplies (Roberti et al. 2017).

To reduce energy demands of existing buildings by improving the thermal performance, researchers have been examining building shapes and various building envelope options. Parasonis et al. (2012) has studied relationships between building geometric parameters (i.e., length, envelope area, and internal floor area) and energy demands (Parasonis et al. 2012). The results provided the optimal building envelope area and compactness for reducing energy uses. Danielski et al. (2012) analyzed that lower shape factor reduces the final thermal energy demands in Nordic climate by testing five existing apartment buildings (Danielski et al. 2012). Premrov et al. (2016) has examined eight building shapes to identify their impacts on energy performance (Premrov et al. 2016). Their study has tested virtual building shapes, and their parameters have been assumed to increment proportionally. This can limit to reflecting actual building topological characteristics. Rashdi and Embi (2016) have also studied impacts of building shape on cooling loads with constraining floor area, volume, and height (Rashdi and Embi 2016). These findings can guide designers to determine the optimal shape for reducing cooling loads. Previous research efforts have focused on recognizing relationships between building geometric parameters and energy performance. The findings can support to establish transformation strategies for individual buildings.

Retrofitting building envelopes have also vigorously studied. Gucyeter and Gunaydin (2012) studied energy-efficient building retrofits by optimizing envelopes strategies for office buildings (Güçyeter and Günaydın 2012). Three different strategies of

retrofitting envelopes have been assessed: reduction of transmission loss, reduction of infiltration loss, and optimization of solar availability. Based on levels of envelope interventions, seven retrofit options re-assembling walls, windows, and floors on ground have been evaluated with measuring heating and cooling energy changes. The researchers proposed to include renewable energy technologies integrated to building envelopes in the future study. Asadi et al (2014) considered to retrofit exterior wall insulation materials, roof insulation materials, window types, solar collector types, and HVAC system types (Asadi et al. 2014). Roberti et al (2017) studied retrofit decisions for a historical building considering the retrofit sets of cooling system, façade insulation, and window replacement based on experts' participations (Roberti et al. 2017). Heo et al. (2012) tested three retrofit alternatives; 1) insulation addition, 2) window replacement, and 3) airtightness (Heo et al. 2012). Building envelope options have a variety of functions, and one of features is that envelopes can be both energy demanders and suppliers.

To decentralize energy generation on buildings, researchers have been investigating renewable energy technologies which can be integrated to existing buildings. Peippo et al (1999) proposed applying building-integrated solar thermal collectors and photovoltaics (PV) (Peippo et al. 1999). Charron and Athienitis (2006) also proposed solar thermal collector and solar PV as applicable renewable energy technologies integrated to building design (Charron and Athienitis 2006). Solar thermal collectors can be a heat storage which can be used to supply hot water and space heating. Solar PV can generate surplus electricity which can be connected to grid and sell to the utility grid systems (Peippo et al. 1999). Gahrooei et al (2016) explored different design scenarios of applying solar PV, and optimized the investment timing of PV for residential buildings by considering the changes

in electricity price, demands, technology prices, and panel sizes (Gahrooei et al. 2016). From the research, they found that expanding sizes of solar panels are not always optimal solutions, phasing investment can improve benefits of the investment, decisions depend on the electricity price, and the uncertainties of electricity prices should be investigated further. As another building-integrated façade, BIQ (Bio-Intelligent Quotient) building, featuring an algae façade, was built in Hamburg, Germany, 2013 (IBA Hamburg 2013; The European Portal For Energy Efficiency In Buildings 2015). The algae sources conduct photosynthesis and generate biofuels to be used for generating heat (Chang et al. 2017; Wilkinson et al. 2016). The potential performance of algae systems has been investigated in urban or building levels (Kim 2013; Quan et al. 2017).

2.1.2 Block Level

On a block level, the performance based on building design scenarios has been evaluated to support an optimized decision considering design options. Lobaccaro and Frontini (2014) tested three design scenarios that have different building shapes and exposed areas to analyze solar availability (Lobaccaro and Frontini 2014). Block-level performance should also consider building parameters as well as urban parameters. According to a research by Van Esch et al. (2012), building parameters such as envelope design and roof shape were considered to evaluate solar accessibility in urban canyon and thermal energy (Van Esch et al. 2012). Furthermore, urban parameters such as street width and street direction were also used for measuring performance outcomes. Chang et al. (2019) studied campus-built forms produced by a generative design approach and evaluated energy demands, solar harvesting potential, and sky view factors (Chang et al. 2019c). The study showed that parameters in campus-built forms consist of the number of

buildings, the number of thermal zones, external wall area, coverage ratio, etc. According to Yang et al. (2012), geometry ratio (height/width) can determine the sky view factor, and thermal properties can determine heat transfer, so block-level heat island effects can be intensified (Yang et al. 2012a).

Zhang et al. (2012) also evaluated sky view factor on façade and ground levels based on existing blocks in different climate conditions (Zhang et al. 2012). Rodriguez-Alvares (2016) investigated current urban fabric for five European cities, and analyzed energy demands of heating, cooling, and lighting based on building and urban parameters (Rodríguez-Álvarez 2016). Morganti et al. (2017) tested 14 urban morphologies and identified potential solar irradiation along with three independent variables of the ratio of built area to the site area, the ratio of vertical surface area to floor area, and the sky factor on the façades (Morganti et al. 2017). The results enable urban planners to incorporate energy performance and solar potential at the preliminary stages of urban planning. Those approaches have isolated the contribution of different parameters individually to understand the influence of factors clearly. However, the isolation can distort the relationships when parameter effects are combined. In this respect, effects of urban building parameters should be analyzed synthetically when impacting on performance indicators.

Even if previous research tested actual built forms without any simplifications, it is still challenging to abstract the complexity of generic forms without disfiguring the performance of the original form (Zhang et al. 2012). In this respect, Stewart et al. (2012) categorized local climate zones for measuring urban heat island effects based on

combinations of estimated block typologies (Stewart et al. 2012). This research showed that standardizing block typologies can measure performance in any city and region by lessening the complexity. In addition, a study testing several building typology options on an existing site was conducted to identify the life cycle of urban typologies (Rodríguez Serrano and Porras Álvarez 2016). This research found that a large energy consumption does not necessarily produce more proportional CO₂ emissions, demonstrating that buildings can reduce CO₂ emissions without saving energy consumption.

2.1.3 Community Level

Reinhart and Cerezo Davila (2016) analyzed energy performance of neighborhoods through a bottom-up approach driven by buildings (Reinhart and Cerezo Davila 2016). Subset of number of buildings, building shape, area, age, use, system, and climate can be used to estimate energy demands at the community level. The research indicated that insufficient information about building use and thermal properties can make reliable prediction of energy use difficult. To quantify environmental impacts of existing buildings in a city level, Stephan and Athanassiadis used existing land use and building footprint data to evaluate life cycle embodied energy of building stocks (Stephan and Athanassiadis 2017). Through the bottom-up approach, embodied energy including material use, energy consumption, greenhouse gas emission, and water use were calculated in their study. In this respect, buildings are still important elements to indicate community-level performance. However, when building performance scales up to urban level, data collection and inconsistencies of data resolution might have problems that undermine accuracy of building performance predictions (Quan et al. 2015b). Detailed building information can be represented as appropriate abstracted forms when scaling up (Kang and

Hong 2015). In other words, appropriate abstractions of data resolution and performance evaluation indicator will be required in the decision at the community level.

On a community level, renewable energy, especially solar potential, has been analyzed to evaluate feasibility of applying solar PV. Freitas et al. (2015) compared solar irradiation of major cities across the world and devised web-based platform to review the different levels of potential (Freitas et al. 2015). Quan et al. (2015a) analyzed solar potentials on building rooftops (Quan et al. 2015a). They evaluated 45,900 buildings in the New York City and compared building energy uses and potential solar power generation when PV installed on about 50% of the rooftops. The energy balance varied by locations, and the annual average of decentralized energy generation by the building-integrated solar PV was 2.69%. Nevertheless, applications of renewable technologies in buildings will create more dynamic energy distributions in urban areas. For example, renewable energy source from biomass energy can provide surplus energy that can provide communities with additional energy capacity (Castro-Lacouture 2015; Chang et al. 2017). When energy loads and resources are distributed in urban area, clear boundaries within a community should be defined (Ton and Smith 2012). The boundaries in a community can be represented by blocks that can be determined street networks (Bürklin and Peterek 2017).

2.2 Performance Evaluation Methods at Multiple Scales

Performance optimization and evaluation methods have been discussed and researched for years, but the methods have been limited to a specific scale even though buildings' performance can influence several scales such as district, city, or region (Nouvel et al. 2015, 2017). Previous research about retrofitting buildings have not measured

dynamic changes or behaviors inside the urban energy system encompassing buildings (Feng et al. 2013; Nouvel et al. 2015). This section reviews tools and performance evaluation criteria of transforming urban buildings at different scales.

On an individual building scale, the energy performance of buildings has been simulated using, e.g., EPC, TRNSYS, EnergyPlus, RADIANCE, and WUFI. (Gahrooei et al. 2016; Ihara et al. 2015; Kämpf and Robinson 2010; Lu et al. 2017; Quan et al. 2015b). Those simulation tools emulate physical properties of buildings. Since those models simplified building details by assuming building parameters (Charron and Athienitis 2006; Yang et al. 2014b), the models cannot accurately represent the performance of actual buildings. Previous research has applied methods of incorporating uncertainties during simulation, such as Monte Carlo, mathematical optimization, and an uncertainty analysis tool (GURA-Workbench) with energy simulation tool (Gahrooei et al. 2016; Lu et al. 2017; Zhang et al. 2016).

Beyond energy performance evaluations, other criteria monetary benefits, technical compatibility, or thermal comfort have been assessed. In order to estimate the building performance with few data, Life Cycle Cost (LCC), Life Cycle Assessment (LCA), and Life Cycle Energy Analysis (LCEA) were presented and integrated to provide the overall performance including economy, energy, material efficiency, environment, and other policy benefits (Iwaro and Mwashia 2013). For incorporate economic benefits in performance evaluation, the following methods: net present value calculation (Hong et al. 2014), probabilistic modeling based on convolution technique (Tina et al. 2006), graph search algorithm (Juan et al. 2010), geometric brownian motion analysis in real option (Gahrooei et al. 2016), multivariate optimization (Peippo et al. 1999) have been studied to

examine energy performance with cost benefits. Technical compatibility as well as structural and thermal performance analysis have been integrated through finite element analysis (Kim 2013). The finite element method was applied to build a database that can provide element alternatives for optimizing building designs (Koo et al. 2014). The thermal comfort criterion could be integrated with the application of the artificial neural network method if there are sufficient responses about the comfort level (Gossard et al. 2013). Genetic Algorithms (GA) were also utilized to generate building design configurations as well as to handle both discrete and continuous parameters (Chantrelle et al. 2011; Charron and Athienitis 2006; Juan et al. 2010). Multi-objective optimization algorithms were developed in MATLAB to evolve building models over generations (Kämpf et al. 2010). Also, multi-criteria decision-making was optimized using weights to test a large set of retrofit options (Asadi et al. 2014). Based on the previous approaches, improvement of reliability of initial populations (retrofit options) can alleviate the disadvantage of GA and maximize benefits of quick iterative optimizations.

On a block scale, performance analysis and relationship analysis are often integrated to establish a theoretical performance that can be replicable to estimate the same forms of urban blocks (Lobaccaro and Frontini 2014; Zhang et al. 2012). While virtual urban forms are modeled and their performance are tested using simplified mathematical formulas, the development of data acquisition using geographic information systems (GIS) and parametric modeling enabled researchers to model existing built forms. Case studies that have used existing built forms and synthetic evaluation of both energy demand and supply have been important on the block level. For example, Reinhart et al. (2013) evaluated operational energy, daylighting, outdoor thermal comfort, walkability in a mixed

use block in Boston, USA, by developing an urban modeling tool (Reinhart et al. 2013). The approach consisted of 3D geometry (Rhinceros)-based modeling and included the measure of building parameters in a block and their relationships with performance.

Statistical inference has enabled designers and planners to develop performance-based design strategies at the early stage (Morganti et al. 2017). Furthermore, statistical models have helped to understand relationships between urban building parameters and multiple performance indicators. Results of urban model simulations are often used to build statistical models (Morganti et al. 2017). Least-square regression analysis was employed to understand relationships among gross space index, façade-to-site ratio, and sky factor (Morganti et al. 2017). Multivariate models were built to understand relationships between performance indicators for energy and sky view factor, including design parameters such as coverage ratio, floor area ratio, etc. (Chang et al. 2019c).

Since data is approximated to analyze community-level performance such as life cycle emissions and energy, the analysis can be simplified by devising a mathematical model (Stephan and Athanassiadis 2017). As being improved computational power, large scale analysis has been empowered by geographical information system (GIS) tools (Freitas et al. 2015). GIS tools are often used for solar radiation analysis (Freitas et al. 2015; Quan et al. 2015b). Simulation methods have been developed to support a bottom-up urban building energy modeling (Reinhart and Cerezo Davila 2016). The simulation methods have been developed into two-folds: 1) simulating a set of buildings by abstracting building details while recognizing uncertainties or 2) modeling urban area including buildings, streets, surrounding vegetations, etc. (Chang et al. 2019c). Energy simulation engines such as EnergyPlus, DOE2, TRNSYS, and IDA-ICE have been widely used

especially where cooling loads are notable (Reinhart and Cerezo Davila 2016). The engines simulate building energy models. Beyond this, Urban Modeling Interface (UMI) has been developed as a plug-in of Rhinoceros 3D, and it parameterizes urban objects including buildings, and conducts EnergyPlus simulation for buildings (Reinhart and Cerezo Davila 2016).

Another approach of urban building energy model tool is ArcGIS based plug-in to integrate spatial and temporal energy consumption patterns (Fonseca and Schlueter 2015). This has been further developed as a computation framework, City Energy Analyst (CEA), to analyze demand, resource, and performance patterns in a neighborhood level (Fonseca et al. 2016). Tools for urban energy systems are to evaluate both energy demand with district energy supply (Shi et al. 2017). To discretize zones of energy patterns, spatial statistics are essential to cluster buildings (Fonseca and Schlueter 2015). Spatial statistics using GIS data and K-means clustering have been identified as an appropriate approach of aggregating buildings' performance while discerning their interactions in a community scale (Fazlollahi et al. 2014; Fonseca and Schlueter 2015).

2.3 Summary of Literature Review

Previous research presented a variety of potential transformable parameters of building forms and performance indicators at different urban scales. Table 1 summarizes research scale, parameters and performance evaluation criteria, and study area of previous literature and this dissertation research.

According to literature review on an individual building level, building envelope renovations are complex decisions because 1) renovations of envelopes should meet

multiple performance criteria, 2) envelopes can require thermal energy as well as provide renewable energy based on their properties, and 3) performance of both traditional materials and renewable sources should synthetically be evaluated.

On a block level, changes in building topological parameters will influence multiple performance in blocks such as energy demands and solar potential, sky exposure, and thermal comfort. There are two manifestations of performance evaluation in a block level. First, detailed data should be simplified without skewing important building parameters even if performance has been measured for existing urban fabric. Second, several building typology parameters should be analyzed together not to skew the relationships between the parameters and performance.

On a community level, buildings' information should be abstracted by simplifying detailed materials or structure to evaluate community-level performance in nonredundant manner. Also, since the potential of renewable sources can change energy distribution dynamically, boundaries within a community should be identified.

In addition, research approach varies by scales. For an individual building, an optimization method to select envelope options should be devised. On a block level, a statistical inference becomes essential to inform performance distributions or changes of typology parameters in a block. On a community level, although energy performance analysis methods have been developed in building-driven analysis or urban objects modeling and simulation, spatial statistics can be useful to consider spatial and temporal conditions.

Table 1 – Summary of literature review

Reference	Analysis Scales			Parameters	Performance / Evaluation criteria			Application scope	Study Area	Existing or Virtual
	Building	Block	Community		Building	Block	Community			
This Study	v	v	v	<u>Building parameters</u> : surface area at each orientation <u>Building typology parameters</u> : floor area, building height, structure, land use <u>Block parameters</u> : energy balance of groups of buildings	Building thermal energy demands Renewable applications Indoor thermal comfort CO2 emissions Economic payback	Building energy demands Renewable applications Indoor thermal comfort Sky view factor	Building energy demands Renewable applications	All buildings	Tokyo, Japan	Existing
(Stephan and Athanassiadis 2017)	-	-	v	Building geometry, and parameters from building archetype (land-use, age, and height)	-	-	Embodied energy, water, and greenhouse gas emissions	All buildings	Melbourne, Australia	Existing
(Freitas et al. 2015)	-	-	v	Climate, building footprints, terrain, LiDAR, imagery	-	-	Solar irradiation	All buildings	Switzerland, Slovakia, US, Portugal	Existing
(Reinhart and Cerezo Davila 2016)	v	-	v	Subset of {Number of buildings, Building shape, area, age, use, system, climate}	Heating loads or Total Energy Unit Intensity (EUI)	-	Heating loads or Total Energy Unit Intensity (EUI)	All buildings	Italy, Greece, Finland Japan, US, UK, Italy, Netherlands, Greece, Switzerland, Ireland, France,	Existing Virtual

									Spain, Germany	
(Quan et al. 2015b)	v	-	v	Land use, building footprint, estimated shading, microclimate zones, and occupancy	Hourly building energy use and roof solar energy production	-	Hourly building energy use and roof solar energy production	All buildings	New York, US	Existing
(Grippa et al. 2018)	-	v	v	Satellite imagery Street block polygons	-	Mapping up-to-date land use		All buildings	Ouagadougou in Burkina Faso and Dakar in Senegal	Existing
(Reinhart et al. 2013)	v	v	-	Building forms, trees, shading objects, window-to-wall ratio, walking paths	Energy use, daylight autonomy, outdoor thermal comfort, walkability	-	-	All buildings	US	Existing
(Rodríguez-Álvarez 2016)	v	v	-	<u>Building parameters:</u> Glazing ratio, Construction type, Thermal capacity, Albedo <u>Urban parameters:</u> Floor Space Index, Ground Space Index, Compactness ratio (envelope area to floor area)	Energy demands: heating, cooling, and lighting	-	-	All buildings	Spain, United Kingdom, France, Germany	Existing
(Morganti et al. 2017)	-	v	-	Gross space index Floor space index Façade-to-site ratio Average building height Volume-area ratio Building aspect ratio	-	Solar availability Sky view factor	-	All buildings	Spain, Italy	Existing

(Rodríguez Serrano and Porras Álvarez 2016)	-	✓	-	Floors Envelope Area Volume Compactness	-	Embodied energy (heating and cooling) CO2 emissions (heating, cooling, domestic hot water)	-	Residential	Spain	Existing site / virtual planning options
(Stewart et al. 2012)	-	✓	-	Aspect ratio, Building surface fraction, Impervious surface fraction, Pervious surface fraction, Average building height, Terrain roughness, Sky view factor	-	<u>Urban heat island effect</u> : Surface admittance, Surface albedo, Heat output	-	All buildings	Not specific	Virtual
(Shi et al. 2017)	-	✓	-	Design parameters, urban context, weather, PV panel cost, new energy technology	-	Energy performance	-	All buildings	Not specific	Virtual
(Chang et al. 2019c)	✓	✓	-	Number of buildings, number of thermal zones, coverage ratio, external wall area, floor area ratio	Energy demands, solar radiation, sky view factor		-	All buildings	Shenzhen, China	Virtual
(Lobaccaro and Frontini 2014)	✓	✓	-	Site terrain, building envelope, building shape, building height	-	Average solar irradiation	-	Commercial	Switzerland	Virtual
(Van Esch et al. 2012)	✓	✓	-	Street width, street direction, roof shape, envelope design	Solar access, heat demand, solar heat gain		-	Residential	Netherlands	Existing
(Zhang et al. 2012)	-	✓	-	Floor area ratio, site area, site coverage, number of stories, area/perimeter ratio	-	Sky view factor on building façade	-	Residential	Netherlands, Spain, France, Singapore	Existing
(Yang et al. 2012a)	-	✓	-	Geometry ratio (Height/Width) Wall surface	-	Sky view factor Solar radiation Air and surface temperature	-	All buildings	Beijing, China	Virtual

				Thermal properties of building materials						
(Parasonis et al. 2012)	√	-	-	Building surface area to floor area, Thermal conductance	Thermal energy through envelopes	-	-	Residential	-	Virtual
(Danielski et al. 2012)	√	-	-	Shape factor (surface area to volume ratio), Thermal conductance, Window area to floor area ratio	Heat demand	-	-	Residential	Sweden	Existing
(Premrov et al. 2016)	√	-	-	Glazing area, Shape factor (surface area to volume ratio), Shape type (Square, Rectangular, L and U shapes)	Cooling energy demand	-	-	All buildings	Slovenia, Germany, Finland	Virtual
(Rashdi and Embi 2016)	√	-	-	Shape factor, Orientation, Shape type (Rectangular, U, T, L, Ellipse, Circle, Courtyard, Square)	Cooling energy demand	-	-	All buildings	Malaysia	Existing
(Chang et al. 2017)	√	-	-	Glazing area - applying biomass façade	Thermal energy generation CO2 emissions	-	-	All buildings	U.S.	Virtual
(Asadi et al. 2012)	√	-	-	Building use, floor area, dimensions and height, enclosure thermal properties, HVAC parameters	Energy consumption Retrofit cost Thermal comfort	-	-	School building	Portugal	Existing
(Roberti et al. 2017)	√	-	-	Façade and roof insulation, Glazing options, cooling systems	Energy demands Indoor thermal comfort Conservation compatibility	-	-	All buildings	Italy	Existing
(Güçyeter and Günaydın 2012)	√	-	-	Transmission and infiltration loss through building envelope materials, solar availability	Heating and cooling energy consumption CO2 emissions Indoor thermal comfort	-	-	Office	Turkey	Existing

					Investment for retrofit					
(Heo et al. 2012)	v	-	-	Wall insulation, window insulation, and airtightness	Energy consumption Payback time	-	-	Office	UK	Existing
(Peippo et al. 1999)	v	-	-	Building geometry, orientation, renewable technology installation (solar thermal collectors and PV), thermal insulation, window types and area, lighting type and control, heat recovery	Building cost Energy saving	-	-	Residential and Office	Finland, France, Italy	Virtual
(Charron and Athienitis 2006)	v	-	-	Building length/width, window types and area on each orientation, overhang, envelope thermal properties, heating and cooling systems, solar thermal collector, roof-integrated PV	Electricity consumption and generation	-	-	Not specific	Canada	Virtual
(Gahrooei et al. 2016)	v	-	-	Investment timing, Solar panel size, Variations of climate condition	Maximum Net Present Value	-	-	Residential	U.S.	Virtual
(Lu et al. 2017)	v	-	-	Applications of wind turbine, bio-diesel generator, and solar PV	Electricity demand and supply Cost CO2 emissions	-	-	Office	Hong Kong	Existing
(Zhang et al. 2016)	v	-	-	Applications of wind turbine and solar PV	Initial investment Energy balance Grid stress	-	-	School building	Hong Kong	Existing

CHAPTER 3. RESEARCH METHODOLOGY

This chapter presents an overall research approach by summarizing specific procedures and techniques to identify urban building transformation strategies at multiple scales and their possible interactions. Figure 3.1 shows an overview of the research workflow that has implemented for transforming urban buildings at each scale and for integrating findings of the empirical studies. To transform urban building parameters at multiple scales, this research conducts four processes: 1) recognizing research problems and questions at each scale, 2) designing an appropriate models or establishing a suitable methodology to address research challenges, 3) implementing the methodology to the test case located in Kyojima, Tokyo, Japan, and 4) analyzing transformable topological or typological parameters and their impacts on performance. Integration strategies are discussed by reviewing findings from the empirical studies conducted in a building, block, and community scales.

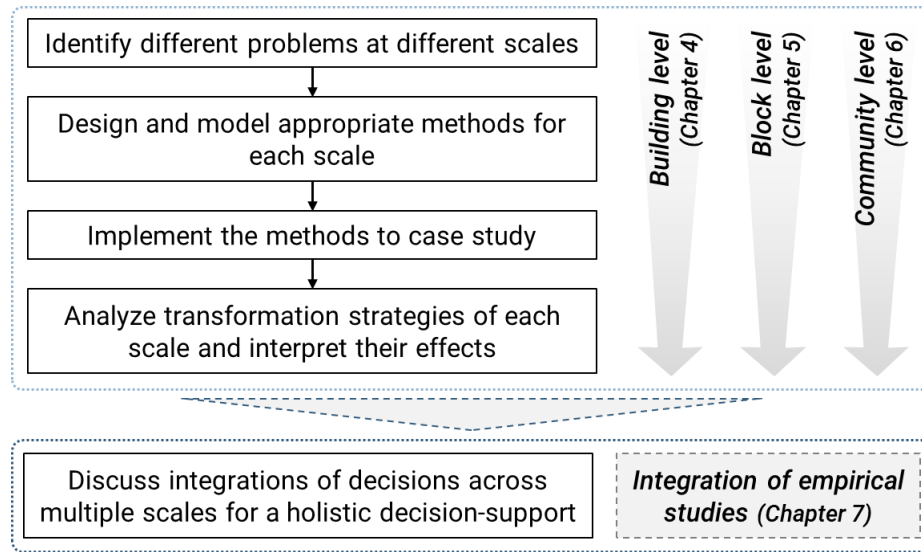


Figure 3.1 – Overall research framework

This research conducts the methodological innovation and integration to design a holistic decision support for multi-level building renovation in the multiple urban scales. Figure 3.2 elaborates research methodologies for three sub-systems: 1) retrofitting buildings' envelopes by incorporating as many as envelope options, 2) reorganizing building typology or topology by considering their multiple performance, and 3) reconfiguring buildings by considering their energy sharing capacity. A multi-objective optimization using evolutionary algorithm for an individual building level is applied for heuristic estimations of performance of selecting a variety of sets of envelope options. On a block scale, Bayesian multilevel modeling is employed to multiple performance and building topological parameters nested in blocks. Then, on a community level, K-nearest neighbor and community clustering are applied and geo-spatial dataset (GIS) is used for spatial analytics. Based on inputs and outputs of methodology at each scale, both top-down and bottom-up decision frameworks are devised for supporting holistic decisions of transforming existing buildings and blocks.

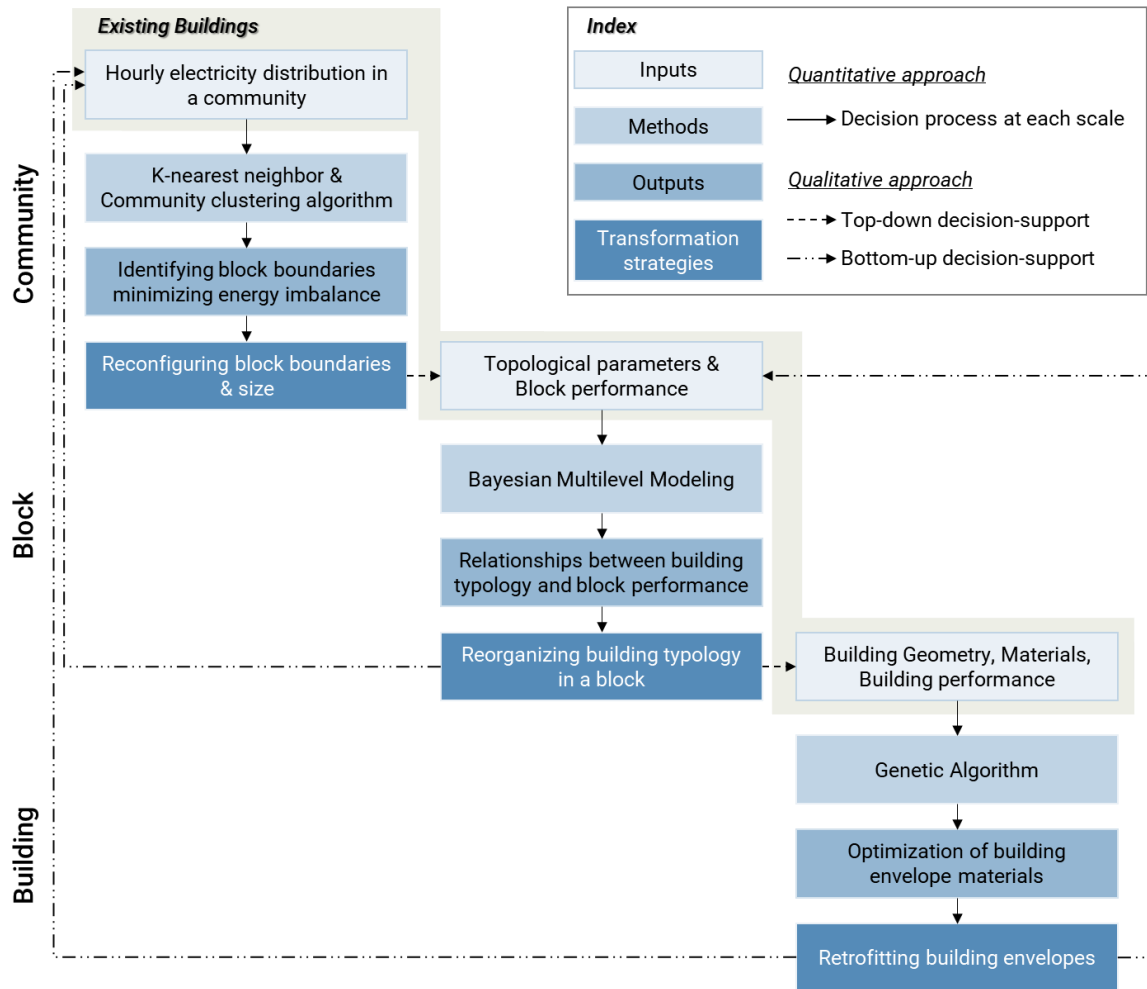


Figure 3.2 – Research Methodology

CHAPTER 4. RETROFITTING BUILDING ENVELOPES ON AN INDIVIDUAL BUILDING

This chapter studies retrofitting building envelopes in an individual building level (Chang et al. 2020a). In an individual building level, approximately 50% of total building energy consumption is impacted by the building envelope elements (Mavromatidis et al. 2013). Building envelope retrofit options can be categorized into two parts: 1) reducing energy demands, and 2) decentralizing energy supplies (Jafari and Valentin 2017; Roberti et al. 2017). Building energy demands can be reduced by applying highly insulated materials (Chantrelle et al. 2011) or energy efficient equipment such as heat recovery systems (Chidiac et al. 2011). The energy supply of buildings can be partially charged by renewable energy (RE) technologies. For example, solar photovoltaic (PV) has been implemented as an energy source integrated in building surfaces (Pagliaro et al. 2010). Although retrofit options can be applied for different purposes, the performance of each option should be estimated collectively to support optimal decisions. However, research in the field of building envelope retrofits has not been fully discussed (Fan and Xia 2017). Additionally, considerations of envelope options have been easily constrained by several pre-conceived experiences about using traditional materials and systems, thereby limiting the potential of improving building performance by retrofitting envelopes.

The decision to adopt new envelope systems is difficult because it is a multi-criteria problem embracing ecological, economic, social, and other dimensions (Asadi et al. 2014). The retrofitting problem also includes constraints such as influences of existing context (Nutmiewicz et al. 2018). Furthermore, the uncertainties in parameter estimates and

performance predictions may make it challenging to ensure the adequacy of the retrofit decisions (Jafari and Valentin 2017). These challenges reclaim a research question about optimization of building envelope retrofit decisions: how can we formulate an optimization framework allowing to incorporate any envelope systems as retrofit options while considering uncertainties under contextual constraints?

This chapter aims to optimize building envelope retrofit decisions while incorporating newly developed façade systems. To achieve the research objectives, four research tasks are devised: 1) identifying multi-objective functions to test retrofit buildings based on common envelope features, 2) identifying uncertainties in building envelope parameters and performance predictions, 3) developing a multi-objective optimization model under uncertainties and built environment constraints, and 4) testing the methodology applied to existing residential buildings.

4.1 Approach for Multi-Objective Optimization Model

Figure 4.1 shows the methodology to build this façade selection models. The following sections divide the methodology in three parts: 1) identifying multi-objectives and decision functions, 2) establishing the framework of considering uncertainties into the decision model, and 3) formulating the multi-objective optimization model using GA. Each step of the methodology will be explained specifically in sections below.

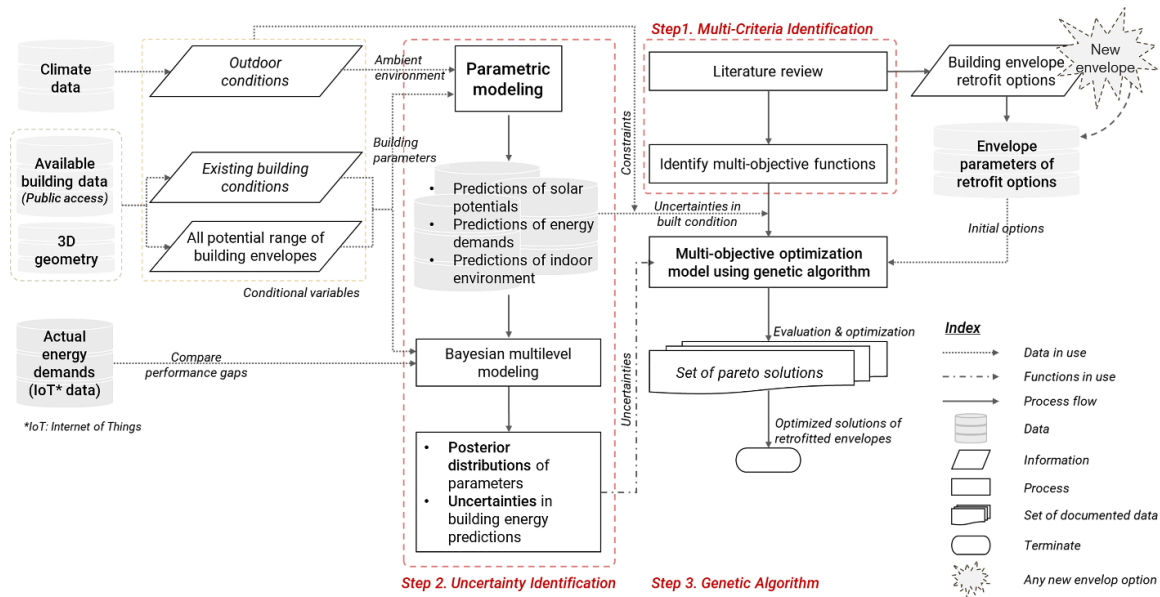


Figure 4.1 – Methodology for selecting building envelopes by using a multi-objective optimization (Chang et al. 2020a)

4.1.1 Multi-criteria for building envelope retrofits

Optimization objectives for retrofit decisions can be summarized as economic, environmental, and social aspects (Jafari and Valentin 2018). Energy performance should consider the balance between energy demand and generation from renewable sources-integrated in building forms (Charron and Athienitis 2006; Quan et al. 2015b). Environmental and economic criteria should also be evaluated to determine an appropriate envelope decision (Chantrelle et al. 2011). Environmental impacts are evaluated by determining the reductions of CO₂ emissions foreseen for the building life cycle (Diakaki et al. 2010). Depending on envelope alternatives, carbon abatement can also be incorporated in life cycle CO₂ emissions (Wilkinson et al. 2017). Economic aspects can be valorized as a payback period commensurate with cash inflow and outflow (Fan and Xia 2017). As input costs, initial investment cost (Cho et al. 2014), energy consumption costs (Cho et al. 2014), maintenance costs (Fan and Xia 2017; Wilkinson et al. 2017), and

environmental costs (Jafari and Valentin 2018) can be considered. As benefits, tax benefits (Govindan et al. 2016) and resale value (Gahrooei et al. 2016; Jafari and Valentin 2017, 2018) can be considered. Multi criteria optimization of social, energy, environmental, and economic aspects presented in Figure 4.2. should be evaluated synthetically to determine optimized envelope retrofits.

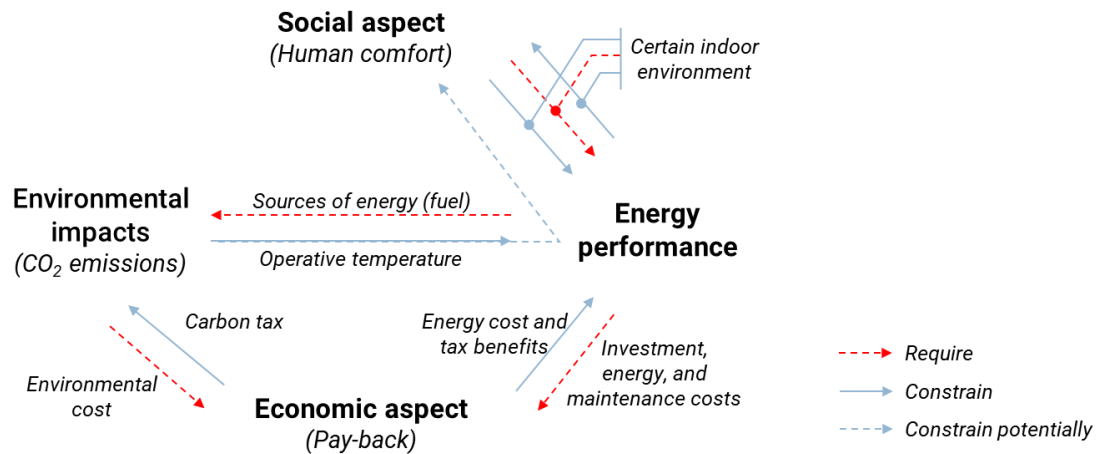


Figure 4.2 – Multi-criteria objectives and their potential relationships

4.1.2 Considering uncertainties and constraints

Uncertainties in building parameters can cause reliable predictions of renewable energy generation and building energy consumption to fail (Zhang et al. 2016). Uncertainties can be categorized into three: physical, design, and scenario parameters (Zhang et al. 2016). Physical properties of building materials are set to calculate energy consumption, and uncertain estimations of the building envelope properties lead to a discrepancy between actual and predicted energy consumption (Jeon et al. 2018). Design parameters are related pre-set working conditions (Zhang et al. 2016), and the design parameters can be obtained from the existing built form, which includes existing building conditions (e.g., shadings, vertical mullions) and surrounding buildings. Uncertainties in

the scenario parameters are originated from climate conditions (i.e., solar radiation) where the buildings and their systems are operated (Cao et al. 2013; Zhang et al. 2016). This chapter identifies uncertainties and incorporates them into decision functions by using the following two parts: parametric modeling and a Bayesian multilevel modeling. In that Bayesian approach can detect posterior uncertainties of parameters for both population level and group level effects (Bürkner 2017), it can eliminate inaccuracy of uncertainty considerations driven by historical assumptions or subjective norms (Nagel and Sudret 2016). The Bayesian multilevel modeling to identifies the distributions of physical parameters and distributions of performance gaps. The framework for considering uncertainties in the building envelope retrofit decisions is devised in Figure 4.3. In the Bayesian multilevel modeling, x denotes explanatory variables, y denotes response variables, ϵ denotes experiment-specific known uncertainties, and i denotes the index of the measurement intervals. The uncertainties are incorporated into the multi-objective optimization as providing uncertainties in physical, design, and scenario parameters.

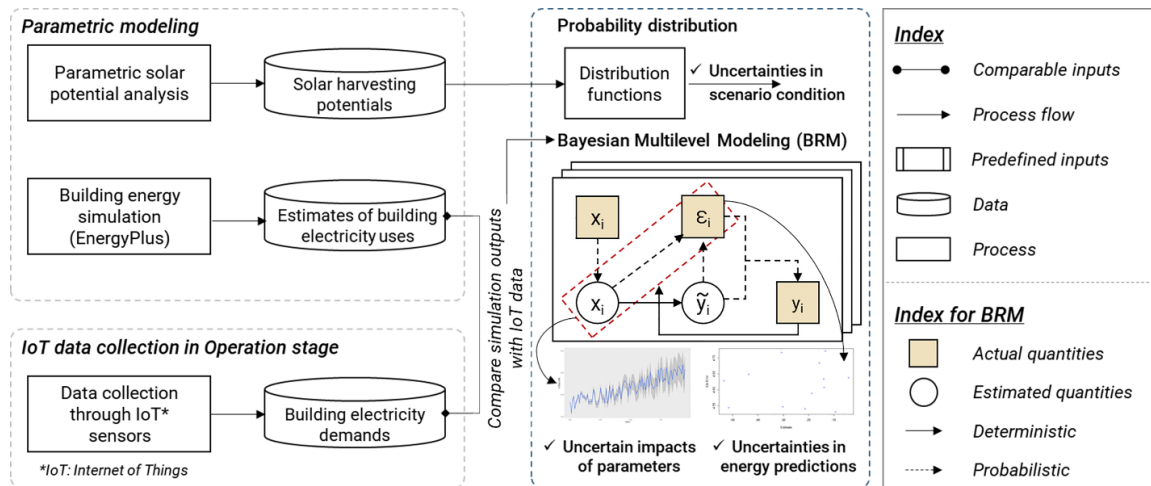


Figure 4.3 – Framework considering uncertainties in physical, design, scenario parameters (Chang et al. 2019a; d, 2020a)

4.1.3 Designing a multi-objective optimization model

A multiple objective optimization (MOO) using the genetic algorithm is modeled in MATLAB computing environment. According to the multi-criteria for building envelope retrofits, decision functions of indoor thermal comfort, energy performance, environmental impacts, and economic aspects are identified by reviewing literature and technical reports. The MOO model can provide Pareto optimal sets by integrating several objective functions into a set of problems (Giagkiozis and Fleming 2012; Miettinen 1999). Sets of solutions will be provided, and decision makers may need another procedure to find out optimal solutions satisfying their requirements among the set (Giagkiozis and Fleming 2012). The Pareto front solutions will be several alternatives optimized in multi-criteria, and decision makers can determine the final implementation among optimal sets. Figure 4.4 presents the framework of designing the multi-objective optimization model.

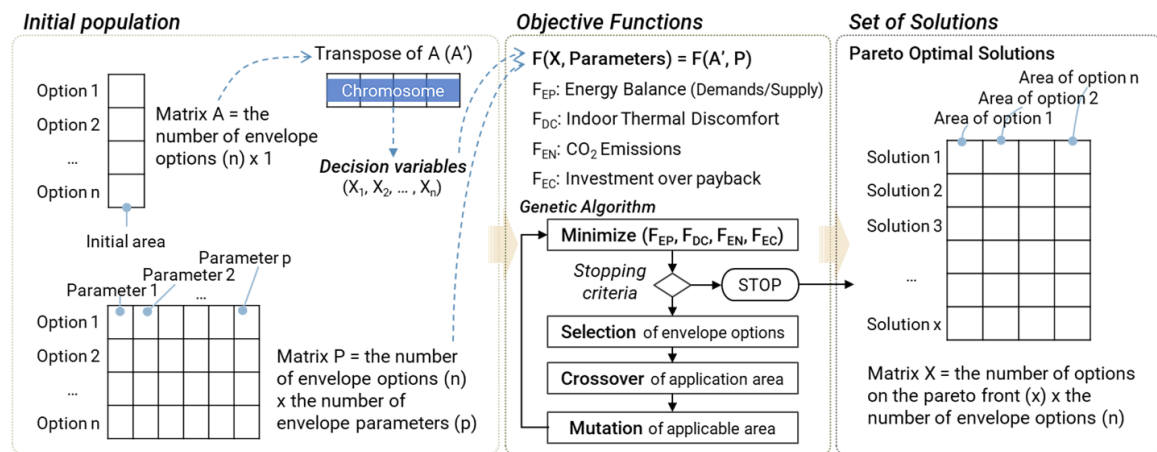


Figure 4.4 – Framework of designing multi-objective model (Chang et al. 2020a)

4.1.3.1 Modeling the multi-objective problem

Based on literature review, objective functions of multi-criteria: energy performance, social aspect (indoor thermal comfort), and environmental impacts (CO₂ emissions) and economic aspects (payback period) are identified and expressed as functions of envelope-related parameters.

1) Energy performance (F_{EP}): thermal energy consumption over generation

Building energy simulation programs analyze building energy consumption by modelling building envelopes and systems (Yang et al. 2012b). This research considers both energy consumption and generation to determine energy performance criteria. Energy performance, F_{EP} , is represented by energy balance: thermal energy consumption over energy generations.

Thermal energy consumption was calculated by using the degree days method. This is a simplified method for estimating energy consumption of small buildings, and has a dominant influence by energy uses (Zhao and Magoulès 2012). The simplified degree days method (Saad Al-Homoud 2001) is presented in the following equation:

$$E_{\text{demands}} = U_{eq} \times A \times (\text{HDD or CDD}) \text{ (kWh/year)} \quad (1)$$

where E_{demands} is energy demand (Watts), U_{eq} is u-value of the overall building surface (W/m²K), A is the surface area (m²), HDD is Heating Degree Days, and CDD is Cooling Degree Days. Degree days are the sum of the degrees exceeding or dropping a certain temperature required heating or cooling yearly. According to the climate design

condition data reported by ASHRAE (ASHRAE 2009), annual cooling and heating degree days and an operative temperature can be determined as climate conditions. A website, <https://www.degreedays.net/>, (BizEE Software 2019) can be used by energy professionals to extract the average HDD and CDD of until recent three years with weather station's location, cooling and heating temperature.

By using different building envelope options, buildings can require various sources of energy. To identify energy generation effects of buildings, renewable sources that are applicable in buildings are reviewed and their energy generating potentials are discussed. Renewable electricity generation sources are categorized into five systems: wind energy, solar photovoltaic (PV), solar thermal, biomass, and small hydro systems (Varun et al. 2009a). Among them, solar photovoltaic, solar thermal, and biomass sources can be applicable as building envelope-integrated systems.

Solar power generation was measured using the following equation (Chang et al. 2019c).

$$E_{pv} = A_{pv} \times \eta_e \times G \text{ (kWh/year)} \quad (2)$$

where A_{pv} is the surface area of the solar PV panels (m^2), η_e is the mean annual power conversion efficiency coefficient, and G is the annual solar irradiation (kWh/m^2). According to the literature review, since the PV module requires a supplementary area including layered areas, the PV module, which has productive circuits, can be placed on 72.5% of the total surface (James et al. 2011). The mean annual power conversion efficiency coefficient was assumed as 0.766 (Hofierka and Kaňuk 2009). In this respect,

annual solar irradiation per unit area was converted hourly averaged solar power generation by using 72.5% of rooftops and 0.766 power conversion efficiency. The annual solar irradiation depends on orientations and surrounding buildings and fluctuates along with the locations of façades and existing building conditions such as shading and the size of panels. To consider existing building conditions and surrounding buildings together, parametric modeling is conducted to predict the potential solar radiation of each orientation.

Solar thermal systems yield energy by multiplying area of collectors with several performance factors (O’Hegarty et al. 2014; Visa et al. 2017), and the energy generations can be simplified by the following equation:

$$E_{st} = A_{st} \times \eta_c \times \eta_s \times G \text{ (kWh/year)} \quad (3)$$

where E_{st} is the electricity energy generations from solar thermal collectors, A_{st} is the surface area of the solar thermal systems (m^2), η_c is the efficiency of the solar thermal collectors, η_s is the efficiency of the systems (e.g., piping, storages), and G is the annual solar irradiation (kWh/m^2). The overall efficiency ($\eta_c \times \eta_s$) is distributed between 0.15 and 0.8 as two peaks and 0.45 as the median (O’Hegarty et al. 2014).

Biomass systems can be integrated into the building envelope as a bioreactor façade. The bioreactor façade, also known as algae façade, can generate biomass about $30kWh/m^2/year$ (Chang et al. 2017; The European Portal For Energy Efficiency In Buildings 2015), and 80% of them can be converted to biogas (The European Portal For Energy Efficiency In Buildings 2015) which can be used for generating electricity or heat energy.

2) Indoor thermal discomfort (F_{DC})

According to the European Committee for Standardization (CEN) (European Committee for Standardization (CEN) 2007), the operative temperature is the value for which the indoor environment can achieve the maximum levels of comfort, which corresponds to $PMV = 0$. The thermal discomfort times can be calculated from the indoor temperature out of the maximum and minimum limits of indoor operative temperature (Atzeri et al. 2016; Penna et al. 2015).

$$T_{o, \max} = 0.33 \times T_{o,o} + 18.8 + 3 \quad (4)$$

$$T_{o, \min} = 0.33 \times T_{o,o} + 18.8 - 3 \quad (5)$$

Where $T_{o,o}$ is the outdoor mean dry bulb temperature, $T_{o,\max}$ is the maximum limit of indoor operative temperature, and $T_{o,\min}$ is the minimum limit of indoor operative temperature.

Outdoor mean dry bulb temperature can be calculated from the mean values of minimum dry bulb temperature and the maximum dry bulb temperature from the EnergyPlus weather file. Discomfort times are when the indoor operative temperature exceeds the boundaries between $T_{o,\min}$ and $T_{o,\max}$. The indoor operative temperature ($T_{o,i}$) can be approximated by calculating the average of the mean radiant temperature of inside surfaces and the indoor dry bulb temperature (Djongyang et al. 2010; Energy 2018). The mean radiant temperature in a zone can be calculated by the following equation (Energy 2018):

$$T_{mr,i} = \frac{\sum \varepsilon_i A_i T_i}{\sum \varepsilon_i A_i} \quad (6)$$

Where $T_{mr,i}$ is the mean radiant temperature in a zone, ε_i is the surface emissivity, A_i is the area of each surface, and T_i is the surrounding surface temperature. The surface temperature of a composite surface can be calculated by the following equation (Energy 2018):

$$T_i = \sqrt[4]{\frac{Q}{\sigma \varepsilon_i}} + T_0 \quad (7)$$

Where Q is the infrared radiant gain from zone (W/m^2), σ is the Stefan-Boltzmann constant ($5.67 \times 10^{-8} W/m^2/K^4$), and T_0 is temperature of absolute zero ($-273.15 \text{ }^\circ\text{C}$). Q , infrared radiant gain, can be determined by following terms:

$$Q_{opaque} = \alpha \times I_{solar} \quad (8)$$

$$Q_{transparent} = \tau \times I_{solar} \quad (9)$$

Where I_{solar} is solar radiation, α is absorptivity (i.e., fraction of energy hitting an object of opaque envelopes), τ is transmissivity (i.e., measure of radiation passing through an object of transparent envelopes). Overall, the indoor thermal discomfort times, F_{DC} , counts all indoor operative temperatures exceeding the maximum and minimum limits, and the values of discomfort times should be minimized.

3) Environmental impacts (F_{EN}): CO₂ emissions

Environment impacts, represented by CO₂ emissions, consider CO₂ emissions related to energy use (Hernandez and Kenny 2010). Lifecycle CO₂ emissions include embodied CO₂ and CO₂ emissions during operations. Lifecycle CO₂ emissions can be normalized using electrical generation units to compare different energy generation methods fairly (World Nuclear Association 2011). Varun et al. (2009) have studied and compared lifecycle CO₂ emissions by energy sources including conventional fossil fuels and renewable sources (Varun et al. 2009a). The objective of environment impacts, F_{EN} , is formulated by adding CO₂ emissions from conventional systems required by the energy balance and CO₂ emissions from renewable systems emitted by renewable energy generations. In addition, in the case of using biomass sources, the CO₂ abatement of algae façades has been analyzed, and it absorbs about 67.4gCO₂/m²/day (Chang et al. 2017; The European Portal For Energy Efficiency In Buildings 2015). Living walls can also sequester CO₂ about 0.14-0.98 kg CO₂/m²/year (one of [0.14, 0.32, 0.41, 0.86, 0.95, 0.98, 0.99] based on a type of vegetations), and green roofs can sequester CO₂ about 0.375-30.12 kg CO₂/m²/year (Charoenkit and Yiemwattana 2016; Marchi et al. 2015)

Table 2 – Lifecycle CO₂ emissions by energy sources (Varun et al. 2009a; World Nuclear Association 2011)

	Systems	gCO ₂ /kWh (Varun et al. 2009a)	gCO ₂ /kWh (World Nuclear Association 2011)		
			Mean	Low	High
Conventional systems	Coal	975.3	888	756	1,310
	Oil	742.1	733	547	935
	Gas	607.6	499	362	891
Renewable systems	Solar PV	53.4-250	85	13	731
	Biomass	35-178	45	10	101
	Solar thermal	13.6-202	-	-	-

4) Economic aspects (F_{EC}): Payback period

Payback period is an important indicator for evaluating economic viability, and is defined as the length of time in which an investment can be recovered while considering temporal values of money (Fan and Xia 2017). The cash inflow consists of installation and maintenance costs. The cash outflow is composed of electricity generation price and tax benefits. Out of building-integrated renewable technologies, solar PV has a tax benefit offering credits about 30% of installation cost (Burns and Kang 2012). Since the payback period (T_p) is the time when the cash paid is recovered, the payback timing can be determined when the net present value is equal to or greater than zero. In this respect, the payback period and net present value can be determined from the following equation:

$$T_p = t, \text{ when } \frac{P_t}{(1+r)^t} \times \frac{E_t}{(1+d)^t} - (C_i + \frac{M_i}{(1+r)^t}) \times A_i + B_i = 0 \quad (10)$$

Where T_p is payback period, t is time (yearly), E_t is the electricity production from envelope options at time t (kWh), P_t is the electricity price at time t (\$/kWh), C_i is installation cost for the envelope options (\$/m²), M_i is maintenance cost for the solar panel (\$/year), A_i is the area of each envelope option, B_i is tax benefits (\$/kWh), d is degradation rate (%) of envelope systems, and r is discount rate (%). Economic effects, F_{EC}, can be formed by minimizing cash inflows including installation and maintenance costs over cash outflows including electricity sales' profits generated from the envelope options plus tax benefits. The F_{EC} is formed to find the year achieving the minimized economic investments over returns for the duration of applying the optimization model.

4.1.3.2 Decision variables and constraints

The multiple objective optimization aims to decide how much each of envelope option can be applicable within the scope of satisfying multi-criteria. The decision variables are a set of areas for envelope options. Assuming that n types of alternative envelope options are available, decision variables can be defined as the following:

$$X_{\text{envelopes in south, north, east, west, roof}} = (X_1, X_2, \dots, X_n)^5 \quad (11)$$

where n = number of envelope options

The available area of applying envelopes should be limited to the existing envelope area of each orientation. The area of applying envelope options should be equal to or greater than zero (0), and the sum of envelope options solved cannot exceed the total area of the existing building envelope. Each envelope option can also possess different constraints. For example, NREL determined that the building integrated solar PV (BIPV) module (c-Si PV system) area should be at least 0.58 m^2 (James et al. 2011). Since solar cells can be installed about 72.5% of the designated area because of layered area (James et al. 2011), the solar PV options should be equal to or greater than 0.80 m^2 (i.e., 0.58 m^2 of the least solar PV module size $\div 0.725$ the proportion of PV module over the entire panel = 0.8). Constraints for each option are also obtained based on literature review and technical reports.

Table 3 shows envelope options for vertical façades and roofs for refurbishing existing buildings. As vertical façade options, 13 options, Exterior Mass wall (EnergyPlus options), External wood frame wall (EnergyPlus options), Exterior metal frame window

(EnergyPlus options), Trombe walls, AAC walls, Double skin façade, Green wall, Vacuum insulation panels, Solar PV (Semi-transparent), Low-e coated window, PCM integrated in wood-lightweight concrete, PCM, and Algae façade, are considered. As roof options, six options, Exterior IEAD roof (EnergyPlus options), Exterior metal roof (EnergyPlus options), Conventional roof, Green roof, Solar PV, and Cool coated roof are considered. Envelope parameters of U-factor (W/m^2K), Absorptivity (Opaque), Transmissivity (Transparent), Emissivity, Installation cost, Maintenance cost, Degradation rate are obtained from literature review.

Table 3 – Envelope options for vertical façades and roofs

Options	U-factor (W/m ² K)	Absorptivity (Opaque)	Transmissivity (Transparent)	Emissivity	Installation cost	Maintenance cost	Degradation rate	Source
Exterior Mass wall (Climate zone 4)	[0.511, 0.553] W/m ² K	0.9	-	0.92				EnergyPlus simulation options
External wood frame wall (Climate zone 2-8)	[0.505, 0.547] W/m ² K	0.9	-	0.78				
Exterior metal frame window (Climate zone 4-6)	3.127 W/m ² K	-	0.888 (Chow et al. 2010) (Clear glass)	0.88 (Khoukhi and Maruyama 2005)				
Trombe walls	1.75 W/m ² K (Jaber and Ajib 2011)	0.9 (Jaber and Ajib 2011)	-	0.84 (Ma et al. 2017)	\$75/m ² (Robbins and Spillman 1980)	15% of capital cost (Jaber and Ajib 2011)	-	Literature review
AAC walls	0.35 W/m ² K (Lindberg et al. 2004)	0.816 (Koči et al. 2012)	-	0.9 (Ghazi Wakili et al. 2015)	\$107/m ² (Moussavi Nadoushani et al. 2017)	\$30/m ² /10 years (Moussavi Nadoushani et al. 2017)	-	
Double skin façade	5.33 W/m ² K (Gratia and De Herde 2004)	-	[0.106, 0.244] (Chan et al. 2009)	0.9 (Pérez-Grande et al. 2005)	\$218-321/m ² (Chan et al. 2009)	-	-	
Green wall	0.144W/mK 0.04m (Wong et al. 2009)	0.05-0.3 (Perini et al. 2013)	-	0.94 (Alexandri and Jones 2008)	\$33-836/m ² (Perini et al. 2013)	-	-	
Vacuum insulation panels	0.6 W/m ² K (Liang et al. 2017)	0.3 (Johansson 2011)	-	0.94 (Johansson 2011); 0.8 (Kwon et al. 2009); 0.05 (aluminum foil at 300 K) (Jang et al. 2011)	\$89-102/m ² (Alam et al. 2011)	-	[1.14, 2.51, 7.76] %/year (Araki et al. 2009)	
Solar PV (Semi-transparent)	0.133 (Wong et al. 2008)	- 0.49 (Park et al. 2010)	0.9 (Wong et al. 2008)	0.84 (Wong et al. 2008)	\$5.02-5.71/W (Biyik et al. 2017; James et al. 2011)	5 - 6% of the installed system's cost (U.S.DOE 2011)	[0.87, 0.95, 0.4, 0.3, 0.96, 0.02, 0.36, 0.23, 0.64] %/year (Jordan and Kurtz 2013)	
Low-e coated window	[1.3, 1.6, 1.8] W/m ² K (Buratti et al. 2013; Gratia and De Herde 2004)	-	0.23 (Buratti et al. 2013)	[0.013, 0.037, 0.16] (Jelle et al. 2015)	\$75.35/m ² (Culp and Cort 2015)	-	-	
PCM integrated in wood-lightweight concrete	[0.15, 0.75] W/mK (Pasupathy et al. 2008) [0.012, 0.030] m (Liu et al. 2017)	0.9 (Liu and Li 2015)	[0.29, 0.40, 0.49, 0.67, 0.9] (Liu et al. 2017; Liu and Li 2015)	0.88 (Liu et al. 2017)	\$4.40-6.60/kg (Biswas and Abhari 2014)	-	-	

	PCM	0.213 W/mK (Park et al. 2019) [0.012, 0.030] m (Liu et al. 2017)				(13kg/m ² (Koschenz and Lehmann 2004))			
	Algae façade	[0.2236, 0.7636] W/m ² K (Cervera Sardá and Vicente 2016)	-	0.718-0.914 (Mertin et al. 2014)	0.04 (Chow et al. 2010) (Tinted Glass)	\$725-1116/m ² (Cervera Sardá and Vicente 2016)	-	-	
2	Exterior IEAD roof (climate zone 2-8)	[0.273, 0.283] W/m ² K	0.9	-	0.7				EnergyPlus simulation options
	Exterior metal roof	[0.312, 0.326] W/m ² K	0.9	-	0.6				
	Conventional roof	1.8 W/mK (Sun et al. 2013) 0.20 m (Sun et al. 2013)	0.9 (Sun et al. 2013)	-	0.93 (Sun et al. 2013)				
	Green roof	[0.124, 0.062, 0.023, 0.036, 0.026, 0.022, 0.014, 0.018] W/m ² K (Wong et al. 2003)	0.6 (Eumorfopoulou and Aravantinos 1998)	0.13(Eumorfopoulou and Aravantinos 1998)	0.95 (Sun et al. 2013)	\$112/m ² (Ascione et al. 2013)	-	-	Literature review
	Solar PV	Same as properties of solar PV on vertical envelopes							
Cool coated roof	0.591 W/m ² K (Mastrapostoli et al. 2014)	[0.0025, 0.0005, 0.01, 0.03] (Levinson et al. 2010)	-	0.9 (Shi and Zhang 2011; Synnefa et al. 2007)	\$22.3/m ² (Ascione et al. 2013)	-	-		

1: Vertical façade systems; 2: Roof systems; \$ = United States Dollar

4.1.3.3 Objective functions

An objective function was formulated based on multi-criteria of energy performance, environmental impacts, and economic aspects. Pareto optimality is presented for the MOO. Since the pareto front presents a set of solutions, the final decision will be made by a decision-maker (Fan and Xia 2017). In the MOO process, energy performance (F_{EP}), indoor thermal discomfort (F_{DC}), environmental impacts (F_{EN}), and economic effect (F_{EC}) are considered as a synthesized objective function (J) in the following equation:

$$J = \text{Min} \{F_{EP} + F_{DC} + F_{EN} + F_{EC}\} \text{ subject to } x. \quad (12)$$

where F_{EP} is the energy balance of the envelope, energy demands over energy generation;

F_{DC} is the predicted discomfort times;

F_{EN} is the environmental impacts of envelope represented by CO_2 emissions during life cycle; and

F_{EC} is the economic aspects of the year minimizing investment costs over the payback prices for 50 years.

4.2 Case Study of Retrofitting Building Envelopes for Residential Buildings in Kyojima, Japan

This section tests the proposed methodology in four residential buildings: two apartments and two wooden houses in North Sumida, Tokyo, Japan. This application conducts four steps: 1) describing input parameters and variables within the study area, 2) identifying uncertainties with parametric modeling and Bayesian multilevel modeling, 3) applying the MOO model, and 4) analyzing the results and findings.

4.2.1 Input parameters and variables

The study area is located in North Sumida, Tokyo, Japan (Figure 4.5). To consider the existing built form and context, 3D geometries of sample buildings and nearby buildings were extruded to represent their height by using a script built in Grasshopper plugged in Rhinoceros 3D. The buildings' 2D polygons and height features were obtained from 2D Shapefile (.shp) and dBASE file (.dbf) to project a geographic information system (GIS) platform. Existing building conditions (e.g., structure, built year), were collected by surveying the households. Building locations and height data were bought from an integrated geospatial system of Zenrin Co. Ltd.(ZENRIN CO. 2018), and building heights were extracted from the digital surface model with 0.5-meter resolutions. Internet of Things (IoT) sensors collected electricity demands every minute for four buildings, and the data was averaged over hourly demands to compare with parametric modeling results. Table 4 presents the overview of building information.

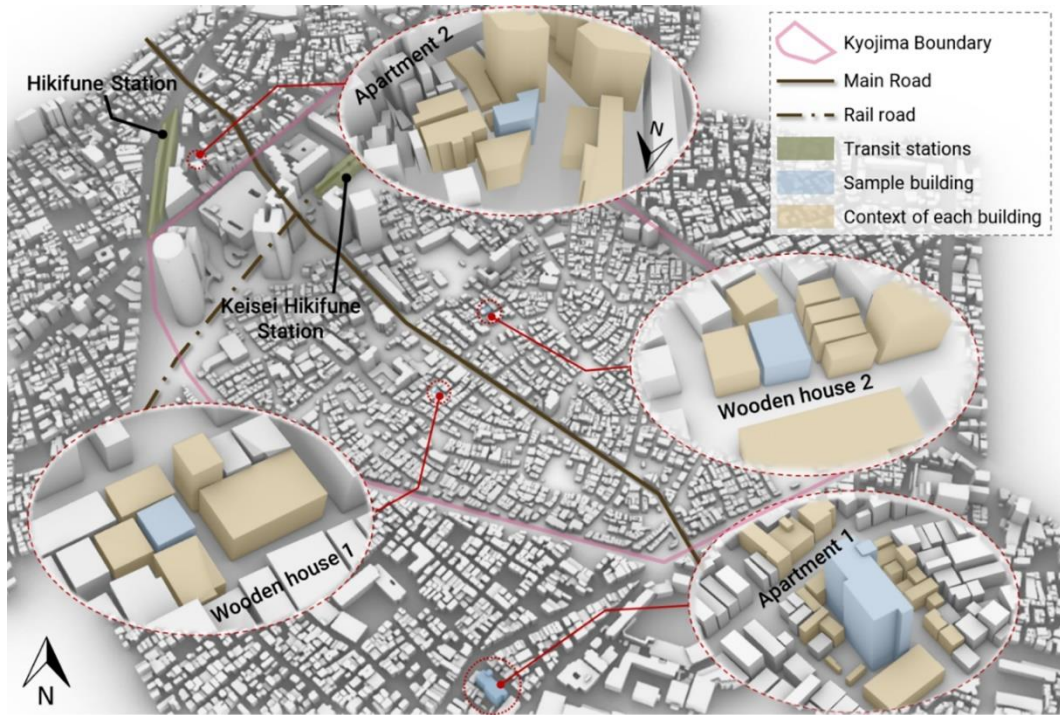

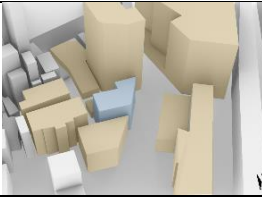
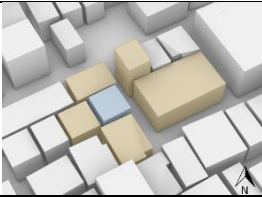



Figure 4.5 – Samples buildings and context in North Sumida, Tokyo, Japan

Table 4 – Overview of Building Information for Sample Buildings

	<i>Apartment 1</i>	<i>Apartment 2</i>	<i>Wooden House 1</i>	<i>Wooden House 2</i>
<i>3D Geometry</i>				
<i>Overview</i>	Age: March 1992 Floor: 12 Height: 34.17 meters Building structure: steel rebar Gross Square Area (GSA): 5,636.98m ²	Age: April 2004 Floor: 4 Height: 13.76 meters Building structure: steel rebar GSA: 467.03m ²	Age: Unknown (prior to 2000) Floor: 2 Height: 6.26 meters Building structure: wood GSA: 64.01m ²	Age: Unknown (prior to 2000) Floor: 2 Height: 6.02 meters Building structure: wood GSA: 103.34m ²

<i>IoT data collection</i>	<u>Collection</u> Location: 6 th Floor	<u>Collection</u> Location: 4 th Floor	<u>Collection</u> Location: 2 nd Floor	<u>Collection</u> Location: 2 nd Floor
	<u>Electricity demands</u> 7/24 13:24PM ~ 8/25 7:58AM	<u>Electricity demands</u> 8/6 18:06PM ~ 9/3 16:26PM	<u>Electricity demands</u> 7/29 11:55AM ~ 8/31 8:47AM	<u>Electricity demands</u> 7/29 10:48AM ~ 8/31 9:17AM

Building envelope options were applied to retrofit existing building envelopes, and current envelope conditions were used for the parametric modeling. Parameters for energy performance objectives, HDD and CDD, were extracted from April 1st, 2018 to April 1st, 2019 when heating degrees of 21°C and cooling degrees of 24°C. Total degree days were 2662.4 (HDD = 2309.9, CDD = 352.5) (BizEE Software 2019). HDD and CDD were detected at the closest weather station from the study area, which is located in 139.76E, 35.69N. Regarding the economic aspects, for the price of electricity, TEPCO, Tokyo Electric Power Company Holdings, charges currently about \$0.23/kWh (25.98 Japanese Yen) for electricity used in the 120 kWh -300kWh range (TEPCO (Tokyo Electric Power Company Holdings) 2016). According to the Bank of Japan (Bank of Japan 2019), the discount rate is 0.30%. Other parameters of economic objective function such as installation and maintenance costs were applied differently for individual options. The useful life of solar PV prolongs between 20 to 30 years, while solar thermal collectors have a lifetime of about 25 to 30 years (Varun et al. 2009b), and green walls mostly prolong more than 50 years (Perini et al. 2013). The optimization model is tested for T = 50 years.

4.2.2 *Uncertainty identification*

Based on the uncertainty identification framework presented in Figure 4.3, uncertain scenarios for solar irradiation are identified by using parametric modeling. The

outputs of energy predictions from parametric modeling are compared with IoT sensor data to determine uncertainties in building physical parameters and performance gaps in energy predictions. A statistical model using Bayesian multilevel modeling is used to identify uncertain impacts of physical parameters and uncertainties of energy predictions (Chang et al. 2019a; d). For this research, uncertainties in CO₂ emissions are directly applied to the MOO model by choosing the lifecycle CO₂ emissions from triangular distribution functions with lower and upper limits. The degradation rates for the envelope systems are randomly selected from the envelope datasets. The outdoor dry bulb temperatures used for calculating indoor thermal discomfort in equations 4 and 5 are randomly selected from the distributions of historical weather data.

4.2.2.1 Uncertainties in design and scenario parameters using parametric modeling

Parametric modeling simulates solar irradiation and building energy consumption by parameterizing building geometries and surrounding buildings to consider shading effects from other components of the buildings or surroundings. The annual average solar irradiation of each orientation is measured from the parametric modeling. The ranges and probability densities of the irradiation on each façade are projected to a triangular distribution and randomly chosen in the MOO model to apply uncertainties of scenarios placing the façade on a certain orientation.

Electricity uses are predicted based on EnergyPlus simulation developed by the U.S. Department of Energy (DOE). Rhinoceros 3D and Grasshopper plugin are used as a platform to model 3D geometry and use a graphical algorithm. Honeybee plugin for the Grasshopper is used to parameterize the subjected buildings into parametric building

components containing physical properties and indicate surrounding buildings as shading objects. The Honeybee tool provides applications to run EnergyPlus simulation (Chang et al. 2019b; Johnson et al. 1984). The electricity uses predicted by EnergyPlus simulation are compared with IoT measured electricity uses, and the probability density of performance gaps, subtracting predicted electricity uses from IoT-measured hourly electricity data is considered. The performance gaps are caused by the errors of predicting electricity uses and uncertainties of physical building parameters. These uncertainties are identified by using Bayesian multilevel modeling.

4.2.2.2 Bayesian multi-level modeling for uncertainty identification

Building envelope parameters influencing the retrofit problem are identified envelope area (m²) and thermal transmittance (U factors: W/m²K). Thermal transmittance is set to follow a normal distribution. Thermophysical properties cannot be exactly measured, even in the detailed models due to persisting randomness (Heo et al. 2012; Macdonald 2002). The standard deviation of uncertainties in thermal transmittance is estimated as 5% (Heo et al. 2012). By using the prior distributions, a Bayesian multilevel additive regression modeling is conducted to consider the errors from performance predictions and uncertainties of physical parameters in building envelopes. The following equation is built to estimate uncertainties as coefficients (β) and prediction errors as intercepts (ε).

$$y_{ij} = \sum_{k=1}^K x_{i,k} \beta_k + \varepsilon_{ij} \quad (13)$$

where i denotes the index of the measurement interval; y_{ij} is the explained variable (i.e., electricity consumptions detected by IoT sensors); $x_{ij,k}$ are regressors from predicted electricity uses analyzed by parametric modeling ($E_{demands}$ in Equation 1), u-value of the entire surfaces (U_{eq} in Equation 1), the total area of building envelopes (A in Equation 1), heating degree days (HDD in Equation 1), and cooling degree days (CDD in Equation 1) ($K=5$); β_k are the fixed regression coefficient including the fixed intercept; ε_i are the mean zero and unknown variance normally distributed disturbance. Table 5 summarizes the estimated coefficients and the intercept, and these are applied to the formula predicting thermal energy consumptions (Equation 1) as additional coefficients.

Table 5 – Estimated effects on uncertainty estimating thermal energy consumption

Effect	Variable	Estimated β (Mean, CI 95%, Significance*)
	Intercept ε_i	2.50 (2.39, 2.62) *
Linear fixed effects	Predicted electricity demands	0.07(0.05, 0.08) *
	U-factors of entire envelopes	-2.07(-2.19, -1.97) *
	Area of envelopes	-0.000012(-0.000016, -0.000009) *
	Heating Degree Days	0.08(0.05, 0.12) *
	Cooling Degree Days	0.00380(0.00025, 0.00736) *

CI: Confidence Interval

4.2.3 Application of multi-objective optimization model

Uncertainties are incorporated into the objective functions as additional coefficients or as an intercept. Decision variables are the area of envelope options for each face: south, north, west, east, and roof. 13 envelope options for the vertical façade and six options for the roof in Table 3 are tested. GA generates 401 sets of envelope options at the beginning, and tests 400 additional sets of population in every generation. GA selects parents

randomly and choose the best option to be a parent for the next generation. Tournament selection criteria is applied to choose the best option out of the set of all possible envelopes (Goldberg et al. 1989; Penna et al. 2015). GA then applies crossover and mutation into the selected parents to create the next generation. While crossover exchanges a part of genes of different chromosomes, mutation randomly alters genes within a chromosome (Goldberg et al. 1989; Penna et al. 2015). This research applies a fixed crossover rate of 0.8 (Penna et al. 2015). Since the optimization problem has a constraint not to exceed the total area of existing envelopes, an “adapt feasible” mutation criteria is applied, and it generates mutation directions randomly considering the last successful or unsuccessful generation (Mosavi et al. 2011; Shahandeh et al. 2015). The multi-objective GA function *gamultiobj* is used, and it uses three criteria to stop the solver. The solver stops if the maximum number of generations reaches 200*number of variables (i.e., the number of variables is the number of envelope options), if the average changes in the spread of the Pareto front over 100 is less than the function tolerance, or if the running time is limited. In other words, the algorithm halts: 1) when the solver tests enough populations, 2) when it can converge objectives or cannot obtain more diversity of population across iterative optimization solutions, or 3) when a designated time is spent. The time to run the solver is not limited in this research.

4.2.4 Case study results and findings

The MOO model calculates four objective functions by adjusting the application area of building envelope options given the constraints of the entire envelope area and the conditions of solar irradiation of each orientation. This model finds Pareto optimal sets of envelope options optimizing four objectives. The total number of Pareto optimal sets are

detected as 70, 70, 91, 98 for north, west, east, and south oriented envelopes respectively in Apartment 1. In Apartment 2, 61, 64, 96, 67 numbers of solution sets are detected for north, west, east, and south oriented envelopes respectively. In Wooden House 1, 78, 64, 80, 103 solutions are found for north, west, east, and south oriented envelopes respectively. In Wooden House 2, 72, 67, 83, 59 solutions for are identified for north, west, east, and south oriented envelopes respectively. For the roof, 100, 81, 67, 76 solutions are found in Apartment 1, Apartment2, Wooden House 1, and Wooden House 2 respectively. One set of solutions, showing a maximum retrofit area, for the east orientation is presented in Figure 4.6~4.7. One set of envelope options on the other orientations and roof is shown in Appendix A. The optimization results and objectives and one example of solution sets when deciding to retrofit the maximum area of envelopes out of sets of solutions.

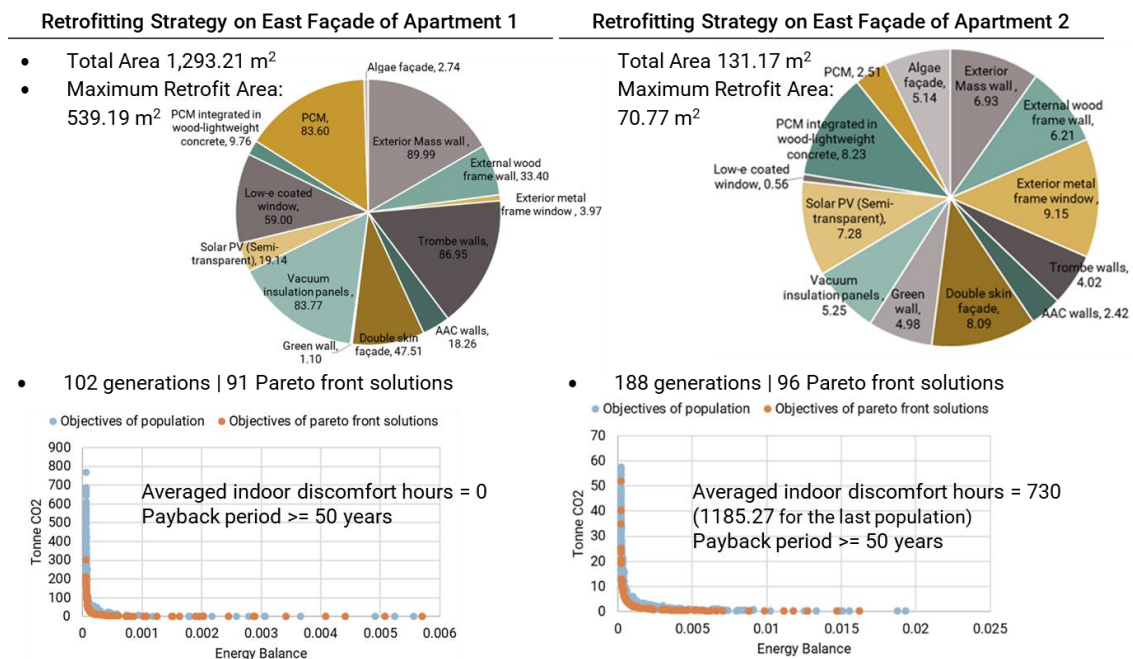


Figure 4.6 – One set of solutions for the east orientation in the apartment 1 (left) and the apartment 2 (right)

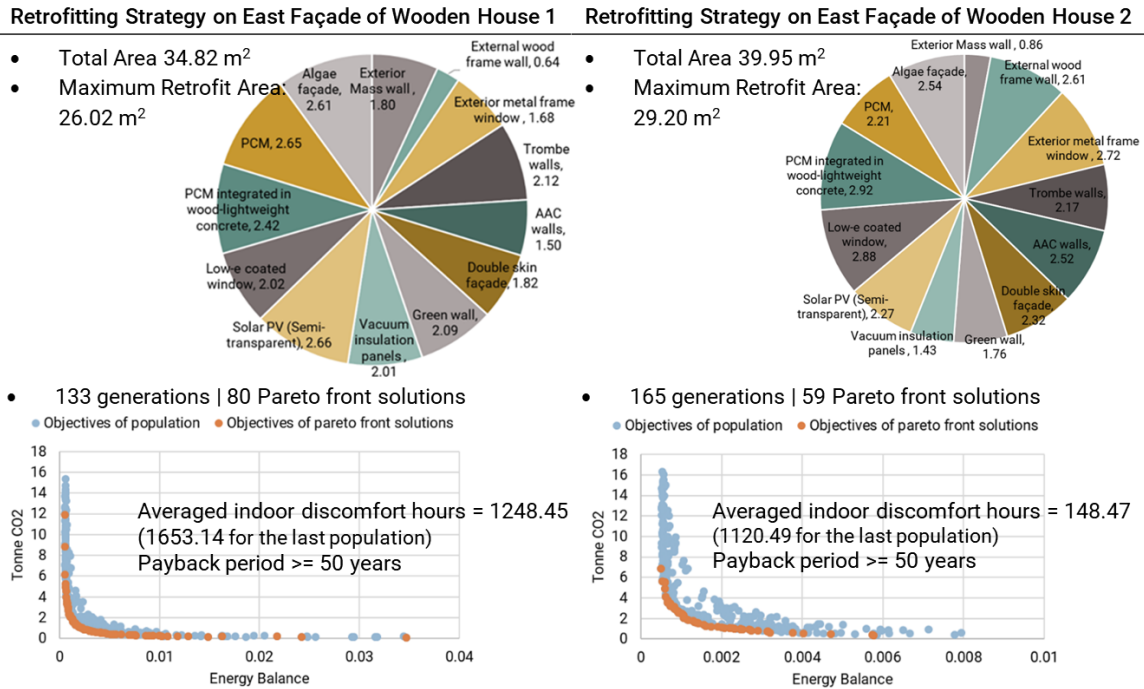


Figure 4.7 – One set of solutions for the east orientation in the wooden house 1 (left) and the wooden house 2 (right)

In Apartment 1, the maximum retrofit areas were 255.11m², 428.64m², 539.19m², and 269.33m² out of 578.97m², 1,303.43m², 1,293.12m², and 575.25m² in north, west, east, and south oriented façades. The roof area can be retrofitted about 367.65m² out of 501.70m² with six options. In Apartment 2, 66.43m² out of 123.05m² on the north façade, 67.90m² out of 151.96m² on the west façade, 70.77m² out of 131.17m² on the east façade, 72.86m² out of 189.37m² on the south façade can be retrofitted at maximum to optimize four objectives of energy, environment, indoor thermal comfort, and payback period. The roof area can be retrofitted 102.90m² out of 116.76m² at maximum. In Wooden House 1, 20.30m² out of 33.09m² on the north façade, 24.33m² out of 34.82m² on the west façade, 26.02m² out of 34.82m² on the east façade, 19.05m² out of 33.09m² on the south façade can be retrofitted at maximum. The roof can be retrofitted about 31.73m² out of 32.00m² at maximum. In Wooden House 2, 25.62m² out of 39.63m² on the north façade, 33.64m²

out of 46.19m² on the west façade, 31.69m² out of 47.42m² on the east façade, 29.20m² out of 39.95m² on the south façade can be retrofitted at maximum. The roof area can be retrofitted 51.51m² out of 51.67m² at maximum.

All solutions can achieve an energy balance of less than 1.0, which means that the energy required from thermal exchange via building envelopes can be satisfied by the energy generated from the envelope-integrated renewable technology systems. Case study can achieve at least 0.35 energy balance after retrofitting building envelopes. Pareto-front solutions can achieve less CO₂ emissions than all sets of envelope options. After retrofitting building envelopes with pareto-front solutions, CO₂ emissions of building envelopes are less than 300 ton per year and 60 ton per year for Apartment 1 and Apartment 2 respectively. For two Wooden Houses, after retrofitting building envelopes with pareto-front solutions, CO₂ emissions can be maintained as less than 30 ton a year. Across the solutions, the retrofitting applications into the south façade had the least impacts of CO₂ emissions.

In the north façade, green walls occupied the widest application out of 13 envelope options for Apartment 1 and Wooden House 2. The north façade in Apartment 2 can be retrofitted by solar PV at the most. In the north façade in Wooden House 1, all envelope options can be applied relatively evenly. In the west façade of Apartment 1, the exterior metal frame window can use up to 83.80m² of traditional materials as defined in ASHRAE 90.1-2010, but the disruptive technology of PCM is followed as the second option, occupying about 81.96 m². Vacuum insulation panels, double skin façade, and PCM integrated in wood-lightweight concrete were the most feasible applications in the west façade for Apartment 2, Wooden House 1, and Wooden House 2 respectively. In the east

façade of both apartments and Wooden House 2, the solutions depended on traditional materials such as exterior mass walls for Apartment 1, exterior metal frame windows for Apartment 2, and exterior mass wall and exterior metal frame windows for the Wooden House 2 as defined in ASHRAE 90.1-2010. On the other hand, in the east façade of Wooden House 1, the retrofitting area is mostly occupied by technical envelope materials or systems including PCM, solar PV, and algae façade. For retrofitting the south façade, AAC walls, low-e coated windows, double skin façade, and PCM integrated in wood-lightweight concrete can be applied at most areas for Apartment 1, Apartment 2, Wooden House 1, and Wooden House 2 respectively. For both apartments, the solution of retrofitting the roof determined that a cool-coated roof can be applied most broadly to minimize energy balance and CO₂ emission with zero discomfort time for 50 years. While the solution for Apartment 1 yielded that a green roof can be applied as the second area, solar PV roof can occupy the second area in the Apartment 2. For both wooden houses, the solution of retrofitting the roofs showed that each roof option can be applied evenly for about 16~17% of the roof area.

4.3 Chapter Conclusions

An optimization study for retrofitting building envelopes was conducted to determine the optimal sets of building envelope options. Functions of energy performance, indoor thermal discomfort, environmental impacts, and economic aspects were formulated using GA to obtain solutions minimizing four objectives. The GA model was tested in four residential buildings in Tokyo and solutions of retrofitting building envelopes were presented for each orientation. The results showed sets of building envelope options, and selected pareto-front solutions with maximum envelope retrofit areas. According to the

case study, at least 33% of vertical envelopes can be retrofitted for better performance (Figure 4.8). In addition, at least 73% of current rooftops can be retrofitted to achieve better performance of energy, environment, and comfort. The solutions vary by individual buildings and envelope orientations. However, the results can only be useful to renovate envelopes for the four buildings considered because the multi-objectives are highly influenced by weather conditions and the surrounding context (e.g., shading effects). For example, Salehi et al. (2019) have shown that comfort times during a year can vary based upon different climate regions (Salehi et al. 2019). Moreover, since the renovations are not actually realized, the results cannot be validated yet without actual renovation data.

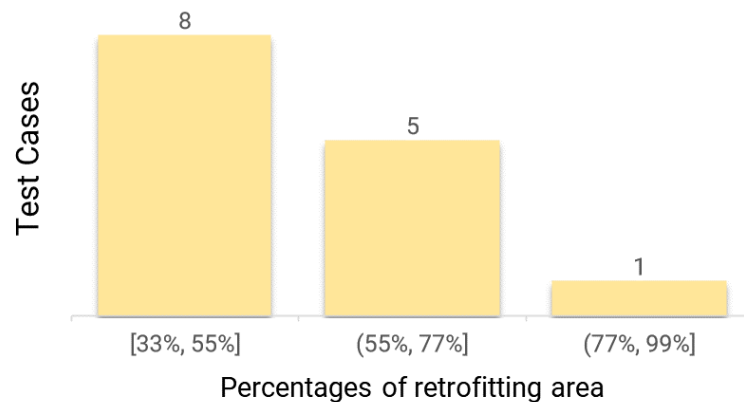


Figure 4.8 – Histogram of retrofitting ratio

Although the results should be further validated with practitioners' perspectives, the modeling process can be partially validated in that the energy predictions were compared with actual data collected through IoT. The approach expanded the utilization of IoT sensor data and provided an uncertainty consideration without burdening energy demand prediction in EnergyPlus simulation. Still, the GA model cannot be fully validated because it is heuristic estimation and the model did not have initial population. Whenever we run the model, the model will show slightly different solutions, and experts need to select the

final option to retrofit. The proposed methodology can become robust by obtaining reliable and practical data of envelope options. Any newly developed envelope materials or systems can be incorporated in the decision-making process as their parameters are provided. A spreadsheet containing envelope options was imported in the optimization model in MATLAB, and the initial options can be modified by a database of envelopes provided by decision-makers. For example, when decision makers intend to determine a window-wall ratio, they can incorporate two options of windows and walls as the envelope options. When they develop or envision an ideal disruptive envelope system, it can be easily written in the spreadsheet and tested in the optimization model. This can support adaptable decision-making in the construction industry by enabling building managers to re-assess the performance of envelope options whenever technology is developed.

After running the MOO model, sets of envelope options were solved to support the decisions for retrofitting building envelopes. However, since the data related to costs has not been fully studied to determine installation cost, maintenance cost and tax benefits, the results show that the payback period cannot be achieved until 50 years of investment for the envelope retrofit solutions. This research has a limitation that there are missing data among envelope parameters. To improve the economic feasibility of envelope retrofit options, research in this field should continue to define and reduce the investment cost of each envelope option. Also, since the envelope retrofitting algorithm was not specified to determine the relative location on each surface, the angle factors determining the mean radiant temperature could not be detailed. Although the solar thermal collector was incorporated in the objective functions, the thermal and solar parameters of this technology could not be found as envelope options. The solutions extracted from the GA model also

presented several sets of envelope options, and the sets should be re-evaluated by decision-makers through subjective judgement. However, the optimization model can consider the decision-makers' interest if they can provide a comparable and quantitative weights across the objectives.

The proposed system can change the paradigm of designing building envelopes, engineering new envelope materials and systems, and innovating re-construction process by evaluating envelope options synthetically. This research envisions that building envelopes can be dynamically transformed along with the development of materials and manufacturing systems in the future. However, the decision-support model should be further reviewed by users and tested with actual renovation projects for validation. Assumptions of envelope option parameters, cost data, and uncertainty considerations can be specified with industry participation. Tests of different regional condition can be also required to generalize the usefulness of the optimization model and the validity of applying diverse envelope options. To promote the paradigm change, design tools and objects should support designers when considering various envelope options synthetically. Also, constructability of retrofitting buildings with various envelopes should be further discussed.

CHAPTER 5. REORGANIZING BUILDING TOPOLOGICAL AND TYPOLOGICAL PARAMETERS ON A BLOCK

This chapter studies block-level building transformation strategies for improving energy efficiency, thermal comfort and visibility performance using bayesian multilevel additive modeling (Chang et al. 2019e, 2020c). Urban form can represent a physical shape of a city, a set of adapted spaces, a system of accessing and transacting, a changing system over time, or a pattern of spatial clustering (Blau et al. 1983). The attributes in urban form: size, density, urban grain, and shape (Lynch 1995), vary by city. Urban form contains a number of components related to the energy performance (Quan et al. 2016). Based on the components and the way people design the pattern of components, a physical density that influences energy consumption can also be measured differently by diverse methods such as population density, floor area ratio (FAR), dwelling unit density, and coverage (Chen et al. 2017; MIT 2011; Quan et al. 2014). The physical densities formed by building typologies can represent geometries of urban form and influence energy performance (Quan et al. 2016). In this respect, buildings are a key determinant of energy dynamics. Building energy consumption is influenced by building density, shape, and typology of the urban context (Quan et al. 2014). Beyond energy consumption, urban block form influences multiple performance indicators of each block including solar access, ventilation, etc. (Sanaieian et al. 2014). For example, layouts of buildings in a block have been studied to understand impacts on multiple performance indicators such as cooling loads and ventilation effects (Javanroodi et al. 2018) or energy balance and sky exposure (Chang et al. 2019c).

Since urban block forms formulated by buildings are interrelated with multiple performance indicators, this chapter addresses a question: How buildings in urban blocks can be changed in order to achieve multiple performance of energy demand, potential PV supply, thermal comfort, and sky view factor? This chapter aims to investigate the relationships among building topological and typological parameters in blocks and multiple block performance to support decisions about reorganizing urban buildings in a block (Chang et al. 2019e). Possible combinations of buildings in a block for energy security and efficiency, thermal comfort, and sky exposure are explored. To achieve the objective, four research tasks are devised: 1) establishing a research methodology, 2) identifying multiple performance indicators in a block, 3) applying the research framework to a case study providing existing building topological and typological parameters, and 4) identifying buildings transformation strategies in a block.

5.1 Approach for Supporting Decisions about Building Typology Transformation

Figure 5.1 shows the research methodology for integrating parametric modeling and statistical modeling. Parametric modeling evaluates three urban building performance indicators: energy demand, thermal comfort, and solar harvesting potential. Based on current topological building parameters, a statistical approach is used to identify relationships between the urban building typology and the respective performance. Considering the solar irradiation of a building with surrounding buildings in the same block, this research identified complex overshadow effects on the site. Bayesian multilevel additive modeling identifies significant variables and detects their impacts on the urban performance indicators. Bayesian multilevel additive modeling has been conducted to compute population effects and group effects of the influential parameters, as well as to

determine non-linearity of them in a certain confidential range (Bürkner 2017). Hence, population effects mean usual regression coefficients. Group effects mean category-wise random constant coefficients to consider different intercept of categories such as building structures and land uses. The Bayesian multilevel additive modeling enables us to validate the posterior deviations of parameters (Nagel and Sudret 2016). This statistical modeling has been conducted through “brms” package in R programming language (Chang et al. 2019d). The results of statistical approaches are used to observe trade-offs among the performance indicators. By recognizing performance variations along with changes in urban buildings typologies, this research established strategies to reorganize the building typology or the combinations of topological parameters in a block.

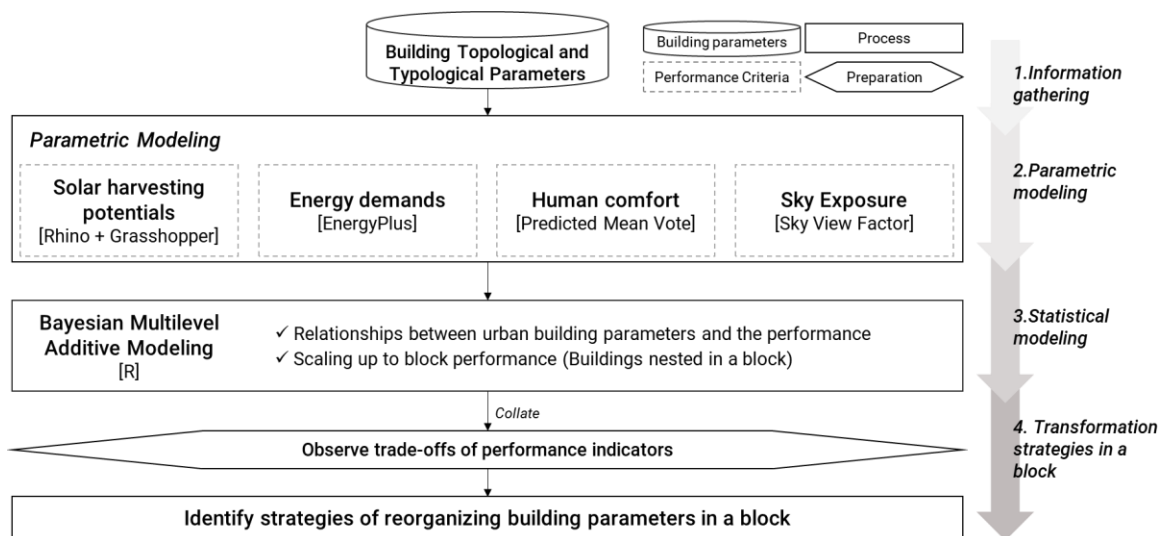


Figure 5.1 – Research methodology for building typology transformation in blocks

Parametric modeling using Rhinoceros 3D and Grasshopper plugin is implemented (Chang et al. 2019b; c). Ladybug plugin for Grasshopper is used to run solar irradiation analysis considering building envelopes of roof and vertical walls with shading effects from nearby buildings. Honeybee plugin for Grasshopper simulates EnergyPlus for

analyzing hourly building energy demands. A method for measuring thermal comfort was developed as Predicted Mean Vote (PMV) and Predicted Percentage of Dissatisfied (PPD) levels in the 1970s (Fanger 1970). Predicted Mean Vote (PMV) represents a thermal comfort of a large population (Magnier and Haghightat 2010). PMV index has been adopted dominantly to measure thermal comfort as an ISO standard by seven scales ranging from -3 (cold) to +3 (hot); cold (-3 PMV), cool (-2), slightly cool (-1), neutral (0), slightly warm (+1), warm (+2), and hot (+3). PMV is a function of air temperature, mean radiant temperature, relative air velocity, air humidity, activity level, and the clothing insulation (Fanger 1970; Yang et al. 2014a). While buildings expected to have high levels of comfort should feature PMV values close to 0 or within ± 0.2 (Frohner and Bánhidi 2007; Hwang and Shu 2011), ± 0.5 PMV values are likely for both new buildings and renovations expected to have a normal level of comfort (European Committee for Standardization (CEN) 2007; Matsui 2018; De Oliveira et al. 2011). PPD and thermally comfortable hours are determined by calculating the PMV index [85], and the indoor environment can achieve about 10% thermal discomfort within ± 0.5 PMV (Wei et al. 2010; Yang et al. 2014a). By estimating the indoor built environment using EnergyPlus engine, a PMV (Predicted Mean Vote) calculator in Ladybug plugin was used to determine the percentages of thermal comfort hours annually. In this research, three measures are evaluated as urban building performance indicators: building energy demand, percentage of indoor thermal comfort, and solar irradiation of building envelopes.

Bayesian multilevel additive modeling is used to consider population effects of building typology parameters as well as group effects of them (Bürkner 2017). Building topological and typological parameters are used to estimate the impacts of multiple

performance. Topological parameters indicate properties of building geometry, and typological parameters can be classifiers of building types as categorical variables. The Bayesian approach can consider uncertainties by providing confidential intervals of regression coefficients and estimating the posterior distributions of parameters (Chang et al. 2019d).

5.2 Case Study of Transforming Building Typology: Kyojima, Tokyo, Japan

5.2.1 Study Area

A superblock in Kyojima 1-chome, Sumida-ward, Tokyo, Japan is composed of 46 blocks and 870 buildings. As presented in Figure 5.2, blocks vary by existing pedestrian street paths and how buildings are organized.

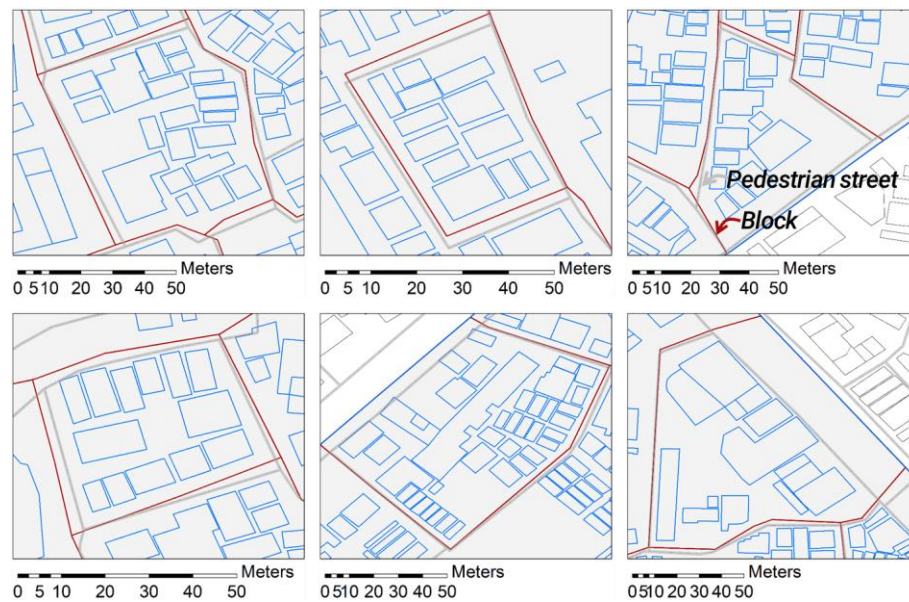


Figure 5.2 – Diversity of building topological and typological parameters in blocks

5.2.2 *Parametric Modelling Results*

Parametric modeling inputs consist of building topology (i.e., building space consisting of topological parameters such as floor area, height, etc.), building structure (e.g., wood, concrete, steel), and building land use (e.g., residential, office, commercial, mixed, special). All window-wall ratios in buildings are assumed to be fixed values of 40% facing north, 25% facing east, and 20% facing south and west. This enables us to compare energy demands of building typologies under controlling building parameters rather than typology alone. Predicted annual building energy demands are presented in Figure 5.3. Based on the energy required to set certain indoor environments (the setpoint of cooling is 23.9°C and the setpoint of heating is 21.1°C), the thermal comfort is calculated using PMV metrics. The percentage of comfort time is indicated in Figure 5.4. As the solar irradiation is influenced by the surrounding context, the solar irradiations on block façades (see Figure 5.5. left) is averaged and projected in Figure 5.5 (right). Sky exposure is analyzed using Ladybug plugin as influencing thermal environment as well as constraining visibility (Figure 5.6).

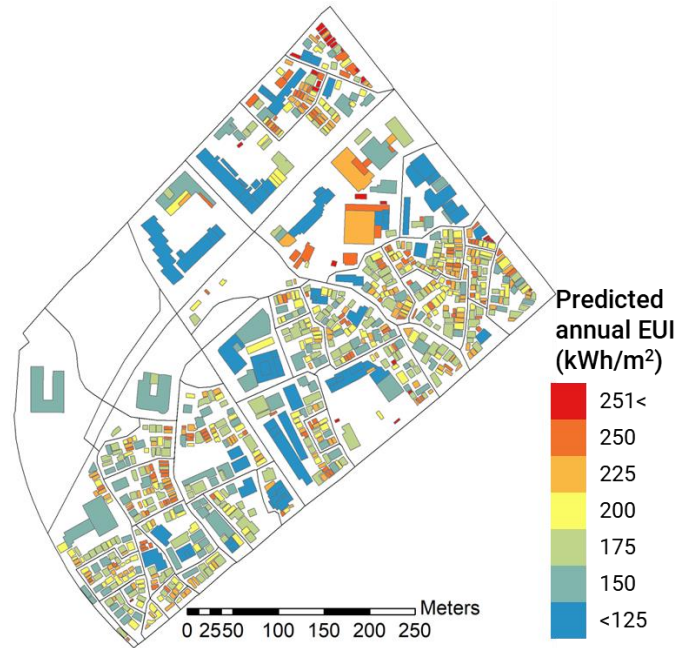


Figure 5.3 – Predicted annual average energy demands using EnergyPlus (kWh/m²)

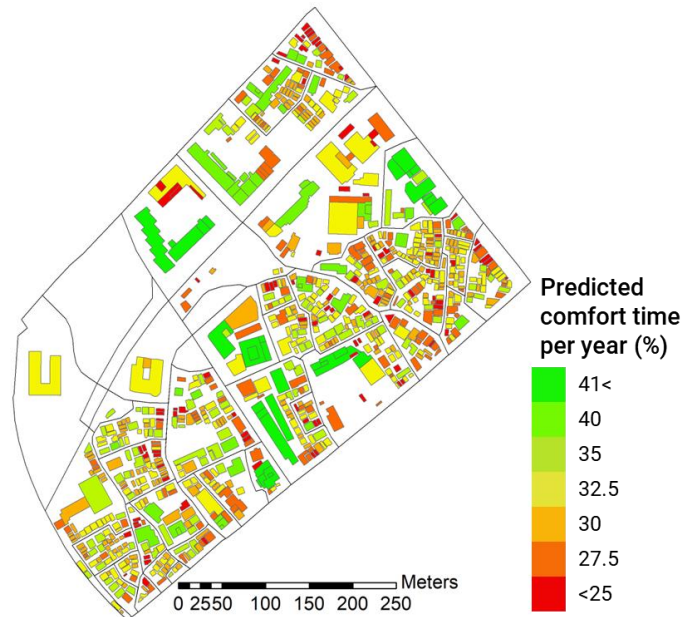


Figure 5.4 – Predicted percentage of comfort hours per year (%)

indicators of energy use intensity, solar irradiation potential, thermal comfort, and sky exposure are considered. After the generalized collinearity test, the dimensions are reduced. The relationships between urban building parameters and performance indicators are then described by implementing a Bayesian multilevel additive modeling.

Rise type is categorized based on the building height. Building height is measured from the ground level, with each story measuring 4 meters. Six rise types are identified: Single tory (1 story), low rise (2 to 7), mid rise (8 to 20), high rise (21 to 130), super high rise (130 to 200), and mega high rise (200 or more). Land use variables are simplified into five types: office, residential, commercial, retail, and mixed. This variable classification takes in into account whether buildings are single or mixed use.

5.2.3.1 Generalized collinearity diagnostics

To recognize the impacts on reliable estimation, the collinearity of coefficients of variables was measured by generalizing the concept of variance inflation (Fox and Monette 1992). An unweighted linear model was formed using regressors and responses. By identifying generalized collinearity, the variables linearly related to each other are eliminated to form a Bayesian multilevel additive modeling. The package “car” in R programming language is used to calculate generalized variance-inflation factors (GVIF) that represent collinearity among regressors (Fox and Monette 1992). DF is the number of coefficients As rule of thumb, the cut-off values of VIF are five or ten to assess the collinearity as strong (Craney and Surles 2007; O’Brien 2007). This research assumed ten as the cut-off value, and the cut-off values for GVIF are calculated by collecting ten with

the number of degrees of freedom (df). Parameters presenting GVIF that exceed the cut-off values are removed from the Bayesian multilevel additive model.

According to generalized collinearity tests, variables in use for block-level performance evaluation have been diagnosed to not include redundant parameters. Height, floor area ratio, and coverage ratio are considered as building topological parameters in a block. Land use, rise type, structure, and use are considered as typology parameters.

Table 6 – Generalized collinearity diagnostics

Predictors \ Responses	VIF	DF	GVIF (VIF^{1/(2*DF)})	Cut-off value for GVIF (10^{1/(2*DF)})	Removed?
Height	1.377303	1	1.173586	3.162278	
Floor Area Ratio	6.696539	1	2.587767	3.162278	
Coverage Ratio	3.683716	1	1.919301	3.162278	
Land Use	2.536916	4	1.12341	1.333521	
Rise Type	1.628583	3	1.08468	1.467799	
Structure	1.707341	2	1.143089	1.778279	
Use	2.127839	1	1.458711	3.162278	
Percentages of households (HH)	28.72606	1	5.359669	3.162278	X
Percentages of office (OF)	36.52032	1	6.043204	3.162278	X
Percentages of vacancies (VA)	649.2415	1	25.48022	3.162278	X
Percentages of others (OT)	343.377	1	18.53043	3.162278	X
HH*OF	13.42696	1	3.664281	3.162278	X
HH*VA	475.2843	1	21.80102	3.162278	X
OF*VA	432.1607	1	20.78848	3.162278	X
HH*OT	433.245	1	20.81454	3.162278	X
OF*OT	891.5852	1	29.85942	3.162278	X
VA*OT	2001.008	1	44.73263	3.162278	X
HH*OF*VA	108.57	1	10.41969	3.162278	X
HH*OF*OT	724.7518	1	26.92121	3.162278	X
HH*VA*OT	1928.125	1	43.91043	3.162278	X
OF*VA*OT	1816.509	1	42.62053	3.162278	X
HH*OF*VA*OT	1373.43	1	37.05981	3.162278	X

5.2.3.2 Bayesian multilevel additive modeling

Package ‘brms’ is used in R programming language to conduct Bayesian multilevel modeling using stan. Subsets of performance indicators are treated by each block to analyze block-level performance. Four models estimating energy demands, solar potential, thermal comfort, and sky exposure were estimated via the Markov-chain-Monte-Carlo method using the No-U-Turn Sampler (NUTS) implemented in Stan and R *brms* package (Bürkner 2017). The NUTS method allows setting parameters automatically thus eliminating the need for any hand-tuning (Hoffman and Gelman 2014). To decrease divergent transitions that can cause biases of posterior samples, the adapt delta, a tuning parameter of the NUTS sampler, was increased to 0.99. Also, the maximum tree depth that is evaluated at each iteration is increased to 15.

The statistical inferences of the parameters in the model are based on four chains, each with 2000 iterations, of which the first 1000 are warm-up to calibrate the sampler as the burn-in period. Total post-warmup samples are 4000. The convergence of the all coefficients in the Bayesian model was checked by identifying \hat{R} values that are 1 or less than 1.05 (Gelman and Rubin 1992).

In the Bayesian model, this research assumed non-linear population effects for continuous variables (e.g., height, floor area ratio, coverage ratio), and linear group effects for categorical variables (e.g., structure, rise type, land use, use). As an assumed example on non-linearity, the influence of floor area ratio on energy demands may be different between wooden and concrete structures.

$$y_{ij} = \sum_{j=1}^J \alpha_j + \sum_{q=1}^Q f_q(z_{ij,q}) + \varepsilon_{ij} \quad (14)$$

where i denotes the index of the measurement interval; j denotes number of group effects of the measurement ($J=4$); y_{ij} is the explained variable; α_j is the random intercept for group effects of structure, land use, rise type, or use (single or mixed), and is assumed to come from a normally distribution with mean zero and unknown variance; $z_{i,q}$ are the regressors from height, floor area ratio, and coverage ratio ($Q=3$) whose impact on y_i are possibly non-linear; $f_q(\cdot)$ are the smoothing spline function as which we used the bivariate tensor spline function recently developed by Wood et al. (2013) for modeling the non-linear impact (Wood et al. 2013), ε_{ij} are the mean zero and unknown variance normally distributed disturbance.

Table 7 shows the estimated mean of posterior distributions for population-level parameters and the estimated standard deviation of posterior distributions for group-level parameters. Also, confidence intervals of standard deviations of estimated coefficients for coverage ratio, floor area ratio, and height are used to form the smoothing splines for non-linear effects (Bürkner 2018). For population-level parameters, the significance of effects is evaluated as to whether the lower and upper 95 percentile confidence intervals do not include zero. According to the results, non-linear populations effects of coverage ratio and floor area ratio significantly influence all performance indicators in blocks. To evaluate the significance of group effects, coefficients of group effects are visualized and evaluated as to whether the coefficients are not zero with 95% percentile confidence. Land use is

significantly influencing energy demand, thermal comfort, and sky exposure. Rise type significantly influences thermal comfort.

While the coverage ratio influences positively energy demands and sky exposure statistically, it has negative impacts on solar potential and thermal comfort. On the other hand, floor area ratio will impact positively the solar potential and thermal comfort, but energy demand and sky exposure will be negatively influenced by the floor area ratio. In addition, group-level effects influence the deviation of multiple performance.

Table 7 – Relationships between urban building performance indicators and building topological and typology parameters

Responses		Energy demands	Solar potential	Thermal comfort	Sky exposure
Effects	Predictors	Estimates (95% CI)			
Non-linear population effect	Coverage ratio [S.d.]	35875.01(1831.39, 82904.40)* [8950.01(3776.00, 17838.24)]	-7322.24 (-11477.48, -3294.62)* [2771.01 (1746.91,4515.71)]	-221.13 (-297.01, -144.54)* [51.21 (29.34,87.42)]	21.47 (16.28, 26.66)* [4.42 (2.58,7.75)]
	Floor area ratio [S.d.]	-183223.47(-350716.84, -56007.29)* [98712.78(56959.11, 166229.76)]	19074.31 (3594.72, 36047.23)* [7048.89 (3743.59,12632.76)]	944.59 (597.84, 1276.75)* [243.34 (139.77,396.29)]	-80.57 (-103.09, -58.65)* [24.23 (15.30,38.04)]
	Height [S.d.]	-8437.07(-32037.11, 7421.12) [4541.37(594.08, 11724.59)]	-8.96(-550.67,418.88) [68.94 (2.17,225.16)]	-2.13(-18.74,8.44) [2.48 (0.07,9.00)]	-0.04(-1.15,1.45) [0.27 (0.01,1.04)]
Linear Group effect	Land Use	642.87(158.19,1742.35)*	15.10(0.54,55.39)	1.23(0.47,3.10)*	0.04(0.00,0.12)*
	Rise Type	583.32(20.47,2402.99)	36.68(1.23,122.92)	3.82(0.77,11.03)*	0.63(0.16,2.30)
	Structure	367.86(8.38,1980.01)	19.21(0.38,87.36)	0.70(0.01,4.16)	0.21(0.02,1.24)
	Use	1116.64(29.28,4698.76)	33.97(0.56,151.08)	4.51(0.57,17.03)	1.60(0.00,11.12)

*: Significance; S.d: Standard deviation

According to the results of Bayesian multilevel additive modeling for each performance indicator and building topological and typological parameters in Table 7,

plots for significant non-linear population effects are presented in Figure 5.7 ~ 5.8. The non-linearity is detected from the results. Any increase in the building coverage ratio in blocks, energy demand and sky exposure are predicted to be reduced. On the other hand, the solar potential and thermal comfort tend to decrease. Interestingly, the non-linear influence of coverage ratio on sky exposure and thermal comfort are saturated around 0.3% and 0.2%, respectively. The height of buildings is not statistically significant to the performance, and its effects are presented in Appendix C. Although it is not significant, the tendency of changing performance can still be observed. When floor area ratio (FAR) increases, predicted energy demands decrease. This finding is also aligned with the finding from previous research conducted by Rodriguez-Alvarez (Rodríguez-Álvarez 2016). By increasing FAR, sky exposure tends to decrease while the solar potential and thermal comfort tend to increase. And also, the non-linear influence of floor area ratio on the three indicators are saturated around 50%.

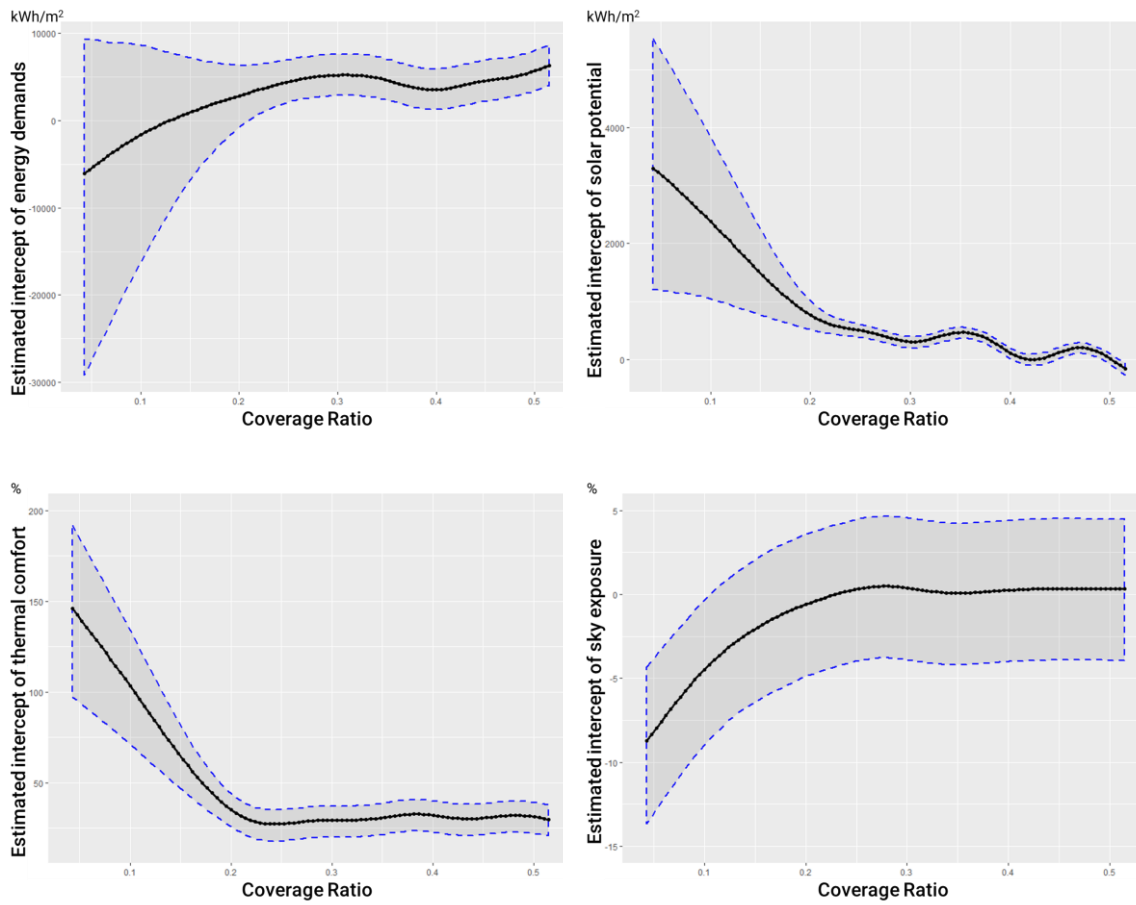


Figure 5.7 – Non-linear population effects of coverage ratio (y coordinates: average energy unit intensity (top-left), solar potential (top-right), average percentages of comfort time (bottom-left), and sky exposure (bottom-right))

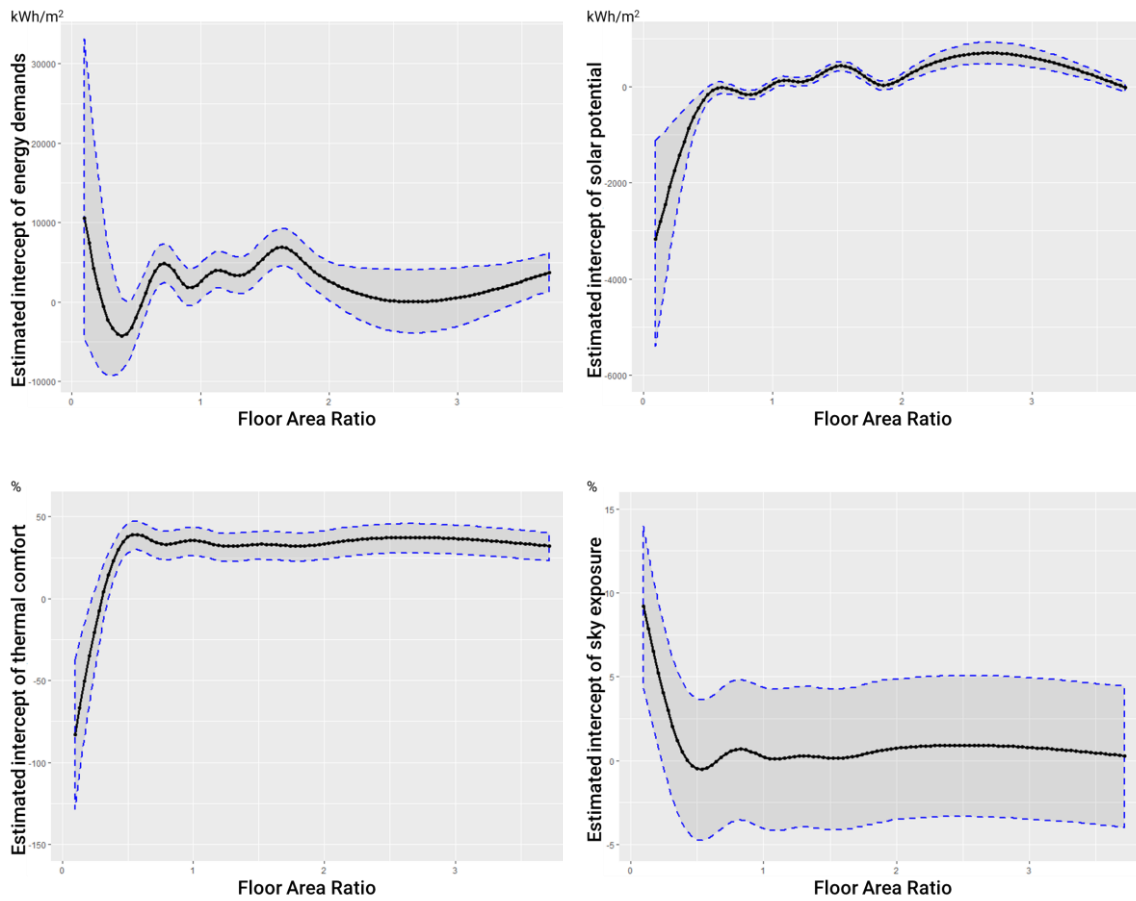


Figure 5.8 – Non-linear population effects of floor area ratio (y coordinates: average energy unit intensity (top-left), solar potential (top-right), average percentages of comfort time (bottom-left), and sky exposure (bottom-right))

According to group-level effects in Table 7, effects of land use on energy demand, thermal comfort, and sky exposure are presented in Figure 5.9 ~ 5.11. Significant impacts of rise type on thermal comfort are presented in Figure 5.12.

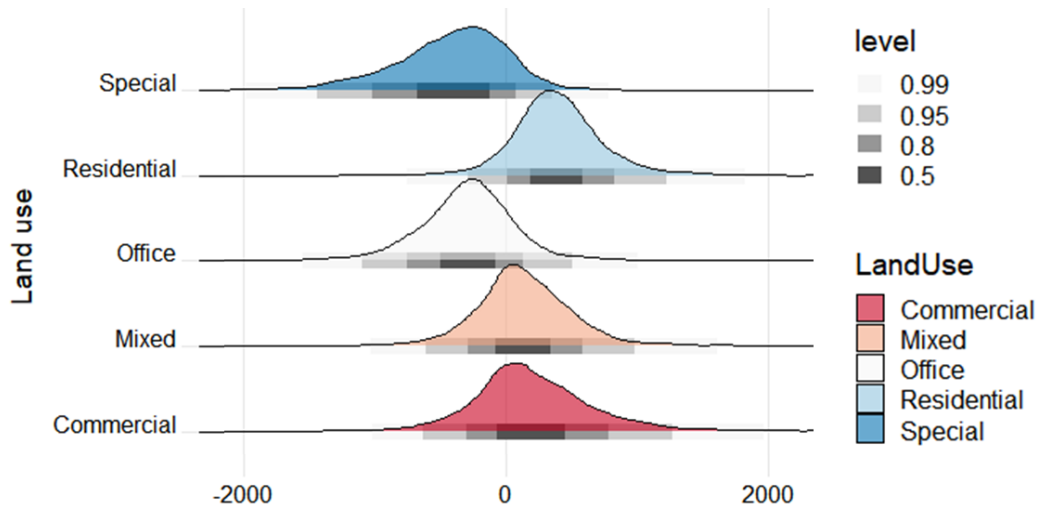


Figure 5.9 – Density estimations of impacts on intercept of energy demands by land use

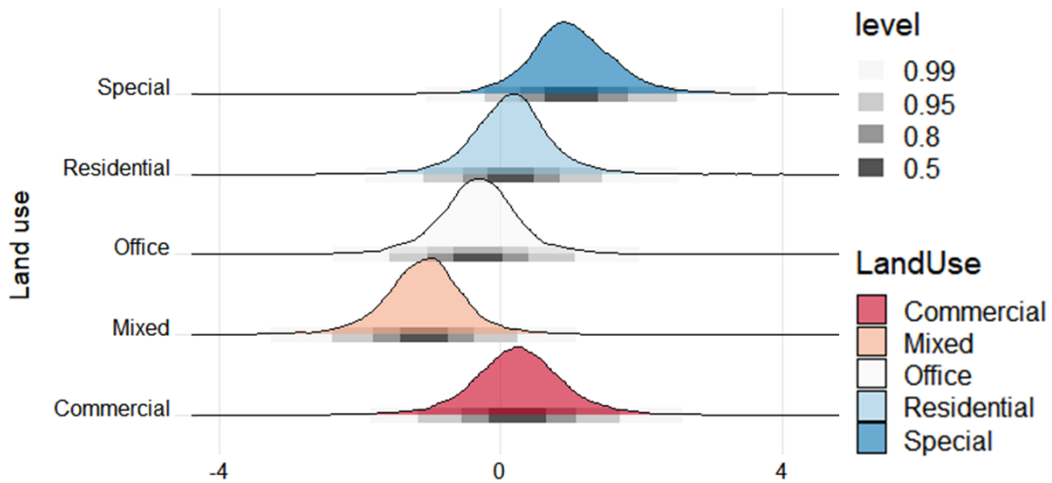


Figure 5.10 – Density estimations of impacts on intercept of thermal comfort by land use

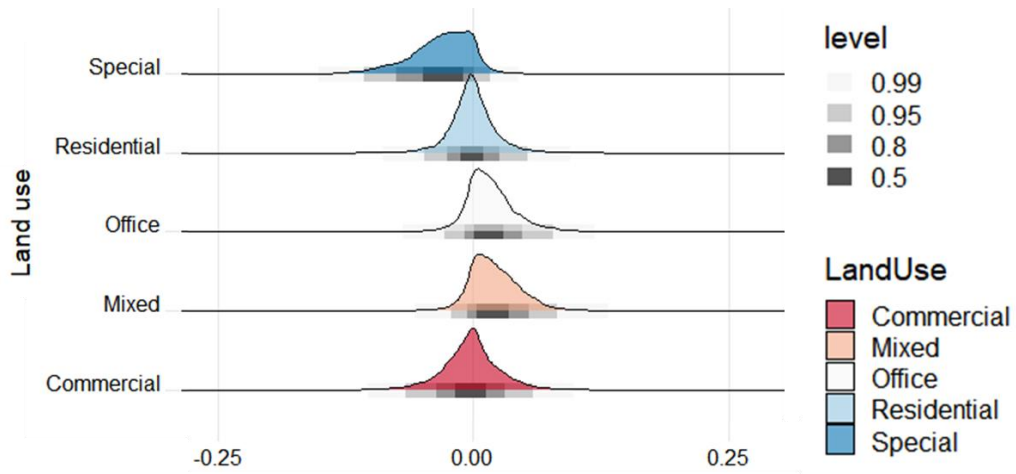


Figure 5.11 – Density estimations of impacts on intercept of sky exposure by land use

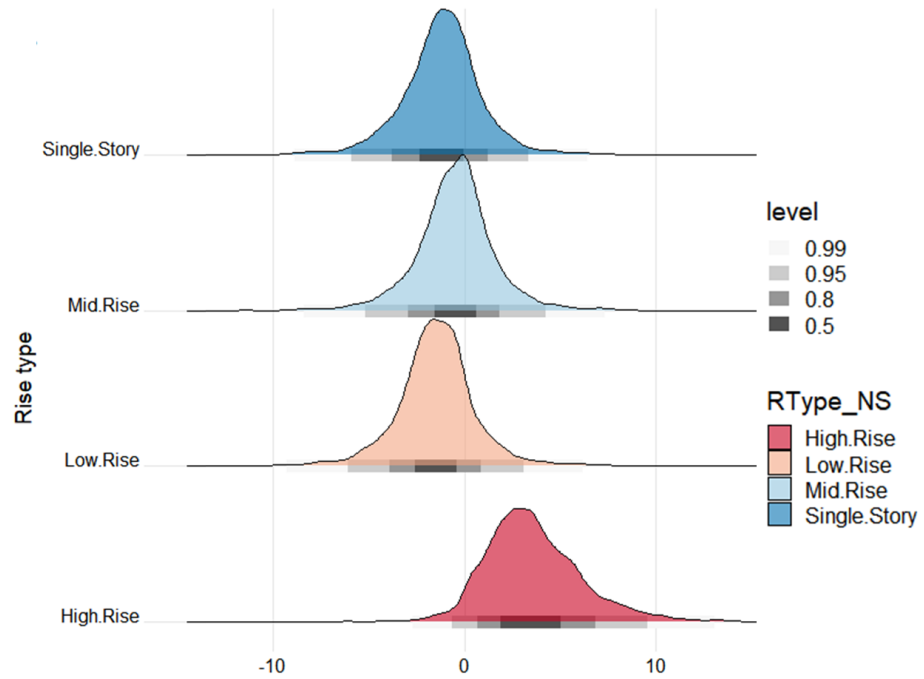


Figure 5.12 – Density estimations of impacts on intercept of thermal comfort by rise type

5.3 Performance Predictions of Building Typologies

Based on the effects of the building parameters, this section reconsiders the potential combinations of building typology in a block to increase solar potential, thermal comfort, and sky exposure while reducing energy demands.

By reducing building coverage ratio, energy performance (i.e., energy demand / supply) can be improved in a block. However, it will correspond to reduce thermal comfort as well as sky exposure. Increasing FAR will provide better energy performance and thermal comfort while losing visibility in a block. Similar impacts of FAR on energy consumption can be observed in previous research (Quan et al. 2014). While the coverage ratio has been discovered as negatively influencing energy performance (Quan et al. 2014), the results in this chapter provides more complex relationships by assuming non-linearity. Coverage ratio around 0.3 and FAR around 0.5 were observed as inflection points where directions of parameters' influences are changed, and trade-offs among performance indicators are changed. Group effects of structure are difficult to be observed because their standard deviations are relatively small. Special land use in blocks tend to provide better energy performance and thermal comfort. Special, residential, and commercial land use in blocks are better to harvest solar power. Office and mixed land use in blocks are better for increasing visibility. High-rise buildings in a block are better for reducing average annual energy demand and improving thermal comfort and sky exposure. Mid-rise buildings in a block harvest solar power better than other rise types. Mixed use buildings provide better thermal comfort environment with less energy demand. The deviations of solar potential and sky exposure are difficult to be observed at a different use category.

Overall, multiple performance in a block level cannot be synthetically achieved given building topological and typological parameters. Based on needs of a certain performance while undermining several other performances indicators, four transformation strategies can be extrapolated.

- 1) Energy performance and comfort improvement while undermining visibility:
Increasing FAR with high-rise buildings of mixed-use purpose on special land use zone.
- 2) Maximization of harvesting solar power while undermining thermal comfort:
Increasing coverage ratio with mid-rise buildings in special, residential, commercial zones.
- 3) Improvement of visibility: reducing coverage ratio and FAR and placing high-rise buildings in office or mix land use zones.
- 4) Improvement of thermal comfort: reducing coverage ratio and increasing FAR by placing high-rise buildings in special and commercial land use zones.

5.4 Chapter Conclusions

This chapter conducted a research to discern impacts of changing building topological parameters on block-level performance including energy performance, thermal comfort, and visibility. The results can contribute to recognizing changes in block performance along with changes in urban building parameters. The better understandings of transformations can support decisions of reorganizing building typologies to improve the performance in a block. By applying a Bayesian multilevel additive modeling, both population-level and group-level effects can be considered as well as linearity and non-

linearity can be considered. Also, since the influences of parameters are estimated in a certain confidential range, tendencies of parameters can be observed even if they are not significant. The impacts of transforming urban building parameters can provide building designers, owners, and managers to establish appropriate retrofit strategies to contribute to block-level performance. In addition, this will provide city planners or city government with potential impacts of retrofitting or redeveloping urban buildings. Then, this information can guide to establishing new category of urban buildings to manage performance-based planning of blocks. However, in that different climate zones may contain different properties, generalizability should be further explored by sufficiently testing the methodology in different communities.

CHAPTER 6. BLOCK BOUNDARIES FOR SHARING ELECTRICITY AMONG BUILDINGS ON A COMMUNITY

The concept of sharing energy within a community was studied to address dynamic energy distribution in urban areas considering buildings and future energy demands of electric vehicles (Chang et al. 2020b; Murakami and Yamagata 2017). This dissertation research focuses on dynamic energy demands and supply of buildings on a community. To alleviate the high-energy demands in urban areas, city-integrated renewable energy including solar, geothermal, wind, and biomass energy has been promoted to substitute current energy generation sources (Kammen and Sunter 2016). Applications of solar photovoltaic (PV) integrated in buildings have been presented one of promising solutions reducing CO₂ emission while producing energy required for building operations (Quan et al. 2015b). Integration of solar PV in buildings decentralize sources of electricity into existing building stocks. Multiple sources and demands have developed the concept of multi-microgrids to integrate them within an existing distribution network (Nunna and Srinivasan 2017). Multi-microgrids can be applied within the same energy network to reduce electricity losses and environmental emissions from the typical distribution grid (Anastasiadis et al. 2010; Bullich-Massagué et al. 2018). To implement microgrids that are groups of interconnected loads and resources decentralized in urban areas, electric boundaries should be clearly defined (Ton and Smith 2012). Boundaries for each microgrid should be designed to minimize the energy imbalance (Nunna and Srinivasan 2017). Several operational boundaries should be adaptable with optimizing power distribution among the multi-microgrids (Wu et al. 2018).

The changes of energy distributions in a community reclaim a research question: how can block size and boundaries be changed by clustering buildings to support an energy sharing architecture? This chapter investigates new block boundaries to support for configuring microgrids that can balance energy uses and generations of buildings integrated solar PV. The objective is to establish the optimized framework of identifying block boundaries for sharing electricity in urban areas when solar energy generation in buildings and hourly electricity demand and supply are collected. This research then explores clustering based Voronoi diagram algorithm to detect clusters that can share electricity among buildings and to identify boundaries among the clusters. Community clustering algorithm can identify self-sufficient subgraphs (Yamagata et al. 2016). By applying the algorithm, this research identifies self-sufficient subgroups of buildings by partitioning the groups to minimize imbalance of energy demand and supply. Voronoi polygons have been used to calculate spatial characteristics such as building coverage ratio beyond parcel geometries, and the method can be used to determine regions belonging to a certain building (Löwe et al. 2019). Voronoi spatial model can handle relationships among spatial components in neighborhood dynamically (Shi and Pang 2000). In this respect, the Voronoi diagram can be applicable to identify boundaries and regions of microgrids where buildings can share electricity each other. The framework is tested to existing buildings in Kyojima 1, North Sumida, Tokyo, Japan. This research can provide electricity sharing boundaries that can be adapted flexibly considering changes in hourly energy demands and supply. This electricity sharing framework will contribute to providing accessible and reliable energy systems.

6.1 Approach for Identifying Electricity Sharing Boundaries

This chapter proposes to apply clustering based Voronoi diagram method to identify electricity sharing boundaries in urban areas that possess various types of electricity demands and supply from buildings (Figure 6.1). R programming language is employed to establish a framework of determining block boundaries. Packages in R built by statisticians and data scientists are used to conduct this research methodology. For example, “fnn” package is used for the fast k-nearest neighbor search algorithms (Beygelzimer et al. 2019), “igraph” package is used to detect community structure using edge betweenness (Csárdi and Nepusz 2006), and “ggvoronoi” is used to visually explore spatial localizations of a region (Garrett et al. 2018).

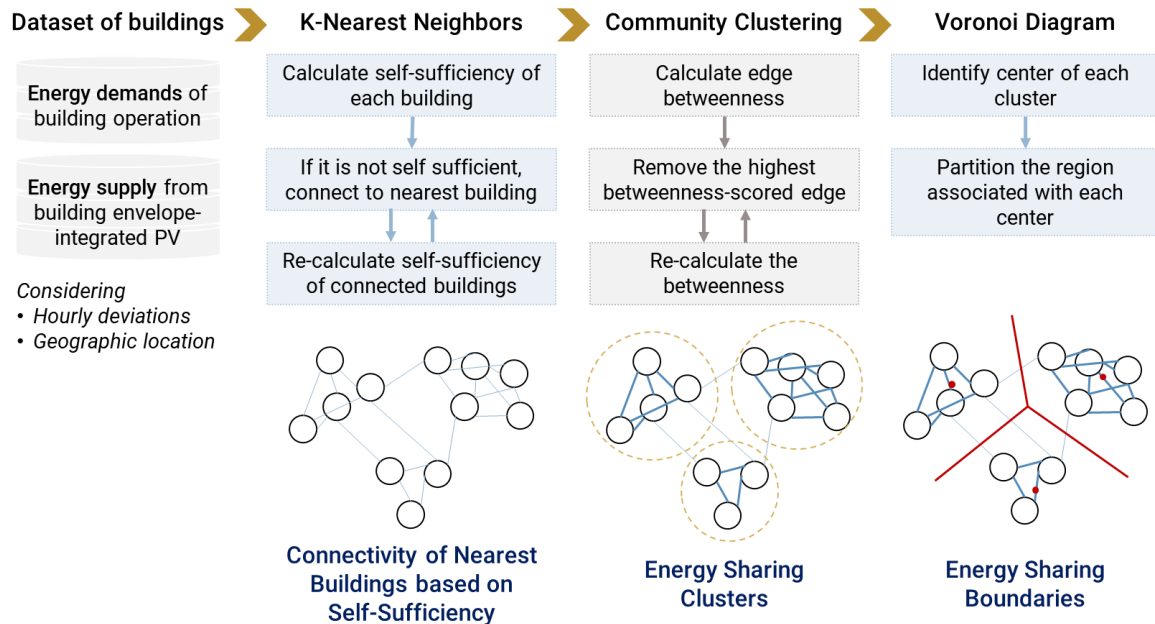


Figure 6.1 – Research methodology to identify block boundaries to support for sharing electricity among buildings (Chang et al. 2020b)

To minimize energy imbalance, the boundary conditions for balanced microgrid should satisfy as the Equation 15 (Wu et al. 2018):

$$P_{Dem}^{K(i)} \leq P_{Sup}^{K(i)} \quad (15)$$

where $P_{Dem}^{K(i)}$ is active energy intensity of the nearest $K(i)$ buildings to the i -th building energy use (kWh/m²), and $P_{Sup}^{K(i)}$ is the renewable energy supply capacity of the nearest $K(i)$ buildings to the i -th building (kWh/m²) (Murakami et al. 2019; Wu et al. 2018). The renewable energy supply capacity of each microgrid has been aggregated solar harvesting potential when PV is installed in building roofs. Block boundaries, where energy imbalance can be minimized, were evaluated by calculating self-sufficiency of spatial and temporal changes of energy demands and supply (Equation 16) (Murakami et al. 2019). Based on the self-sufficiency, buildings are connected to nearest buildings, and the network will be used to identify the block boundaries for sharing electricity.

$$\sum_{t=hour}^T S_{K(i),t} = \max \left(0, \sum_{t=hour}^T \sum_{k(i)}^{K(i)} (P_{Sup}^{k(i)} - P_{Dem,Building}^{k(i)}) \right) \quad (16)$$

Where t is hourly supply and demand, and this research considered time from $t=1$ to $T=24$. $S_{K(i),t}$ is the self-sufficiency of $K(i)$ buildings from i -th building at a certain time of the day. $k(i)$ is the k -th nearest building from the i -th building.

To identify the communities, edges connecting energy networks among buildings are removed iteratively using possible “betweenness” (Newman and Girvan 2004). Vertex and edge betweenness are calculated by the number of shortest paths (geodesics) going

through a vertex or an edge. Then, the clustering algorithm, calculating the edge betweenness, removing the edge having the highest betweenness scores, re-calculating the betweenness, and iterating this process to identify possible community boundaries. Edge betweenness means the number of shortest paths passing through the edge, and it represents how many travels that can be made over the edge for reaching to other nodes. Based on this definition, an example of edge betweenness scores is presented in Figure 6.2.

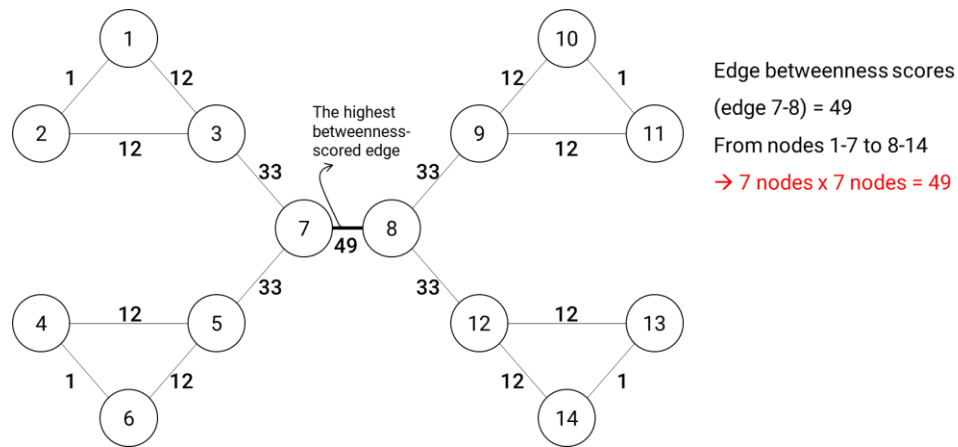


Figure 6.2 – An example of edge betweenness

The clustering method optimize the modularity measure Q:

$$Q = \sum_i (w_{ii} - a_i^2) = \text{Tr}(\mathbf{W}) - \|\mathbf{W}^2\| \quad (17)$$

where \mathbf{W} denotes a community network matrix. w_{ii} , the elements of \mathbf{W} , indicates the fraction of edges in the network connected vertices in the community. a_i , the sum of each i -th row elements of \mathbf{W} , denotes the expected value of the fraction in the same community when a network is randomly connected. $\text{Tr}(\cdot)$ means the trace operator, and $\|\cdot\|$ means the sum of all elements of the argument. Based on the optimal (maximum) modularity measure, we estimate \mathbf{W} matrix by dividing the network graph matrix which

we estimated to meet self-sufficiency for minimizing energy imbalance. If the random connectivity is better than the number of within-community edges, the modularity gets closer to 0. When the modularity Q is closer to 1, it is better to partition clusters (Newman and Girvan 2004). Based on the clusters of buildings, Voronoi regions, which are convex polygons sharing boundaries with surrounding Voronoi vertices, are identified as new block boundaries that can be basis of multi-microgrids.

6.2 Case Study of Reconfiguring Block Boundaries: Kyojima, Tokyo, Japan

The framework is tested to existing buildings in Kyojima 1, North Sumida, Tokyo, Japan. The site area is about 214,825m², there are 870 existing buildings, and 46 existing block boundaries. The scope of study area is presented in Figure 6.3. 870 buildings are considered to share electricity use and potential solar power in this community. Since a community's spatial span, which is defined based on an administrative super-block, is between 400 and 1,000 meters, buildings within the area can share same local climate zone (Stewart et al. 2012).

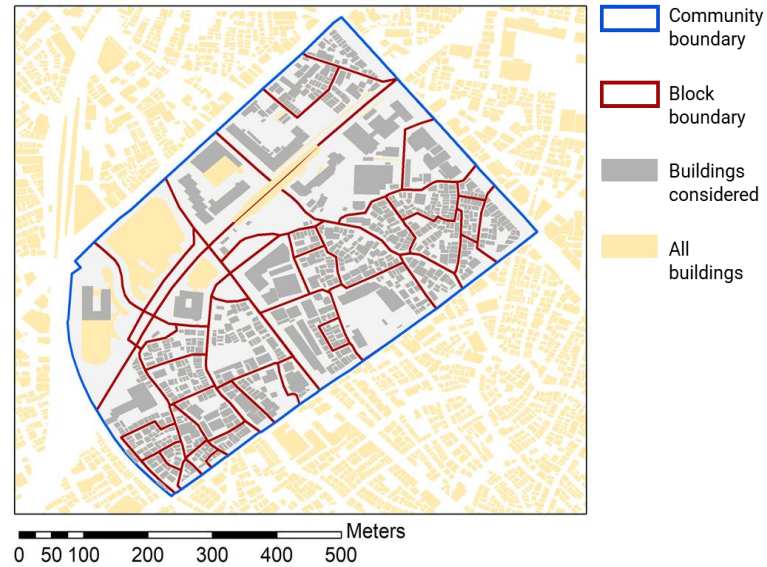


Figure 6.3 – Study area of a community scale

6.2.1 Data Acquisition

Building polygon, height, and land use data have been collected by Zenrin Co. Ltd. (ZENRIN CO. 2018), in GIS data format (.shp and .dbf), and the buildings are projected into 3D graphics in Rhinoceros 3D. Rhinoceros and Grasshopper plugin has been used to parameterize 3D polysurface of buildings into space or room requiring energy. Honeybee plugin for Grasshopper has been used to run EnergyPlus simulation. Solar harvesting potentials on rooftop of buildings are analyzed using ArcGIS Solar Radiation Tool. Hourly averaged annual solar harvesting potentials have been detected.

The process of acquiring hourly energy demands and supply is presented in Figure 6.4. Building energy demands were measured using EnergyPlus simulation engine, and heating loads, cooling loads, and electricity for lighting and equipment were produced. Since electricity is used for cooling in general, cooling, lighting, and equipment loads were aggregated to require electricity, and their hourly average electricity demands were

detected by creating a macro in Excel. To measure solar radiation on rooftops of buildings in a community, “Area Solar Radiation Tool” provided in ArcGIS 10.7 was used. This tool requires Raster format of topography (Quan et al. 2015b). This study provided buildings shapes and heights for radiation analysis.

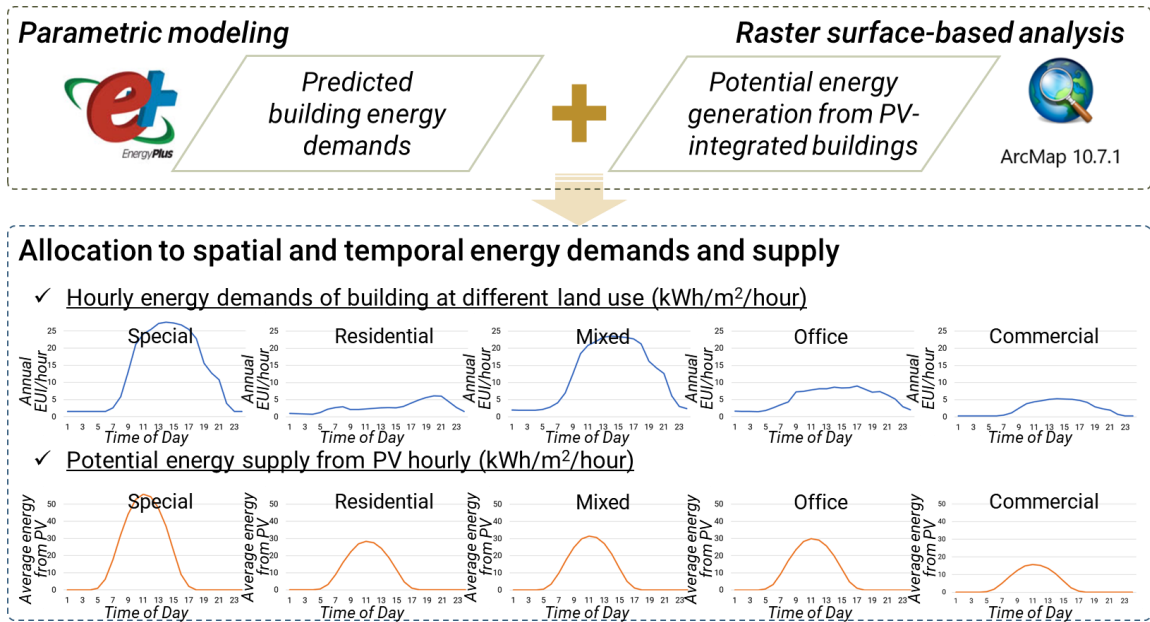


Figure 6.4 – Data acquisition for temporal energy supply and demand of buildings

Results of estimating hourly averaged electricity demands on 12PM and 6PM during a day are projected in Figure 6.5.

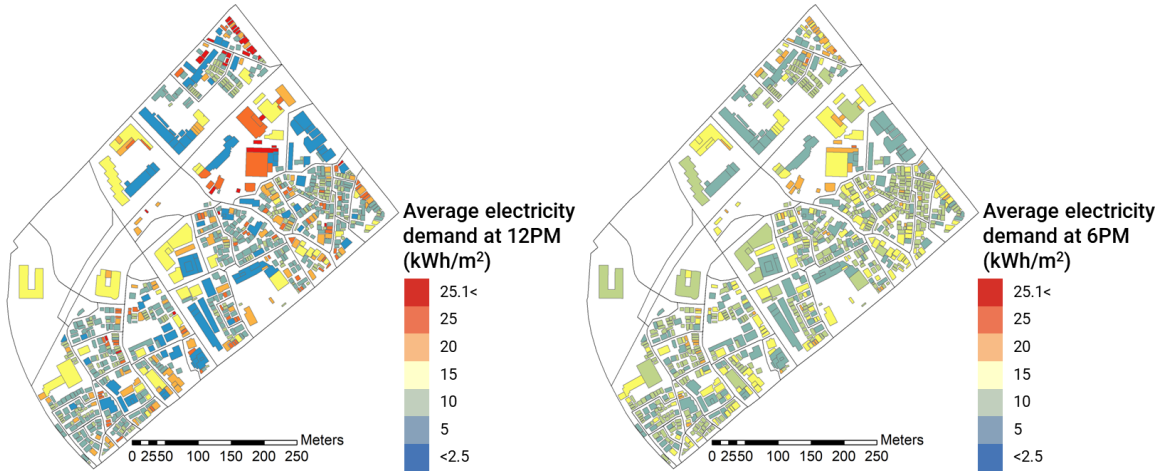


Figure 6.5 – Examples of hourly electricity demand: 12PM (left), and 6PM (right)

Solar irradiation on rooftops on buildings in the community is shown in Figure 6.6 (left), and total annual solar irradiation per unit rooftop area is also presented in Figure 6.6 (middle). From the solar irradiation, electricity energy generation of Solar PV was calculated using the Equation 2 in Chapter 4.

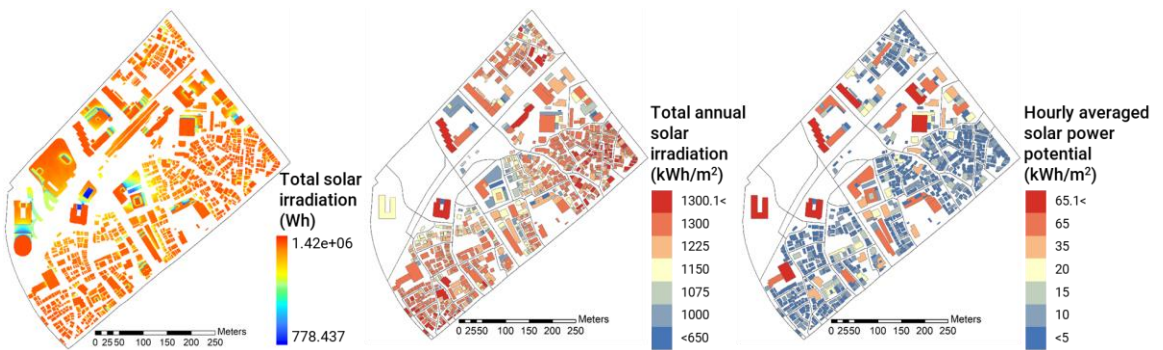


Figure 6.6 – Solar power generation potential: solar irradiation on rooftop (left), total annual solar irradiation (middle), and hourly averaged solar power (right)

6.2.2 Buildings' Connectivity

Based on the estimation of hourly electricity demand and potential solar supply, buildings can share electricity with nearby buildings to decentralize energy distribution networks in urban areas. To begin with, the connectivity for sharing energy among buildings has been detected by calculating biggest self-sufficiency among nearest buildings (Equation 16). Fast k-nearest neighbor searching algorithm was used to identify optimized networks of buildings to be able to share electricity. Figure 6.7 (Left) shows the connectivity for sharing electricity among nearest buildings considering demands and supply averaged for the 24 hours. Figure 6.7 (Right) presents the number of connected buildings that ranges from one to twelve.

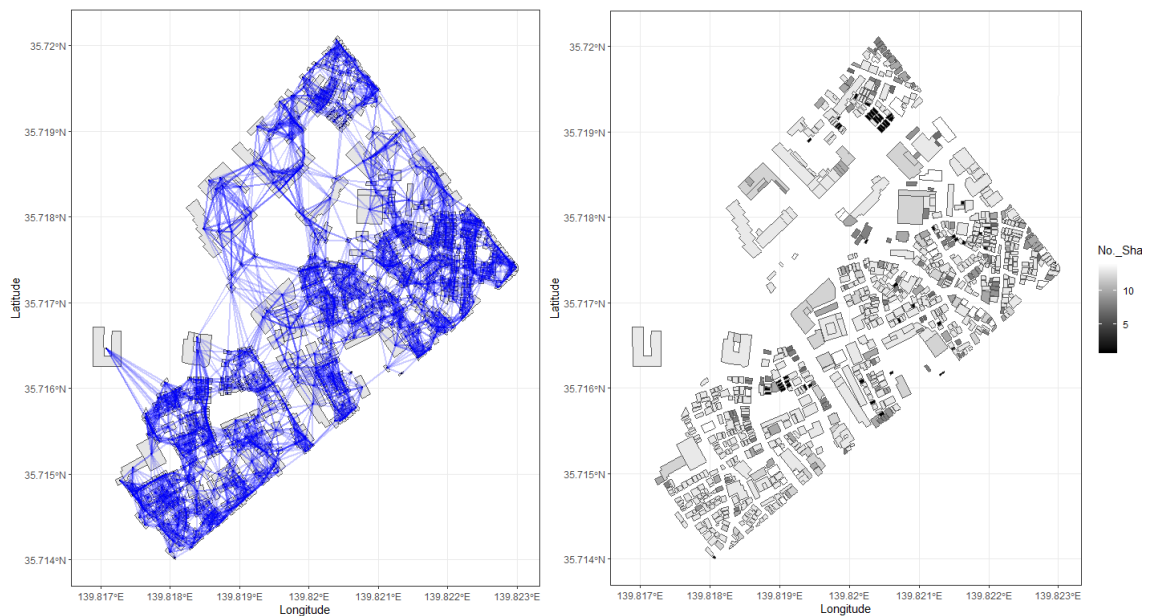


Figure 6.7 – Connectivity for sharing electricity among nearest buildings (Left); number of neighboring buildings for sharing energy (Right)

According to hourly demand and supply during the data (Figure 6.8), potential solar power supply can be maximized during 11AM ~1PM while estimated electricity demands were maximized during 5 ~ 7PM. Buildings' connectivity during those time periods are also estimated to observe temporal changes in sharing electricity.

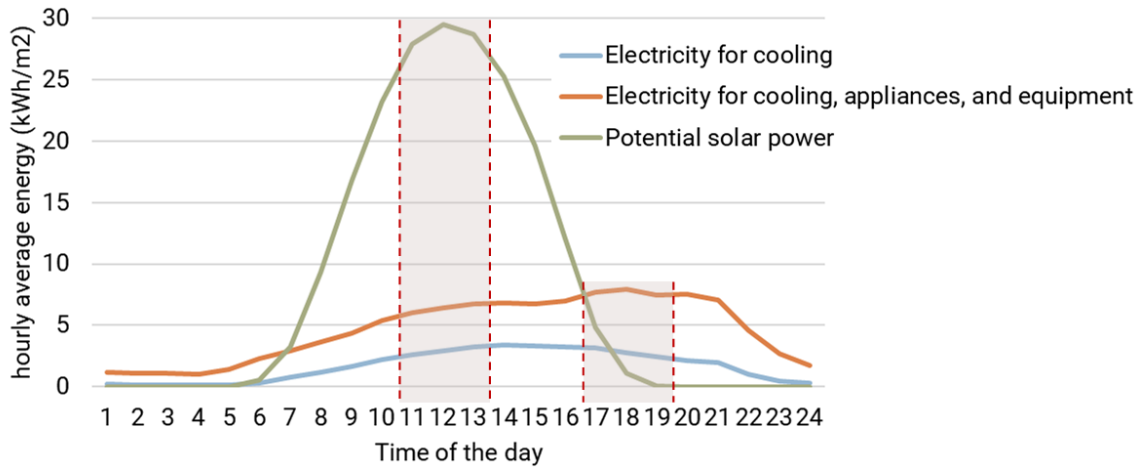


Figure 6.8 – Hourly demand and supply during the time of the day

During 11AM to 1PM, high potential solar power provided more connections than annual averaged connectivity. Also, while annual averaged networks offer 12 neighboring buildings at maximum, 36 buildings in the community can share electricity with 102 buildings surrounded that building during 11AM to 1PM. Figure 6.9 shows connectivity among buildings to share electricity during 11AM to 1PM when buildings can obtain maximum solar power potentially during the day.

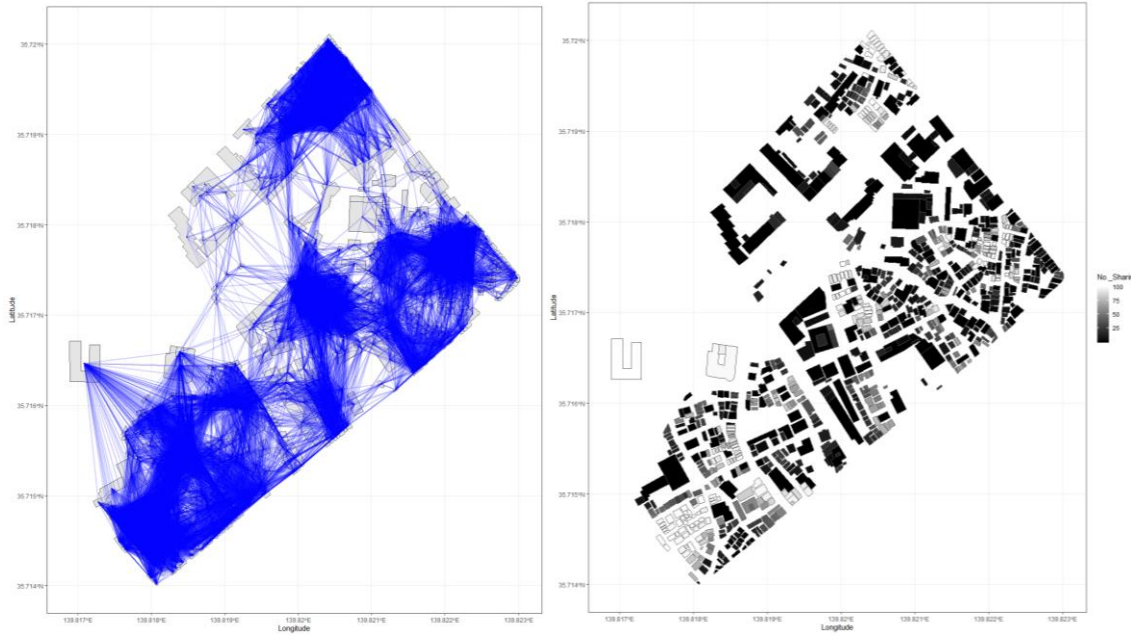


Figure 6.9 – Connectivity for sharing electricity among nearest buildings during 11AM ~ 1PM (Left); number of neighboring buildings for sharing electricity 11AM ~ 1PM (Right)

During 5PM to 7PM, only 58 buildings out of 870 can only share electricity. Among 58 connected buildings, 11 buildings can share electricity with four to nine buildings nearby. Seven buildings can share electricity with 12 to 16 buildings nearby. Eight buildings can share electricity more than 100 buildings surrounded them. The buildings' connectivity and numbers of buildings sharing electricity are presented in Figure 6.10. During the time, potential solar power becomes very low in overall. However, in the southwest part of the community, several office buildings' electricity demands decrease while the buildings can provide relatively higher solar potentials because of their higher height and broader roof area than surrounding buildings. Those several office buildings can be connected to surrounded small detected houses for sharing their electricity. Meanwhile, buildings in other parts of the community could not achieve either collective self-sufficiency or proximity of sharing electricity.

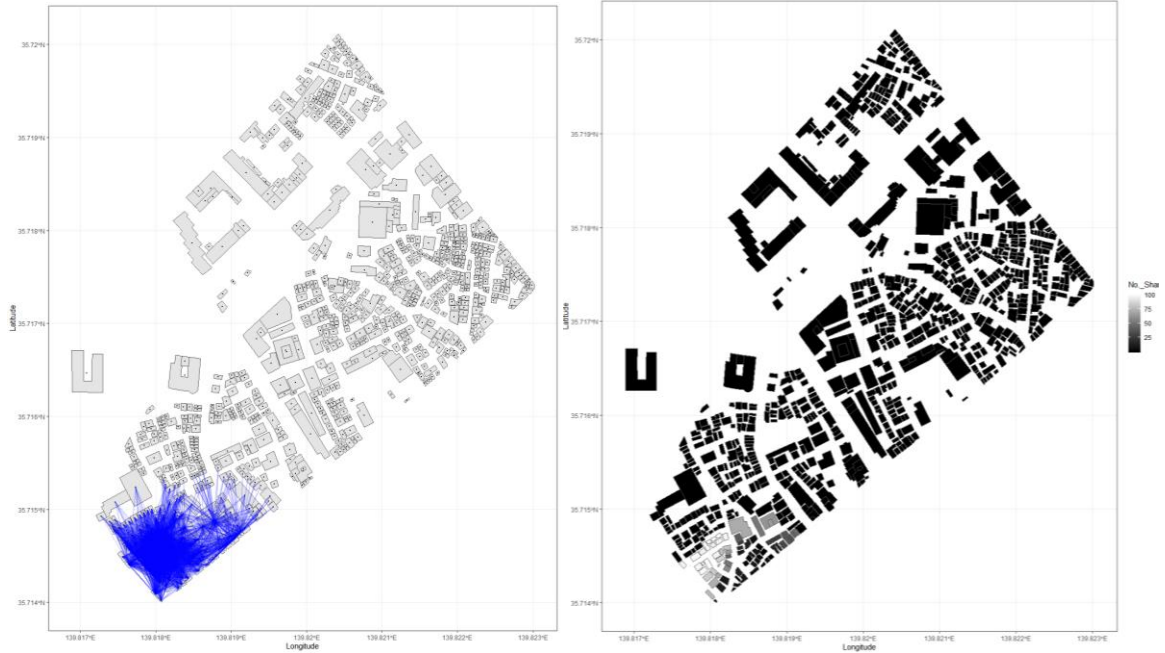


Figure 6.10 – Connectivity for sharing electricity among nearest buildings during 5 ~ 7PM (Left); number of neighboring buildings for sharing electricity 5 ~ 7PM (Right)

6.2.3 Block Boundaries to Share Electricity

This research then compares the connectivity and expected random connectivity measured by spatial nearest using the community clustering algorithm (Newman and Girvan 2004). The algorithm is based on the modularity as presented in the section 6.1 to decide the number of clusters to maximize the modularity. This community in the case study showed the estimate of Q was 0.8455926. In that the modularity which is higher than 0.7 is rare (Newman and Girvan 2004), blocks can be partitioned based on hourly averaged electricity during a year.

Based on the subgroups of buildings, Voronoi diagram algorithm is conducted to identify centroids of clusters of buildings and convex polygons representing block

boundaries. While current administrative block boundaries are 46, Voronoi diagram based on clustering identified 13 boundaries sharing electricity (see Figure 6.11).



Figure 6.11 – Current administrative block boundaries (Left); Clustering-based Voronoi diagram (Right)

During 11AM to 1PM, the modularity was 0.7204888, and the groups of buildings can be regrouped to 28 (Figure 6.12). However, during 5PM to 7PM, a majority of buildings cannot share electricity with nearby buildings because of the lack of potential solar power. The connectivity was correspondingly small, and the modularity was 0.1323828, The small modularity led to increase of the number of clusters to 708. In this trial, the clustering based Voronoi diagram cannot create block boundaries.

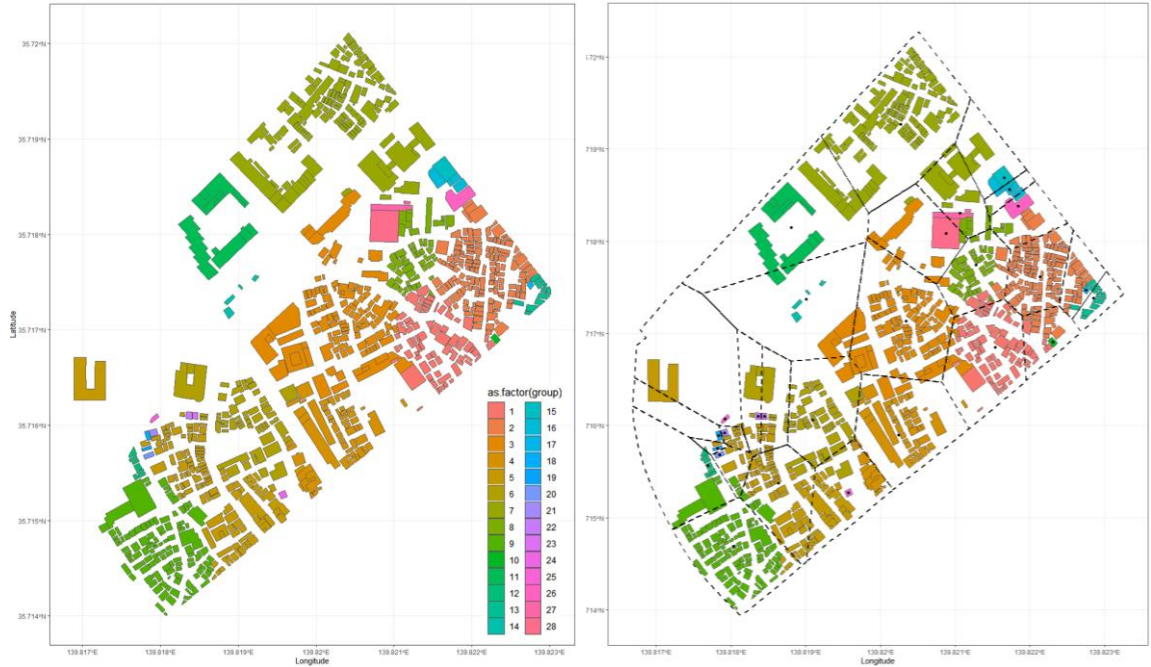


Figure 6.12 – Connectivity for sharing electricity among nearest buildings during 11AM ~ 1PM (Left); number of neighboring buildings for sharing electricity 11AM ~ 1PM (Right)

6.3 Chapter Conclusions

This chapter studied a methodology using energy performance analysis of buildings in a community, spatial statistics, machine learning techniques such as k-nearest neighbors, graph or network mining such as community clustering algorithm, and two-dimensional Euclidean distance calculations of Voronoi diagram. The research design was employed to determine block boundaries and size based on electricity self-sufficiency of buildings within the community in Kyojima, Tokyo, Japan. This chapter identified that there are changes in block boundaries and sizes whenever energy distributions in urban area are varied. The proposed block boundaries can be utilized for transaction boundaries to share electricity in the future when the micro-grids are adapted in the community. The boundaries can also be adapted to spatiotemporal distributions of solar power capacity and building

energy efficiency. In addition, the clusters of buildings and block boundaries can be employed for maintenance zones, site layout for planning redevelopment and construction, and guidelines of green community certifications. This algorithm can also be easily replicated in other built forms when geospatial data of energy demanding facilities and energy distributions are acquired. This algorithm can also be integrated with future mobility systems such as electric vehicles (EVs) (Chang et al. 2020b). Adopting EVs will provide more dynamic energy distributions in urban area by providing battery capacity or requiring charging stations. In this respect, energy demands of charging infrastructure can be added in this research framework. Also, when potential solar power gets lower from 7PM to 6AM, remained energy on EVs' battery can be discharged for powering buildings. In the future, Vehicle-to-Buildings-to-Grids will be able to be projected based on this research implementation.

CHAPTER 7. INTEGRATED DECISION SUPPORT FRAMEWORK FOR URBAN BUILDING TRNASFORMATIONS

This chapter delves into interrelationships among transformation strategies at multiple scales based on lessons learned from optimization and evaluation at each scale. Transformable parameters and their impacts on performance have been observed at each scale, and their relationships across scales are observed.

When reconfiguring block boundaries, temporal scopes projected different energy distributions spatially, and led to change number of buildings that can share electricity, building connectivity, number of clusters of buildings, and block boundaries and size. When reorganizing building typology on a block, building topological parameters of coverage ratio and FAR were common significant variables for multiple performance of energy demand, solar potential, thermal comfort, and visibility. Also, group effects deviated each performance in different standard deviations. When retrofitting building envelopes, building exterior area, orientations, and envelope options were given for optimizing sets of envelopes. Although the decisions at each scale are siloed, the inputs and outputs can be related across three scales. In this respect, this chapter observes interdependent relationships across building transformation decisions at multiple scales of community, block, and individual building.

7.1 Interrelated Parameters

At multiple scales, different concepts of transformation issues were discussed. On a community scale, in that buildings are endpoints of distributing electricity, block boundaries configured by sharing electricity among nearby buildings in a community were studied. On a block scale, in that buildings are nested in a block and determine multiple performance on a block level, building parameters within a block were analyzed to estimate the block performance. On an individual building scale, in that sets of building envelopes influence multiple performance of buildings, an optimization approach was conducted to evaluate collective performance of diverse envelop options. By reviewing methodological inputs and outputs of each scale (Table 8), parameters that can potentially be interrelated are explored.

Table 8 – Methodological inputs and outputs

	Inputs	Outputs
Community scale	Spatial distributions of buildings	<ul style="list-style-type: none"> • Buildings' connectivity • Number of buildings sharing electricity • Clusters of buildings • Block boundaries
Block scale	<ul style="list-style-type: none"> • Coverage ratio • Floor area ratio (FAR) • Height • Land use • Structure • Rise type • Use (single or mixed within a building) 	Changes in multiple block performance (energy demand, solar harvesting potential, thermal comfort, sky exposure)
Building scale	<ul style="list-style-type: none"> • Envelope area • Envelop options 	Application area for sets of envelop options

According to the input and output variables, and their influences each other, the potential interrelationships and the key variables are explored in Figure 7.1. Key variables are identified as auxiliary variables directly driving other variables, variables formed by convergence of other variables, or constant solely influencing performance evaluation of each level significantly. On a building scale, envelope area that consists of vertical façade area, roof, and floor area will be key variables that determine applicable area of retrofitting building envelopes by sets of possible options. On a block scale, land use, rise type, coverage ratio, and FAR will be key variables that determine block-level multiple performance. In that height will directly form rise type or FAR, height is also considered as a key variable. On a community scale, spatial distributions of buildings will be a key variable that can change potential capacity of sharing electricity.

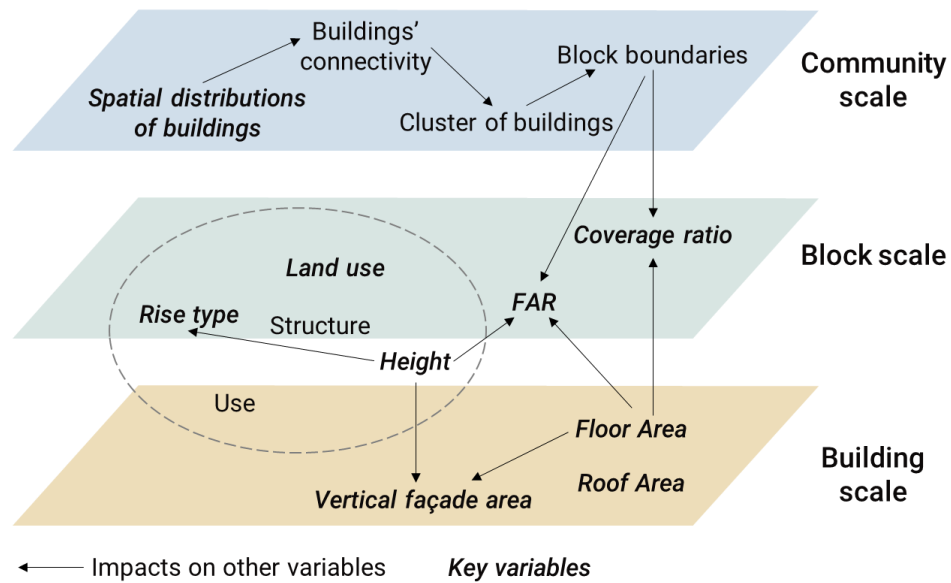


Figure 7.1 – Potential interrelationships among variables

7.2 Integrated Decision Support Framework: Top-down and Bottom-up

7.1.1 Top-down decision framework

Based on the interrelationships among variables at each scale as well as their impacts studied in Chapter 4 ~ 6, a top-down decision framework is built in Figure 7.2. On a community scale, reconfigurations of block boundaries will be normatively decided by desires or social norms of sharing electricity or requiring micro-grids to save energy and transmission loss. After block boundaries reconfigured, buildings' topological parameters within block such as coverage ratio and FAR will be changed. The changes of topological parameters derive changes in multiple performance in a block. Correspondingly, energy demand and solar potential in a block level will be singled out to individual buildings. The performance changes allocated to individual buildings can require retrofitting building envelopes. In Figure 7.2, positive effects indicate findings from empirical studies, and normative effects are based on value judgement by stakeholders of buildings and a community.

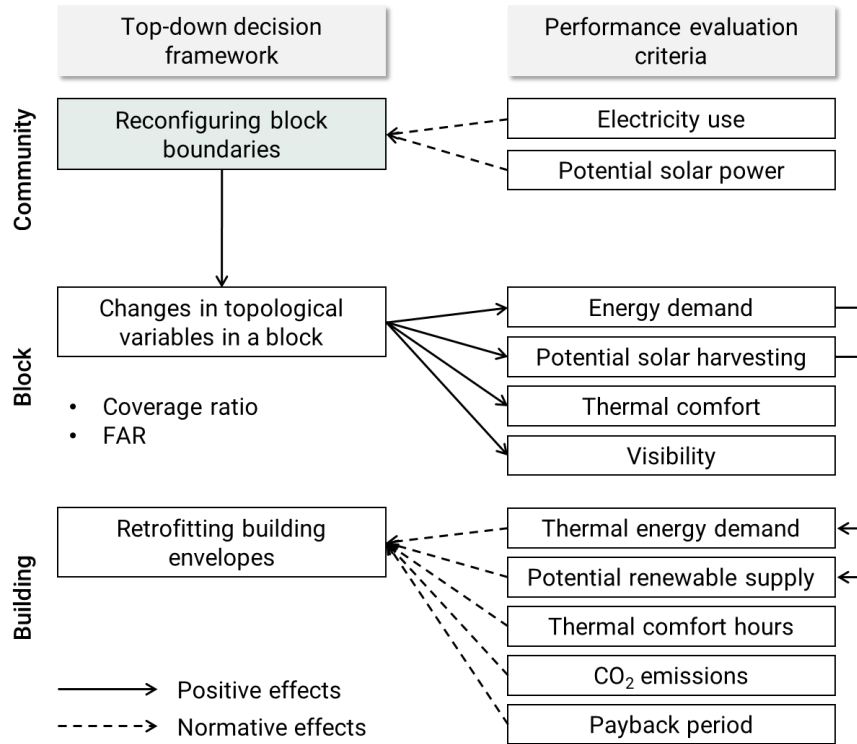


Figure 7.2 – Top-down decision framework

7.1.2 Bottom-up decision framework

A bottom-up decision framework is built in Figure 7.3. Bottom-up decision framework can begin with applying transformation strategies of an individual buildings scale. After retrofitting building envelopes, building energy and comfort performance will be changed, and this can release or restrict typology configurations in a block to achieve a certain degree of block-level performance. The changes of typology can influence the block-level performance that can vary energy distributions on a community. Afterwards, based on the community's willingness, block boundaries can be reconfigured to share electricity among buildings.

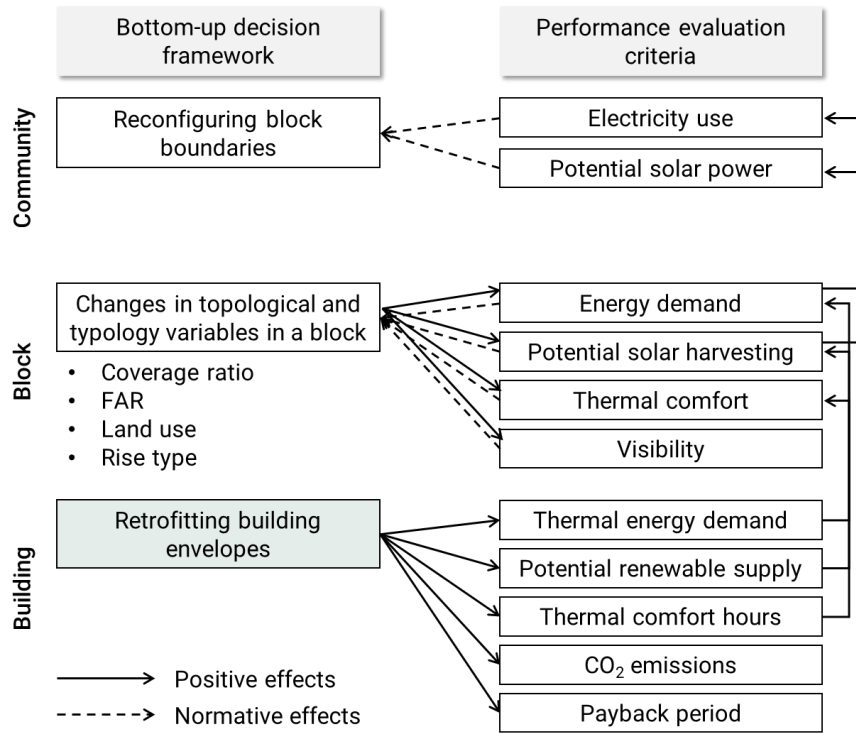


Figure 7.3 – Bottom-up decision framework

7.3 Performance Comparisons of Integrated Decisions

This section explores how the transformations in a community level and in an individual building level can influence block-level performance. The reconfigured block boundaries in Chapter 6 are assigned new block categories to all buildings, and energy performance improvement of individual buildings in Chapter 4 is also applied for approximating energy performance of buildings after retrofitting building envelopes. Then, the new dataset incorporating the new block assignment and the energy performance improvement is used to recognize changes in multiple performance in a block level. Figure 7.4 ~ 7.7 compares average performance of the existing blocks and the proposed blocks. Block scales in this research can be manageable in analysis as the focal scale between buildings and communities (Yang 2012).

Average energy demand of new blocks can be very much improved (Figure 7.4) because impacts of retrofitting building envelopes on energy performance were only considered influencing energy demand while the effects can also change potential renewable energy generation. The median of average solar potential of new blocks is decreased, but highest 25 quartile values are much more increased compared with the existing blocks (Figure 7.5). The median and highest 25 quartile values for average thermal comfort and visibility on blocks are slightly improved than the performance of the existing blocks (Figure 7.6 ~ 7.7).

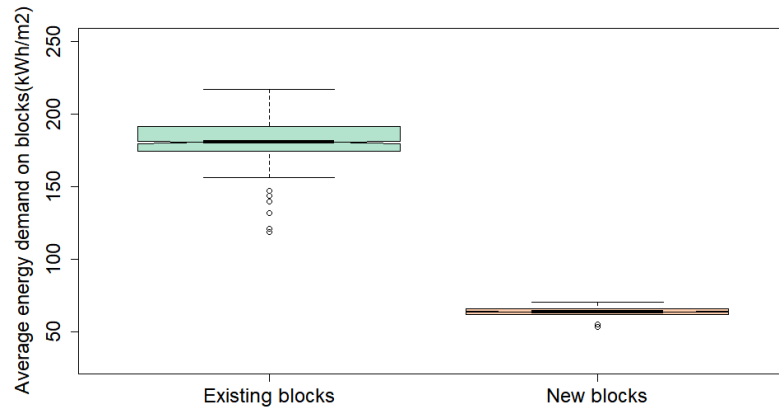


Figure 7.4 – Comparing changes in average building energy demand on blocks

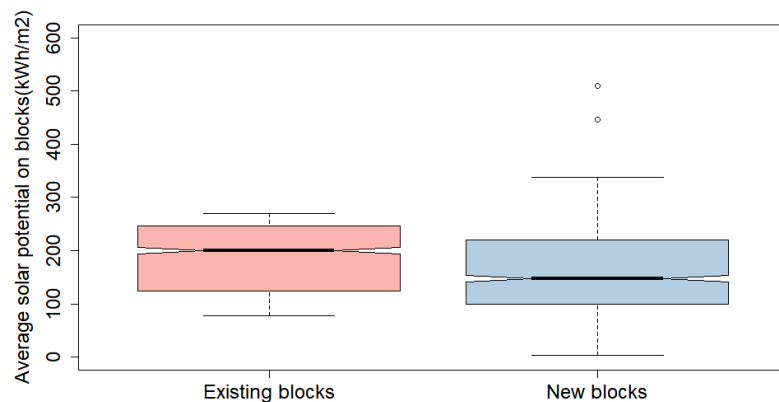


Figure 7.5 – Comparing changes in average building-integrated solar potential on blocks

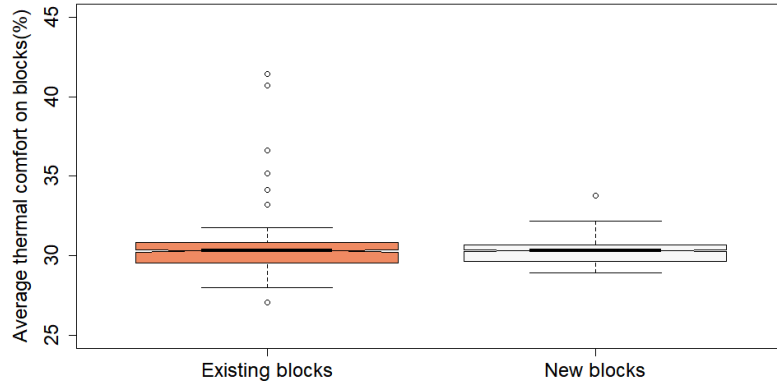


Figure 7.6 – Comparing change in average percentages of thermal comfort on blocks

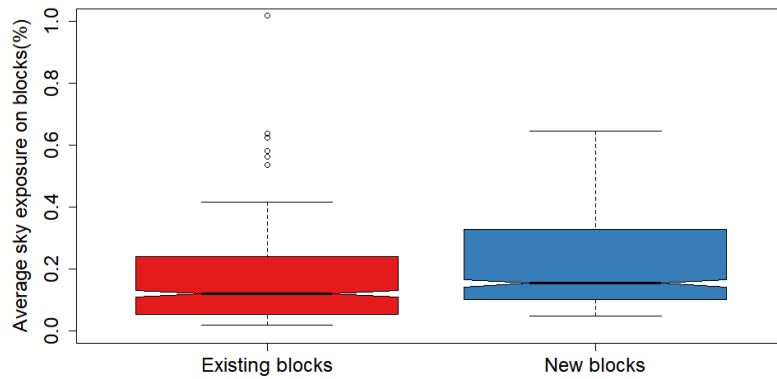


Figure 7.7 – Comparing changes in average visibility on blocks

7.4 Chapter Conclusions

This chapter was devised to explore interrelationships of variables and performance across multiple scales of community, block, and building. From the top-down perspective, block boundaries determine block size and correspond changes in block coverage ratio, FAR, and combinations of building typology within a block. From the bottom-up perspective, building topological parameters such as height, floor area, etc. influence other topological variables such as coverage ratio as well as building typological parameters such as rise type. In addition, the changes of transformable parameters will affect multiple performance indicators at each scale. Performance indicators are also networked among

multiple scales. For instance, the block-level building energy demand was singled out energy demand of buildings in a block. The energy demand can impose different levels of thermal energy demand through building envelopes in an individual building level. Also, the amount can be singled out hourly demands and provide temporal fluctuations for energy distribution in a community level. Based on the observations, a decision of one scale will influence decisions in other scales. In this respect, decisions of transforming buildings should be collaboratively implemented after scrutinizing changes of parameters and impacts of the changes.

CHAPTER 8. CONCLUSIONS

This chapter concludes this thesis by summarizing the research framework and major findings, drawing research implications from the results, discussing contribution and limitations, and suggesting future research initiatives.

8.1 Conclusion

Transformations of urban buildings require different strategies at different scales, and changes in one scale influence performance indicators in other scales. In this respect, this research devised to investigate appropriate transformation strategies at multiple scales of an individual building, a block, and a community and explore their interrelationships.

First, research objective on an individual building scale was to optimize selections of envelope options when retrofitting buildings. This research found that at least 33% of current vertical envelopes of buildings in the case study can be retrofitted to improve energy performance, environmental impacts of CO₂ emissions, and indoor thermal comfort. However, the economic feasibility was challenging to be paid back in 50 years but there is still an opportunity to improve if an economic envelope option emerges in the future. Since the genetic algorithm was formed to incorporate any newly developed materials in the optimization process, building engineers or managers can address future development of economic envelope options.

Second research objective was to reorganize building typology that can improve multiple performance indicators in a block level. The Bayesian multilevel additive model was applied to analyze relationships between a variety of variables and multiple indicators

of energy demand, potential solar supply, thermal comfort, and visibility. This research discovered that tradeoffs of block-level performance indicators were influenced by building topological or typological parameters. Based on the results, reducing coverage ratio with an increase in FAR by raising building height can improve energy performance by reducing energy demand. However, collections of mid-rise buildings will provide better solar harvesting potential than groups of high-rise buildings due to the shading effects. The information of building parameters and their effects on multiple performance was detected in the Chapter 5.

Third research objective was to reconfigure block boundaries that can support decisions of sharing energy on a community. To achieve the goal, spatial clustering and Voronoi diagram algorithm were utilized to consider spatiotemporal distributions of electricity demand and supply. According to the case study applied in a community located in Tokyo, Japan, existing 46 blocks can be redefined into 13 blocks that can share electricity. When micro-grids become necessary to be formed in a community, the proposed block boundaries can function as guidelines on the top of existing physical blocks (i.e., street networks, zones, etc.). Also, the algorithm can be replicable with geo-spatial data of buildings and their electricity demand and supply. The algorithms can quickly provide new block boundaries whenever analysis period is changed. The reconfigurable block boundaries were studied in Chapter 6.

Finally, the interrelated parameters were discerned in Chapter 7. Based on the interactions, both bottom-up and top-down decisions can be implemented, and transformation of block boundaries and building envelopes can correspondingly changes in performance on a block level.

8.2 Research Implications

This research framework and findings can be used for policymaking, practice, theory, and future research works.

First, this research discerned improvement of energy performance, environmental impacts (CO₂ emissions), and thermal comfort hours by retrofitting building envelopes. And sets of envelope options presented in Table 3 cannot be collectively achieved to get payback within 50 years of investment. It indicates that necessity of different investment timing based on the availability of reducing levelized cost of energy of technology options or price of high-performance material. This study found that rooftops are preferable to be retrofitted than vertical envelopes since the maximum retrofittable envelope areas much larger in rooftops than vertical façades.

Second, this research identified that building parameters on a block influence block performance of energy demand, solar harvesting potential, thermal comfort, and sky exposure. A major finding is that we cannot avoid trade-offs among four performance indicators. Still, city planners and building managers can plan combinations of building typology in a block by being informed of the relationships. This research extracted four strategies for reconfiguring building typologies in a block: 1) energy performance and comfort improvement while undermining visibility, 2) maximization of solar harvesting potential while undermining thermal comfort, 3) visibility improvement, and 4) thermal comfort improvement.

Third, this research found that existing block boundaries should be reconsidered to form energy sharing boundaries based on predicted electricity uses and potential solar

power generations. The new block boundaries can be separations for managing energy distributions. In that clear definitions of boundaries have been required to implement micro-grids in urban area (Ton and Smith 2012), this empirical study established a methodology identifying clear boundaries based on energy balance of demand and supply for groups of buildings. In this research, by identifying the number of buildings that can share electricity and the boundaries vary hourly, the boundaries should be managed hourly basis and the future micro-grid energy distribution systems can envision hourly adaptations for distributing electricity. Also, the boundaries will define energy sharing zones in which energy transactions occur. This will support future decentralized and shared electricity markets that can resiliently accommodate real-time electricity needs in an urban area. The definition of boundaries will enable policy makers to devise principles related to sharing and distributing electricity.

This research also explored integrated decision frameworks that can be driven by a community or individual building level. Impacts of retrofitting building envelopes can reduce energy demands in a block level. Also, although block boundaries were reconfigured based on self-sufficiency of energy demands and supply, new blocks can offer better thermal comfort and visibility on average. The reconfigured blocks functioned for reducing averaged energy demands in a block even if the solar potential in new blocks is decreased. The integrated decision frameworks provide information of impacts of transforming buildings and blocks at different scales. Both top-down and bottom-up decision frameworks should be employed in practice to optimize performance changes and adapt driving forces.

8.3 Contribution

Although decisions of renovating buildings in a certain scale influence other scales in an urban area, the decisions should be differentiated to address different challenges and goals varied by scales. In this respect, this research thrust was tailored decisions at each scale, and investigates interactions of the decisions across multiple scales. This research will contribute to both academia and practice.

In the academia, this research will contribute to a body of knowledge about the interrelationships between building design and construction parameters considering multiple performance indicators at multiple scales in urban areas. For example, while previous study has been simplified impacts of building parameters by assuming linearity (Chang et al. 2019c), this research broadened understandings of the building parameters by considering spatiotemporal distributions on a community level, non-linear population-level and group-level effects synthetically on a block level, and performance evaluation of set of envelopes rather than one single option on an individual building level. The findings can support to discuss the complexity theory across multiple scales of urban building transformations.

The research efforts will also contribute to making appropriate decisions for investment, regulations, or guidelines when renovating physical building assets at different scales in urban areas. The impacts of transforming urban building parameters can provide building designers, owners, and managers a framework to appropriately consider renovation strategies to contribute to block-level performance. In addition, this will provide city planners or city government with potential impacts of retrofitting or redeveloping

urban buildings. Then, the information can guide to establishing a new category of urban buildings to manage performance-based planning of blocks. From the city government perspective, this research can be employed to investigate the energy sharing potential and adapt block boundaries based on real-time energy demand and supply of buildings. For city planners, building engineers, and building managers, this study improves building parameters' assessment on a block level for reviewing alternative building typologies. The optimization method for retrofitting building envelopes will reduce time to evaluate sets of envelope options by substituting current processes of reviewing applicable envelope options one by one. Integrating inputs and outputs of multiple scales will contribute to examining overall impacts in the urban area while focusing on a certain scale.

Since many cities are at the tipping point trying to become more resilient, increasingly focusing on sustainability, economic feasibility, and human well-being, a better understanding of the impact of built forms at multiple scales will support urban development decisions for the future smart and connected communities.

8.4 Limitations

This research has several limitations. First, transformation strategies at each scale were employed only one case study located in Tokyo, Japan. Since energy performance is highly related to climate zones, different regions should be further investigated. The spatial boundary can also correspondingly change influential factors in the block-level performance as well as context uncertainties in the building-level optimization. In addition, value of the optimization model should be further investigated by validating with experts' point of view. Objective functions in the model can also be broadened by incorporating

other decision criteria as well as diverse energy conversion methods. Moreover, the quantitative relationships among inputs and outputs at multiple scales should be further investigated to consolidate a holistic decision-making system.

8.5 Future Research

One of weakness of this research is that interrelationships were explored with qualitative measures, but quantifying the sequential inputs and outputs is necessary to consolidate a holistic decision-making system.

On-going research project, smart community in Shinagawa, Tokyo, Japan, will replicate the research efforts and suggest practical agenda for transforming an existing community to be smart and connected community in the future.

In addition, energy distributions will be more dynamic when electric vehicles (EVs), unmanned aerial vehicles (UAV), etc. are incorporated into an urban area in the future. Although this research suggested virtual block boundaries that can support managing electricity sharing when adopting micro-grid systems, future works can be developed to address how smart grid systems actually work by considering proximity advantage and transmission cost, transaction mechanism, and energy storage systems, etc. Requirements of improving the block performance and better understanding of complex impacts of building parameters can drive to suggest atypical building typology in the future. In addition, a GA model for optimizing the selections of building envelopes is required to be further validated the modeling process and feasibility of solutions. Moreover, different scenarios of retrofitting buildings envelopes can be tested to achieve energy-efficient community and to provide reliable transformation strategies. Quantitative

approach considering interdependencies among inputs and outputs at multiple scales can be further explored in the future.

For the future research, three research questions are driven from the research conducted in this thesis.

- 1) How much the optimization model of selecting building envelope options is valuable in practical applications?
- 2) Can we re-define building typology that can optimize multiple performance in a block level?
- 3) How will energy distributions be changed when energy demand and supply become more dynamic (e.g., EVs)? and how smart grid systems works?

APPENDIX A. OPTIMIZED ENVELOPE SELECTION OPTIONS FOR RESIDENTIAL BUILDINGS, KYOJIMA, TOKYO, JAPAN

Table 9 – Optimized Envelope Selection Option for Apartment 1

	Optimization Results & Objectives	Maximum Retrofit Area (m ²)
<i>North façades</i>	<ul style="list-style-type: none"> • 102 Generations • 70 pareto front solutions • Objectives of population (blue dots) • Objectives of pareto front solutions (orange dots) <p style="text-align: center;">Tonnes CO2</p> <p style="text-align: center;">Energy Balance</p> <p style="text-align: center;">Averaged indoor discomfort hours = 0 Payback period >= 50 years</p>	<ul style="list-style-type: none"> • Retrofit Area 255.11m² • Total Area 578.97m² <p style="text-align: center;">Retrofit Area Breakdown (m²):</p> <ul style="list-style-type: none"> Algae façade, 3.90 Exterior Mass wall, 27.53 External wood frame wall, 18.07 Exterior metal frame window, 7.31 Trombe walls, 14.08 AAC walls, 28.40 Double skin façade, 20.48 Green wall, 31.99 Vacuum insulation panels, 22.16 Solar PV (Semi-transparent), 32.35 Low-e coated window, 6.36 PCM integrated in wood-lightweight concrete, 19.79 PCM, 22.69
<i>West façades</i>	<ul style="list-style-type: none"> • 106 generations • 70 pareto front solutions • Objectives of population (blue dots) • Objectives of pareto front solutions (orange dots) <p style="text-align: center;">Tonnes CO2</p> <p style="text-align: center;">Energy Balance</p> <p style="text-align: center;">Averaged indoor discomfort hours = 0 Payback period >= 50 years</p>	<ul style="list-style-type: none"> • Retrofit Area 428.64m² • Total Area 1,303.43m² <p style="text-align: center;">Retrofit Area Breakdown (m²):</p> <ul style="list-style-type: none"> Algae façade, 17.55 Exterior Mass wall, 47.74 External wood frame wall, 18.36 Exterior metal frame window, 83.80 Trombe walls, 3.96 AAC walls, 8.42 Double skin façade, 23.44 Green wall, 47.64 Vacuum insulation panels, 4.12 Solar PV (Semi-transparent), 18.70 Low-e coated window, 37.67 PCM integrated in wood-lightweight concrete, 35.26 PCM, 81.96

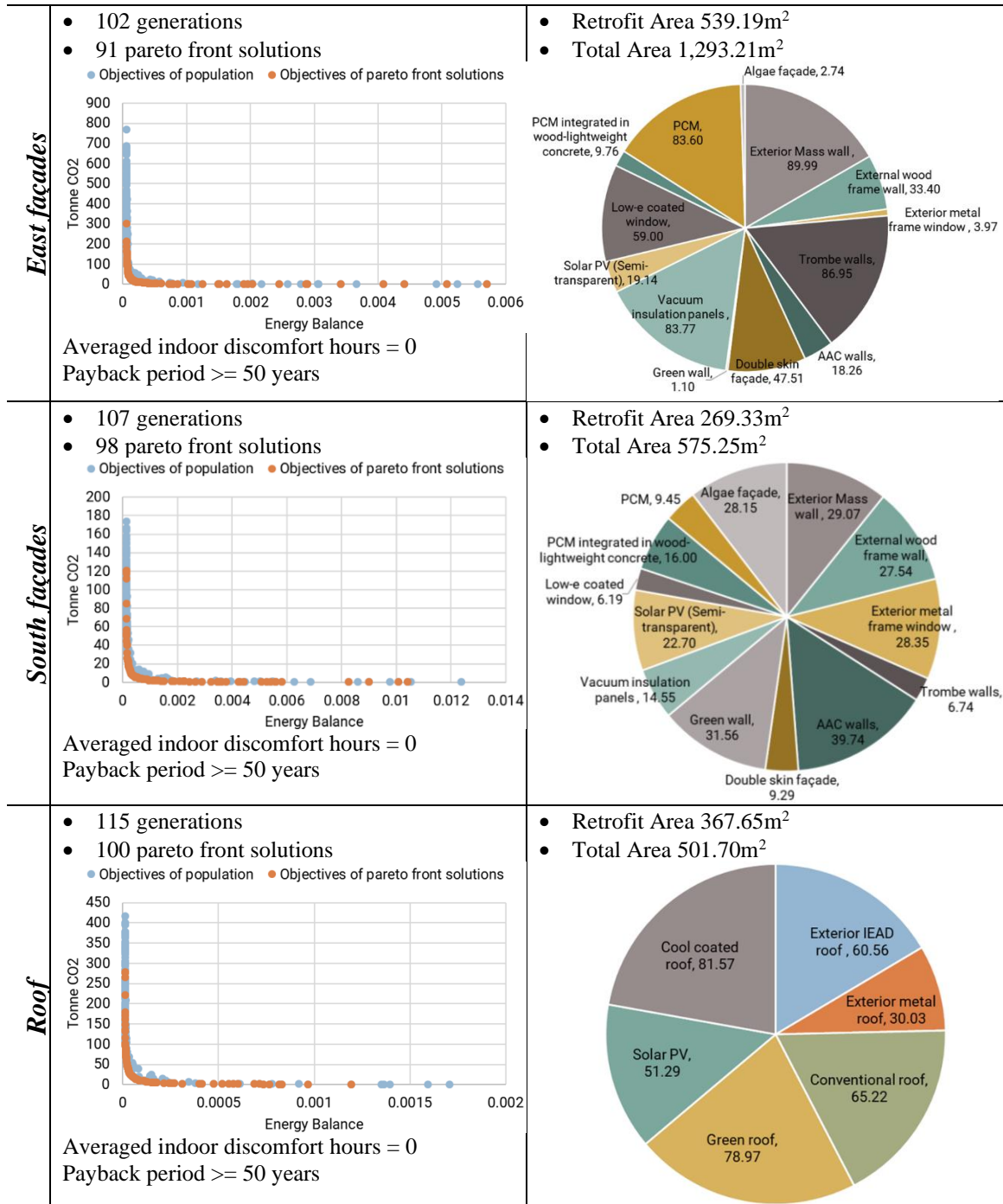


Table 10 – Optimized Envelope Selection Option for Apartment 2

	Optimization Results & Objectives	Maximum Retrofit Area (m ²)																												
<i>North façades</i>	<ul style="list-style-type: none"> 107 generations 61 pareto front solutions Objectives of population (blue dots) Objectives of pareto front solutions (orange dots) <p>Averaged indoor discomfort hours = 0 Payback period >= 50 years</p>	<ul style="list-style-type: none"> Retrofit Area 66.43m² Total Area 123.05m² <table border="1"> <caption>Retrofit Area Distribution for North Façades</caption> <thead> <tr> <th>Measure</th> <th>Area (m²)</th> </tr> </thead> <tbody> <tr><td>Algae façade</td><td>5.64</td></tr> <tr><td>Exterior Mass wall</td><td>6.31</td></tr> <tr><td>External wood frame wall</td><td>4.39</td></tr> <tr><td>External metal frame window</td><td>4.63</td></tr> <tr><td>Trombe wall</td><td>1.95</td></tr> <tr><td>AAC walls</td><td>6.84</td></tr> <tr><td>Double skin façade</td><td>7.73</td></tr> <tr><td>Green wall</td><td>2.89</td></tr> <tr><td>Vacuum insulation panels</td><td>4.65</td></tr> <tr><td>Solar PV (Semi-transparent)</td><td>8.55</td></tr> <tr><td>Low-e coated window</td><td>4.56</td></tr> <tr><td>PCM integrated in wood-lightweight concrete</td><td>4.59</td></tr> <tr><td>PCM</td><td>3.71</td></tr> </tbody> </table>	Measure	Area (m ²)	Algae façade	5.64	Exterior Mass wall	6.31	External wood frame wall	4.39	External metal frame window	4.63	Trombe wall	1.95	AAC walls	6.84	Double skin façade	7.73	Green wall	2.89	Vacuum insulation panels	4.65	Solar PV (Semi-transparent)	8.55	Low-e coated window	4.56	PCM integrated in wood-lightweight concrete	4.59	PCM	3.71
Measure	Area (m ²)																													
Algae façade	5.64																													
Exterior Mass wall	6.31																													
External wood frame wall	4.39																													
External metal frame window	4.63																													
Trombe wall	1.95																													
AAC walls	6.84																													
Double skin façade	7.73																													
Green wall	2.89																													
Vacuum insulation panels	4.65																													
Solar PV (Semi-transparent)	8.55																													
Low-e coated window	4.56																													
PCM integrated in wood-lightweight concrete	4.59																													
PCM	3.71																													
<i>West façades</i>	<ul style="list-style-type: none"> 102 generations 64 pareto front solutions Objectives of population (blue dots) Objectives of pareto front solutions (orange dots) <p>Averaged indoor discomfort hours = 0 Payback period >= 50 years</p>	<ul style="list-style-type: none"> Retrofit Area 67.90m² Total Area 151.96m² <table border="1"> <caption>Retrofit Area Distribution for West Façades</caption> <thead> <tr> <th>Measure</th> <th>Area (m²)</th> </tr> </thead> <tbody> <tr><td>Exterior Mass wall</td><td>5.54</td></tr> <tr><td>External wood frame wall</td><td>3.66</td></tr> <tr><td>External metal frame window</td><td>4.52</td></tr> <tr><td>Trombe walls</td><td>1.16</td></tr> <tr><td>AAC walls</td><td>2.59</td></tr> <tr><td>Double skin façade</td><td>6.05</td></tr> <tr><td>Green wall</td><td>4.63</td></tr> <tr><td>Vacuum insulation panels</td><td>9.23</td></tr> <tr><td>Solar PV (Semi-transparent)</td><td>8.61</td></tr> <tr><td>Low-e coated window</td><td>6.73</td></tr> <tr><td>PCM integrated in wood-lightweight concrete</td><td>2.58</td></tr> <tr><td>PCM</td><td>4.97</td></tr> <tr><td>Algae façade</td><td>7.62</td></tr> </tbody> </table>	Measure	Area (m ²)	Exterior Mass wall	5.54	External wood frame wall	3.66	External metal frame window	4.52	Trombe walls	1.16	AAC walls	2.59	Double skin façade	6.05	Green wall	4.63	Vacuum insulation panels	9.23	Solar PV (Semi-transparent)	8.61	Low-e coated window	6.73	PCM integrated in wood-lightweight concrete	2.58	PCM	4.97	Algae façade	7.62
Measure	Area (m ²)																													
Exterior Mass wall	5.54																													
External wood frame wall	3.66																													
External metal frame window	4.52																													
Trombe walls	1.16																													
AAC walls	2.59																													
Double skin façade	6.05																													
Green wall	4.63																													
Vacuum insulation panels	9.23																													
Solar PV (Semi-transparent)	8.61																													
Low-e coated window	6.73																													
PCM integrated in wood-lightweight concrete	2.58																													
PCM	4.97																													
Algae façade	7.62																													
<i>East façades</i>	<ul style="list-style-type: none"> 188 generations 96 pareto front solutions Objectives of population (blue dots) Objectives of pareto front solutions (orange dots) <p>Averaged indoor discomfort hours = 730 (1185.27 for the last population) Payback period >= 50 years</p>	<ul style="list-style-type: none"> Retrofit Area 70.77m² Total Area 131.17m² <table border="1"> <caption>Retrofit Area Distribution for East Façades</caption> <thead> <tr> <th>Measure</th> <th>Area (m²)</th> </tr> </thead> <tbody> <tr><td>Exterior Mass wall</td><td>6.93</td></tr> <tr><td>External wood frame wall</td><td>6.21</td></tr> <tr><td>External metal frame window</td><td>9.15</td></tr> <tr><td>Trombe walls</td><td>4.02</td></tr> <tr><td>AAC walls</td><td>2.42</td></tr> <tr><td>Double skin façade</td><td>8.09</td></tr> <tr><td>Green wall</td><td>4.98</td></tr> <tr><td>Vacuum insulation panels</td><td>5.25</td></tr> <tr><td>Solar PV (Semi-transparent)</td><td>7.28</td></tr> <tr><td>Low-e coated window</td><td>0.56</td></tr> <tr><td>PCM integrated in wood-lightweight concrete</td><td>8.23</td></tr> <tr><td>PCM</td><td>2.51</td></tr> <tr><td>Algae façade</td><td>5.14</td></tr> </tbody> </table>	Measure	Area (m ²)	Exterior Mass wall	6.93	External wood frame wall	6.21	External metal frame window	9.15	Trombe walls	4.02	AAC walls	2.42	Double skin façade	8.09	Green wall	4.98	Vacuum insulation panels	5.25	Solar PV (Semi-transparent)	7.28	Low-e coated window	0.56	PCM integrated in wood-lightweight concrete	8.23	PCM	2.51	Algae façade	5.14
Measure	Area (m ²)																													
Exterior Mass wall	6.93																													
External wood frame wall	6.21																													
External metal frame window	9.15																													
Trombe walls	4.02																													
AAC walls	2.42																													
Double skin façade	8.09																													
Green wall	4.98																													
Vacuum insulation panels	5.25																													
Solar PV (Semi-transparent)	7.28																													
Low-e coated window	0.56																													
PCM integrated in wood-lightweight concrete	8.23																													
PCM	2.51																													
Algae façade	5.14																													

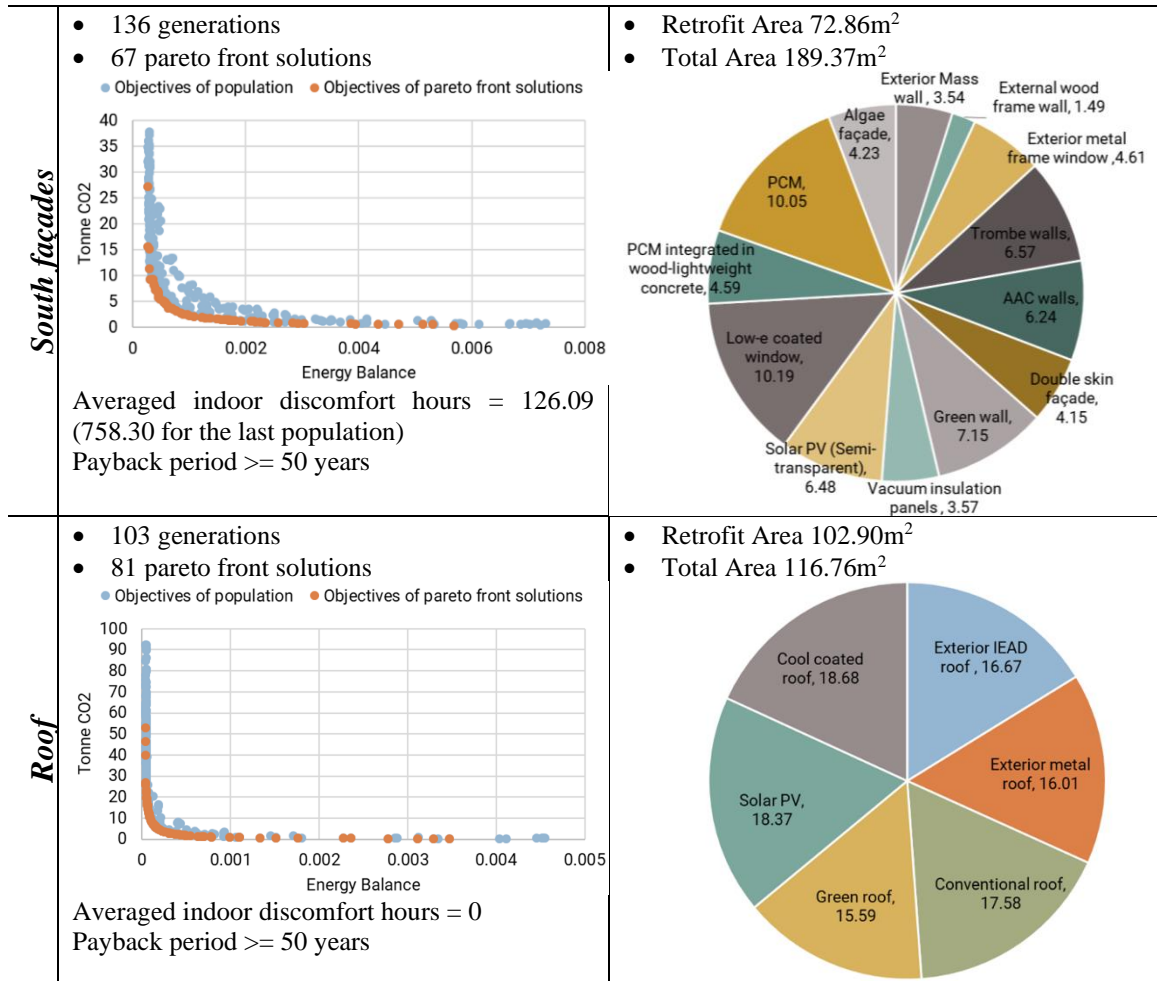
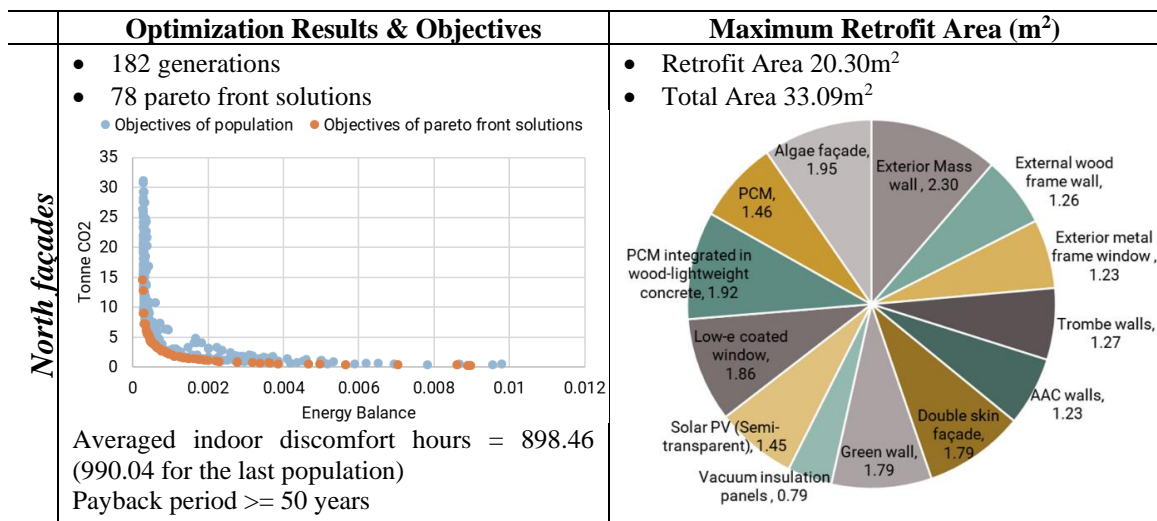
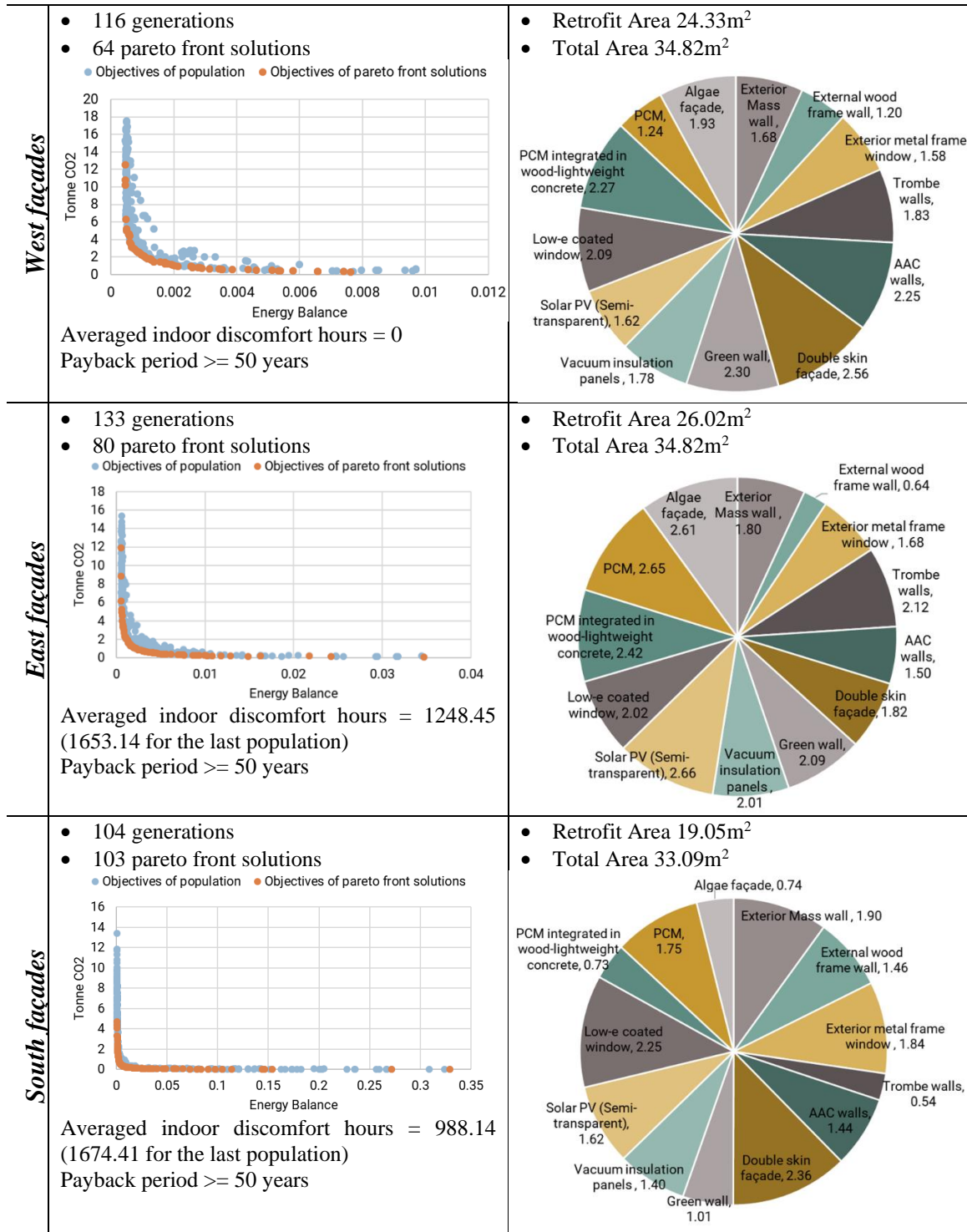


Table 11 – Optimized Envelope Selection Option for Wooden House 1





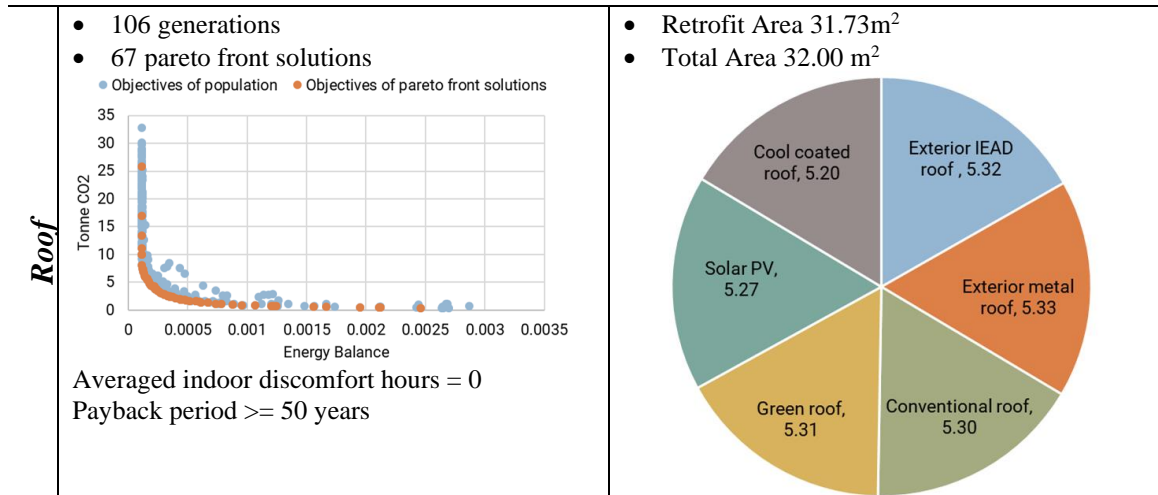
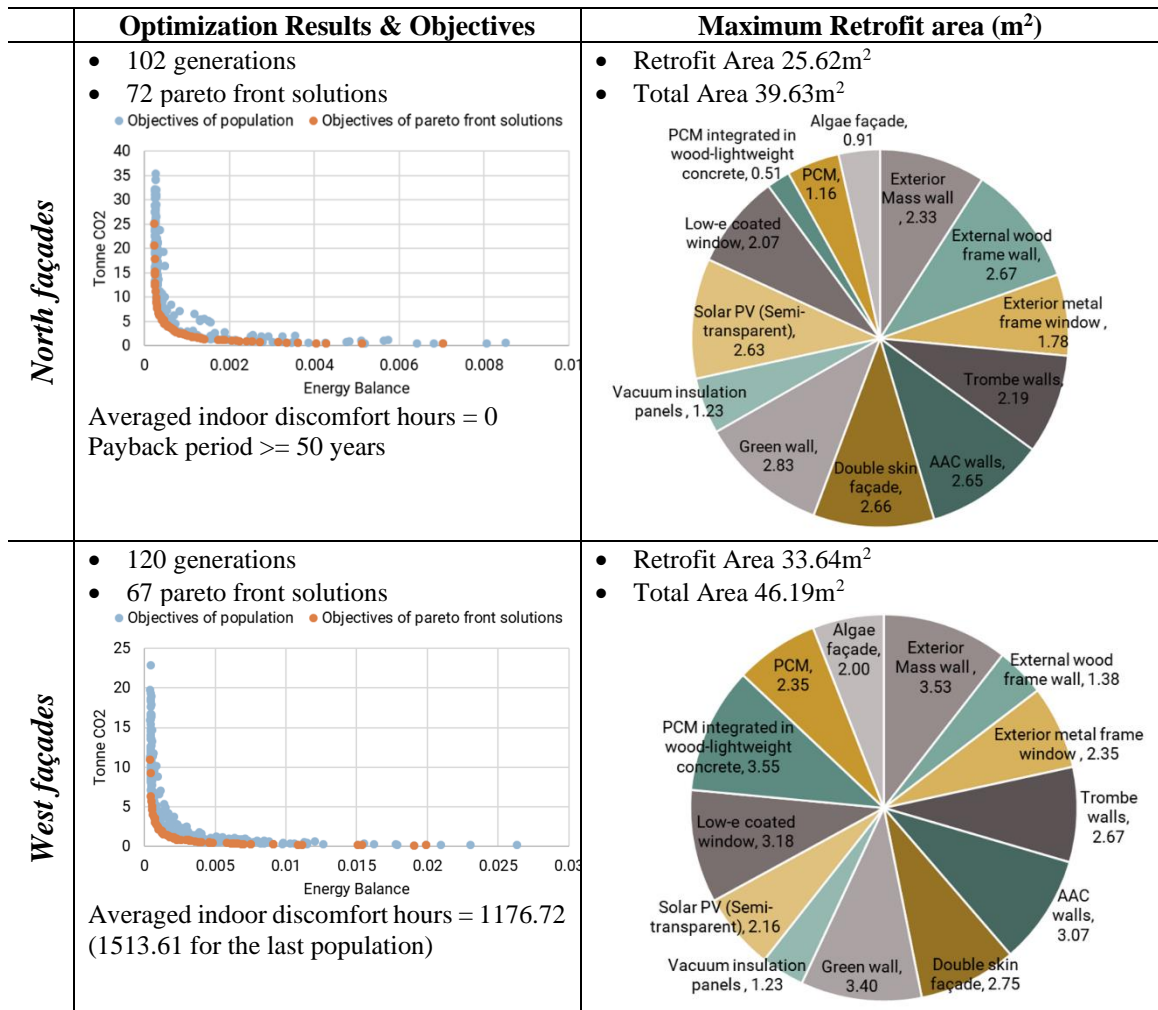
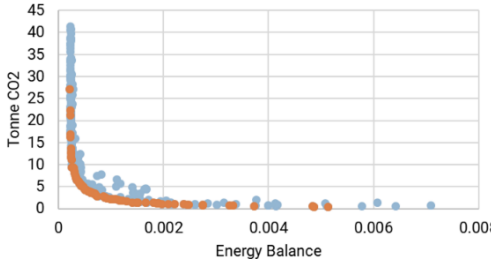
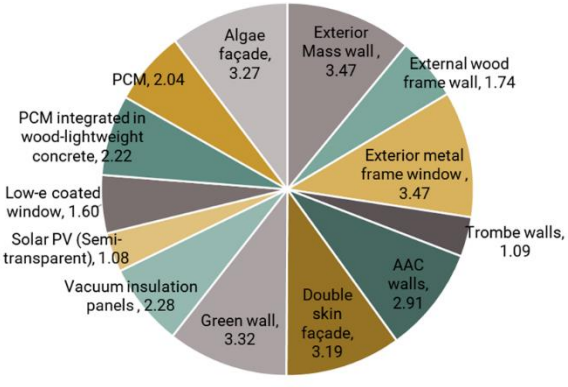
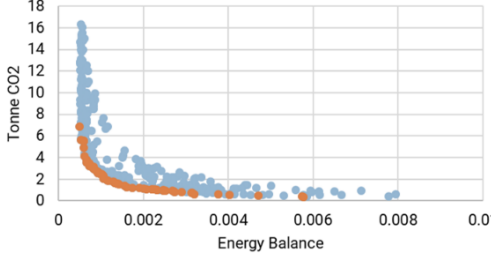
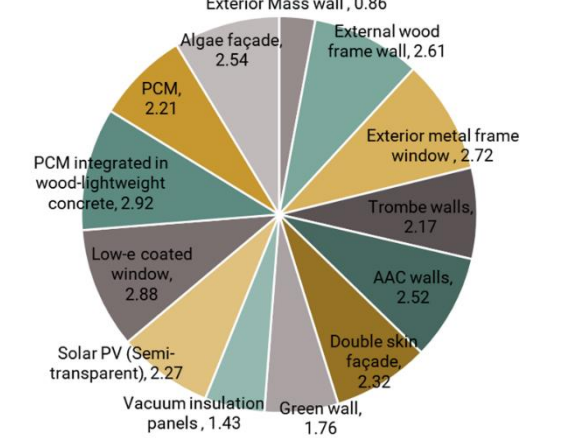
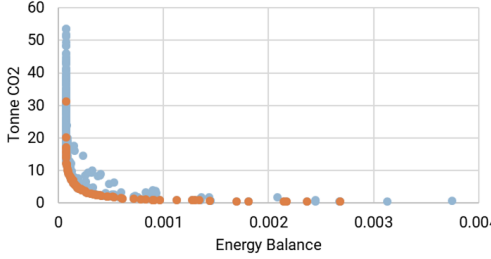
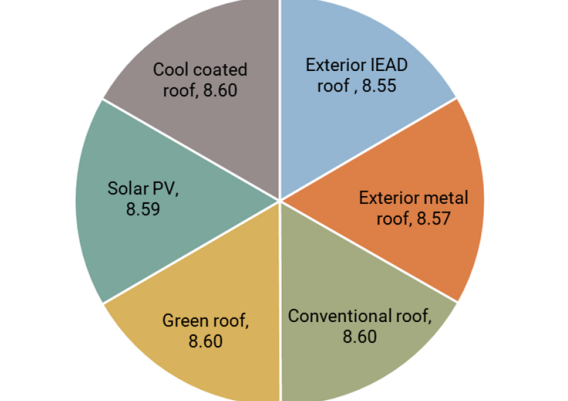


Table 12 – Optimized Envelope Selection Option for Wooden House 2



<p>East façades</p> <ul style="list-style-type: none"> • 102 generations • 83 pareto front solutions • Objectives of population (blue dots) • Objectives of pareto front solutions (orange dots)  <p>Averaged indoor discomfort hours = 0 Payback period \geq 50 years</p>	<ul style="list-style-type: none"> • Retrofit Area 31.69m² • Total Area 47.42m²  <table border="1"> <caption>Area Distribution for East Façades</caption> <thead> <tr> <th>Material</th> <th>Area (m²)</th> </tr> </thead> <tbody> <tr><td>Algae façade</td><td>3.27</td></tr> <tr><td>Exterior Mass wall</td><td>3.47</td></tr> <tr><td>External wood frame wall</td><td>1.74</td></tr> <tr><td>Exterior metal frame window</td><td>3.47</td></tr> <tr><td>Trombe walls</td><td>1.09</td></tr> <tr><td>AAC walls</td><td>2.91</td></tr> <tr><td>Double skin façade</td><td>3.19</td></tr> <tr><td>Green wall</td><td>3.32</td></tr> <tr><td>Vacuum insulation panels</td><td>2.28</td></tr> <tr><td>Solar PV (Semi-transparent)</td><td>1.08</td></tr> <tr><td>Low-e coated window</td><td>1.60</td></tr> <tr><td>PCM integrated in wood-lightweight concrete</td><td>2.22</td></tr> <tr><td>PCM</td><td>2.04</td></tr> </tbody> </table>	Material	Area (m ²)	Algae façade	3.27	Exterior Mass wall	3.47	External wood frame wall	1.74	Exterior metal frame window	3.47	Trombe walls	1.09	AAC walls	2.91	Double skin façade	3.19	Green wall	3.32	Vacuum insulation panels	2.28	Solar PV (Semi-transparent)	1.08	Low-e coated window	1.60	PCM integrated in wood-lightweight concrete	2.22	PCM	2.04
Material	Area (m ²)																												
Algae façade	3.27																												
Exterior Mass wall	3.47																												
External wood frame wall	1.74																												
Exterior metal frame window	3.47																												
Trombe walls	1.09																												
AAC walls	2.91																												
Double skin façade	3.19																												
Green wall	3.32																												
Vacuum insulation panels	2.28																												
Solar PV (Semi-transparent)	1.08																												
Low-e coated window	1.60																												
PCM integrated in wood-lightweight concrete	2.22																												
PCM	2.04																												
<p>South façades</p> <ul style="list-style-type: none"> • 165 generations • 59 pareto front solutions • Objectives of population (blue dots) • Objectives of pareto front solutions (orange dots)  <p>Averaged indoor discomfort hours = 148.47 (1120.49 for the last population) Payback period \geq 50 years</p>	<ul style="list-style-type: none"> • Retrofit Area 29.20 m² • Total Area 39.95 m²  <table border="1"> <caption>Area Distribution for South Façades</caption> <thead> <tr> <th>Material</th> <th>Area (m²)</th> </tr> </thead> <tbody> <tr><td>Algae façade</td><td>2.54</td></tr> <tr><td>External wood frame wall</td><td>2.61</td></tr> <tr><td>Exterior metal frame window</td><td>2.72</td></tr> <tr><td>Trombe walls</td><td>2.17</td></tr> <tr><td>AAC walls</td><td>2.52</td></tr> <tr><td>Double skin façade</td><td>2.32</td></tr> <tr><td>Green wall</td><td>1.76</td></tr> <tr><td>Vacuum insulation panels</td><td>1.43</td></tr> <tr><td>Solar PV (Semi-transparent)</td><td>2.27</td></tr> <tr><td>Low-e coated window</td><td>2.88</td></tr> <tr><td>PCM integrated in wood-lightweight concrete</td><td>2.92</td></tr> <tr><td>PCM</td><td>2.21</td></tr> <tr><td>Exterior Mass wall</td><td>0.86</td></tr> </tbody> </table>	Material	Area (m ²)	Algae façade	2.54	External wood frame wall	2.61	Exterior metal frame window	2.72	Trombe walls	2.17	AAC walls	2.52	Double skin façade	2.32	Green wall	1.76	Vacuum insulation panels	1.43	Solar PV (Semi-transparent)	2.27	Low-e coated window	2.88	PCM integrated in wood-lightweight concrete	2.92	PCM	2.21	Exterior Mass wall	0.86
Material	Area (m ²)																												
Algae façade	2.54																												
External wood frame wall	2.61																												
Exterior metal frame window	2.72																												
Trombe walls	2.17																												
AAC walls	2.52																												
Double skin façade	2.32																												
Green wall	1.76																												
Vacuum insulation panels	1.43																												
Solar PV (Semi-transparent)	2.27																												
Low-e coated window	2.88																												
PCM integrated in wood-lightweight concrete	2.92																												
PCM	2.21																												
Exterior Mass wall	0.86																												
<p>Roof</p> <ul style="list-style-type: none"> • 102 generations • 76 pareto front solutions • Objectives of population (blue dots) • Objectives of pareto front solutions (orange dots)  <p>Averaged indoor discomfort hours = 0 Payback period \geq 50 years</p>	<ul style="list-style-type: none"> • Retrofit Area 51.51m² • Total Area 51.67 m²  <table border="1"> <caption>Area Distribution for Roof</caption> <thead> <tr> <th>Material</th> <th>Area (m²)</th> </tr> </thead> <tbody> <tr><td>Cool coated roof</td><td>8.60</td></tr> <tr><td>Exterior IEAD roof</td><td>8.55</td></tr> <tr><td>Exterior metal roof</td><td>8.57</td></tr> <tr><td>Conventional roof</td><td>8.60</td></tr> <tr><td>Green roof</td><td>8.60</td></tr> <tr><td>Solar PV</td><td>8.59</td></tr> </tbody> </table>	Material	Area (m ²)	Cool coated roof	8.60	Exterior IEAD roof	8.55	Exterior metal roof	8.57	Conventional roof	8.60	Green roof	8.60	Solar PV	8.59														
Material	Area (m ²)																												
Cool coated roof	8.60																												
Exterior IEAD roof	8.55																												
Exterior metal roof	8.57																												
Conventional roof	8.60																												
Green roof	8.60																												
Solar PV	8.59																												

APPENDIX B. BAYESIAN MULTILEVEL MODELS FOR BLOCK-LEVEL PERFORMANCE ESTIMATION BY BUILDING PARAMETERS

1. Model to fit energy demand averaged in each block

```
brm(blockEnergy ~ s(CoverageRatio)+s(FAR)+s(Height)+(1|LandUse)+(1|RType_NS)  
+(1|Use)+(1|structure), data=dat, chains =4, core=31, control = list(adapt_delta = 0.99,  
max_treedepth = 15))
```

2. Model to fit solar potential of building facades in each block

```
brm(solarBlock ~ s(CoverageRatio)+s(FAR)+s(Height)+(1|LandUse)+(1|RType_NS)  
+(1|Use)+(1|structure), data=dat, chains =4, core=31, control = list(adapt_delta = 0.99,  
max_treedepth = 15))
```

3. Model to fit sky exposure in each block

```
brm(SkyExposur ~ s(CoverageRatio)+s(FAR)+s(Height)+(1|LandUse)+(1|RType_NS)  
+(1|Use)+(1|structure),data=dat, chains =4, core=31, control = list(adapt_delta = 0.99,  
max_treedepth = 15))
```

4. Model to fit thermal comfort averaged in each block

```
brm(blockcomf ~ s(CoverageRatio)+s(FAR)+s(Height)+(1|LandUse)+(1|RType_NS)  
+(1|Use)+(1|structure),data=dat, chains =4, core=31, control = list(adapt_delta = 0.99,  
max_treedepth = 15))
```

APPENDIX C. RELATIONSHIPS BETWEEN BUILDING HEIGHTS AND MULTIPLE PERFORMANCE IN BLOCKS

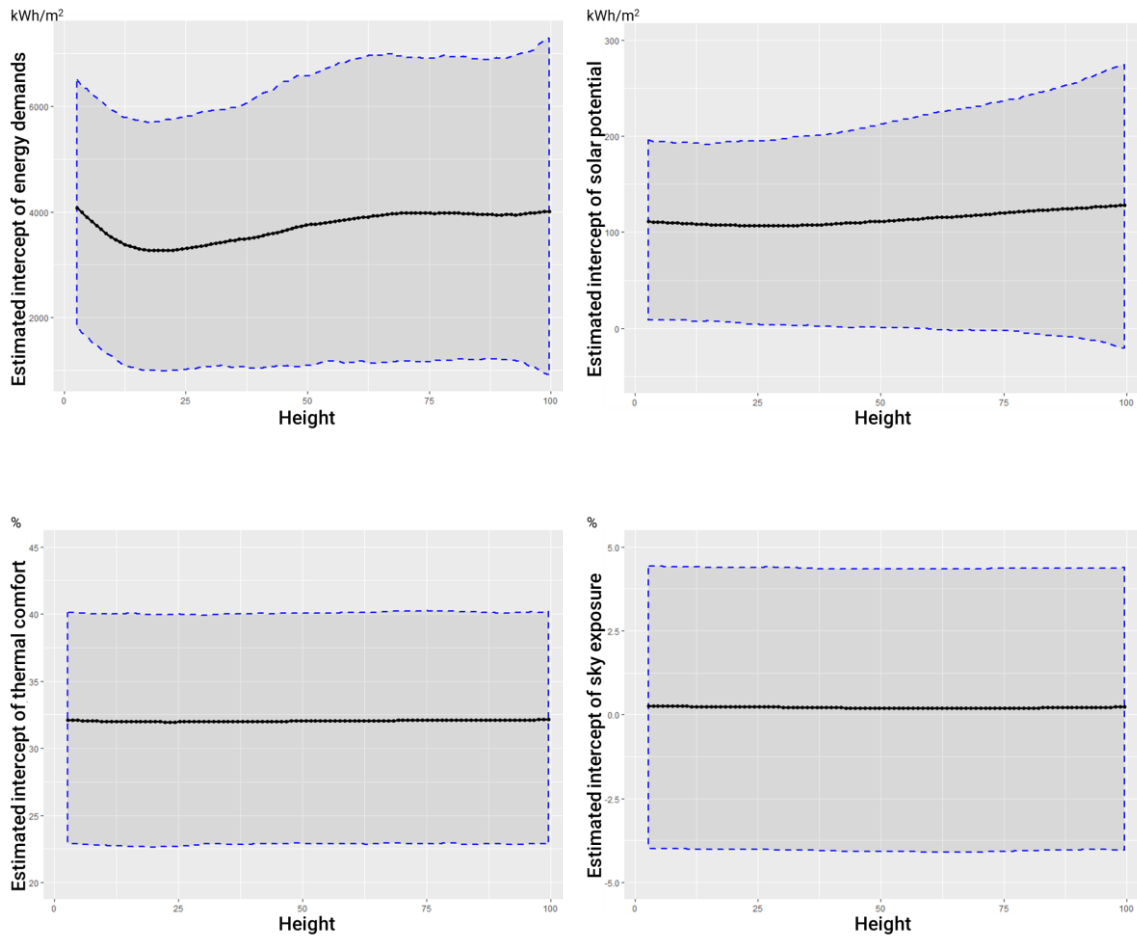


Figure 8.1 – Non-linear patterns of block-level performance by building height (y coordinates: average energy unit intensity (top-left), solar potential (top-right), average percentages of comfort time (bottom-left), and sky exposure (bottom-right))

REFERENCES

- Alam, M., Singh, H., and Limbachiya, M. C. (2011). “Vacuum Insulation Panels (VIPs) for building construction industry – A review of the contemporary developments and future directions.” *Applied Energy*, Elsevier, 88(11), 3592–3602.
- Alexander, C., Ishikawa, S., York, M. S.-N., and 1977, U. (1977). *A Pattern Language: Towns, Buildings, Construction*. Oxford University Press, New York.
- Alexandri, E., and Jones, P. (2008). “Temperature decreases in an urban canyon due to green walls and green roofs in diverse climates.” *Building and Environment*, Pergamon, 43(4), 480–493.
- Anastasiadis, A. G., Tsikalakis, A. G., and Hatziaargyriou, N. D. (2010). “Operational and environmental benefits due to significant penetration of Microgrids and topology sensitivity.” *IEEE PES General Meeting*, IEEE, 1–8.
- Araki, K., Kamoto, D., and Matsuoka, S. (2009). “Optimization about multilayer laminated film and getter device materials of vacuum insulation panel for using at high temperature.” *Journal of Materials Processing Technology*, Elsevier, 209(1), 271–282.
- Asadi, E., Silva, M. G. da, Antunes, C. H., and Dias, L. (2012). “A multi-objective optimization model for building retrofit strategies using TRNSYS simulations, GenOpt and MATLAB.” *Building and Environment*, Pergamon, 56, 370–378.
- Asadi, E., Silva, M. G. da, Antunes, C. H., Dias, L., and Glicksman, L. (2014). “Multi-objective optimization for building retrofit: A model using genetic algorithm and artificial neural network and an application.” *Energy and Buildings*, Elsevier, 81, 444–456.
- Ascione, F., Bianco, N., de’ Rossi, F., Turni, G., and Vanoli, G. P. (2013). “Green roofs in European climates. Are effective solutions for the energy savings in air-conditioning?” *Applied Energy*, Elsevier, 104, 845–859.
- ASHRAE. (2009). “ASHRAE climatic design conditions 2009/2013/2017.” *American Society of Heating, Refrigerating and Air-Conditioning Engineers*, <<http://ashrae-meteo.info/>> (Jun. 15, 2018).

- Atzeri, A. M., Cappelletti, F., Tzempelikos, A., and Gasparella, A. (2016). “Comfort metrics for an integrated evaluation of buildings performance.” *Energy and Buildings*, Elsevier, 127, 411–424.
- Bank of Japan. (2019). “The Basic Discount Rate and Basic Loan Rate (Previously Indicated as ‘Official Discount Rates’): 日本銀行 Bank of Japan.” *Bank of Japan*, <<https://www.boj.or.jp/en/statistics/boj/other/discount/discount.htm/>> (Apr. 11, 2019).
- Batty, M. (2013). *The New Science of Cities*. MIT Press, Cambridge, MA.
- Bazaz, A., Lwasa, S., Bertoldi, P., Markgraf, C., Buckeridge, M., Newman, P., Cartwright, A., Revi, A., Coninck, H. de, Rogelj, J., Engelbrecht, F., Schultz, S., Jacob, D., Shindell, D., Hourcade, J.-C., Singh, C., Klaus, I., Solecki, W., Kleijne, K. de, Steg, L., and Waisman, H. (2018). *Summary of urban policy makers: what the ipcc special report on global warming of 1.5°C means for cities*.
- Beygelzimer, A., Kakadet, S., Langford, J., Arya, S., Mount, D., and Li, S. (2019). *Package “FNN.”*
- Biswas, K., and Abhari, R. (2014). “Low-cost phase change material as an energy storage medium in building envelopes: Experimental and numerical analyses.” *Energy Conversion and Management*, Pergamon, 88, 1020–1031.
- Biyik, E., Araz, M., Hepbasli, A., Shahrestani, M., Yao, R., Shao, L., Essah, E., Oliveira, A. C., del Caño, T., Rico, E., Lechón, J. L., Andrade, L., Mendes, A., and Atlı, Y. B. (2017). “A key review of building integrated photovoltaic (BIPV) systems.” *Engineering Science and Technology, an International Journal*, Elsevier, 20(3), 833–858.
- BizEE Software. (2019). “Heating & Cooling Degree Days - Free Worldwide Data Calculation.” *BizEE Software*, <<https://www.degreedays.net/>> (Apr. 3, 2019).
- Blau, J. R., Gory, M. La, and Pipkin, J. S. (1983). *Professionals and Urban Form*. State University of New York Press, Albany, New York.
- Bullich-Massagué, E., Díaz-González, F., Aragiús-Peñalba, M., Girbau-Llistuella, F., Olivella-Rosell, P., and Sumper, A. (2018). “Microgrid clustering architectures.” *Applied Energy*, Elsevier, 212, 340–361.

- Buratti, C., Moretti, E., Belloni, E., and Cotana, F. (2013). “Unsteady simulation of energy performance and thermal comfort in non-residential buildings.” *Building and Environment*, Pergamon, 59, 482–491.
- Bürklin, T., and Peterek, M. (2017). *Basics urban building blocks*. Birkhäuser Architecture; 1 edition (October 5, 2007).
- Bürkner, P.-C. (2017). “brms: An R Package for Bayesian Multilevel Models using Stan.” *Journal of Statistical Software*, 80(1).
- Bürkner, P.-C. (2018). “Advanced Bayesian Multilevel Modeling with the R Package brms.” *The R Journal*, 10/1, 395–411.
- Burns, J. E., and Kang, J.-S. (2012). “Comparative economic analysis of supporting policies for residential solar PV in the United States: Solar Renewable Energy Credit (SREC) potential.” *Energy Policy*, Elsevier, 44, 217–225.
- Cao, S., Hasan, A., and Sirén, K. (2013). “On-site energy matching indices for buildings with energy conversion, storage and hybrid grid connections.” *Energy and Buildings*, Elsevier, 64, 423–438.
- Castro-Lacouture, D. (2015). “Resource Management and Closed-Loop Systems: Advancing Sustainable Performance Metrics.” *Proceedings of the Measurement Science for Sustainable Construction and Manufacturing Workshop Volume II. Presentations*, U.S. Department of Commerce.
- Cervera Sardá, R., and Vicente, C. A. (2016). “Case Studies on the Architectural Integration of Photobioreactors in Building Façades.” *Nano and Biotech Based Materials for Energy Building Efficiency*, Springer International Publishing, Cham, 457–484.
- Chan, A. L. S., Chow, T. T., Fong, K. F., and Lin, Z. (2009). “Investigation on energy performance of double skin façade in Hong Kong.” *Energy and Buildings*, Elsevier, 41(11), 1135–1142.
- Chang, S., Castro-Lacouture, D., Dutt, F., and Yang, P. P.-J. (2017). “Framework for evaluating and optimizing algae façades using closed-loop simulation analysis integrated with BIM.” *Energy Procedia*, 143(World Engineers Summit – Applied Energy Symposium & Forum: Low Carbon Cities & Urban Energy Joint Conference, WES-CUE 2017, 19–21 July 2017, Singapore), 237–244.

- Chang, S., Castro-Lacouture, D., Matsui, K., and Yamagata, Y. (2019a). “Planning and Monitoring of Building Energy Demands under Uncertainties by Using IoT Data.” *Proceedings of 2019 ASCE International Conference on Computing in Civil Engineering*, American Society of Civil Engineers, June 17-19, Atlanta, GA, USA.
- Chang, S., Castro-Lacouture, D., and Yamagata, Y. (2020a). “Decision support for retrofitting building envelopes using multi-objective optimization under uncertainties.” *Journal of Building Engineering*, Accepted.
- Chang, S., Saha, N., Castro-Lacouture, D., and Pei-Ju Yang, P. (2019b). “Generative design and performance modeling for relationships between urban built forms, sky opening, solar radiation and energy.” *Energy Procedia*, Elsevier, 158, 3994–4002.
- Chang, S., Saha, N., Castro-Lacouture, D., and Yang, P. P.-J. (2019c). “Multivariate relationships between campus design parameters and energy performance using reinforcement learning and parametric modeling.” *Applied Energy*, Elsevier, 249, 253–264.
- Chang, S., Yoshida, T., Binder, R. B., Yamagata, Y., and Castro-Lacouture, D. (2020b). “Energy sharing boundaries integrating buildings and vehicles tangled in spatial and temporal changes.” *Construction Research Congress 2020*, American Society of Civil Engineers, Tempe, Arizona, U.S.A., Accepted.
- Chang, S., Yoshida, T., Castro-Lacouture, D., and Yamagata, Y. (2020c). “Block-level Building Transformation Strategies for Improving Energy Efficiency, Thermal Comfort and Visibility Performance Using Bayesian Multilevel Additive Modeling.” *Applied Energy*, Under Review.
- Chang, S., Yoshida, T., Castro-Lacouture, D., Yamagata, Y., and Matsui, K. (2019d). “An Ontology to Sustainability Provision System of Energy Demands and Indoor Thermal Comfort by Integrating Building Energy Models with IoT – Focusing on Residential Building in Kyojima, Tokyo.” *Proceedings of CIB World Building Congress 2019*, CIB World Building Congress, June 17-21, Hong Kong.
- Chang, S., Yoshida, T., Tobey, M., Yamagata, Y., and Yang, P. P.-J. (2019e). “Transformative model of urban buildings optimizing energy demands, solar harvesting potential, and indoor thermal comfort.” *The 11th International Conference on Applied Energy*, Aug 12-15, Västerås, Sweden.
- Chantrelle, F. P., Lahmidi, H., Keilholz, W., Mankibi, M. El, and Michel, P. (2011). “Development of a multicriteria tool for optimizing the renovation of buildings.”

Applied Energy, Elsevier, 88(4), 1386–1394.

- Charoenkit, S., and Yiemwattana, S. (2016). “Living walls and their contribution to improved thermal comfort and carbon emission reduction: A review.” *Building and Environment*, Pergamon, 105, 82–94.
- Charron, R., and Athienitis, A. (2006). “The Use of Genetic Algorithms for a Net-Zero Energy Solar Home Design Optimisation Tool.” *PLEA2006-The 23rd Conference on Passive and Low Energy Architecture*, Geneva, Switzerland.
- Chen, Y.-J., Matsuoka, R. H., and Liang, T.-M. (2017). “Urban form, building characteristics, and residential electricity consumption: A case study in Tainan City.” *Environment and Planning B: Urban Analytics and City Science*, SAGE PublicationsSage UK: London, England, 239980831769015.
- Chidiac, S. E., Catania, E. J. C., Morofsky, E., and Foo, S. (2011). “Effectiveness of single and multiple energy retrofit measures on the energy consumption of office buildings.” *Energy*, Pergamon, 36(8), 5037–5052.
- Cho, J., Yoo, C., and Kim, Y. (2014). “Viability of exterior shading devices for high-rise residential buildings: Case study for cooling energy saving and economic feasibility analysis.” *Energy and Buildings*, Elsevier, 82, 771–785.
- Chow, T., Li, C., and Lin, Z. (2010). “Innovative solar windows for cooling-demand climate.” *Solar Energy Materials and Solar Cells*, North-Holland, 94(2), 212–220.
- Craney, T. A., and Surles, J. G. (2007). “Model-Dependent Variance Inflation Factor Cutoff Values.” *Quality Engineering*, 14(3), 391–403.
- Csárdi, G., and Nepusz, T. (2006). “The igraph software package for complex network research.” *International Journal of Computer Systems (IJCS)*, 1695, 1–9.
- Culp, T. D., and Cort, K. A. (2015). *Energy Savings of Low-E Storm Windows and Panels across US Climate Zones*. Richland, Washington .
- Danielski, I., Fröling, M., and Joelsson, A. (2012). “The impact of the shape factor on final energy demand in residential buildings in nordic climates.” *In: World Renewable Energy Forum, WREF 2012, Including World Renewable Energy Congress XII and Colorado Renewable Energy Society (CRES) Annual Conference*, Denver, CO, 4260–

4264.

- Derrible, S. (2017). "Urban infrastructure is not a tree: Integrating and decentralizing urban infrastructure systems." *Environment and Planning B: Urban Analytics and City Science*, SAGE PublicationsSage UK: London, England, 44(3), 553–569.
- Diakaki, C., Grigoroudis, E., Kabelis, N., Kolokotsa, D., Kalaitzakis, K., and Stavrakakis, G. (2010). "A multi-objective decision model for the improvement of energy efficiency in buildings." *Energy*, 35(12), 5483–5496.
- Djongyang, N., Tchinda, R., and Njomo, D. (2010). "Thermal comfort: A review paper." *Renewable and Sustainable Energy Reviews*, Pergamon, 14(9), 2626–2640.
- Dumbaugh, E., and Rae, R. (2009). "Safe Urban Form: Revisiting the Relationship Between Community Design and Traffic Safety." *Journal of the American Planning Association*, Taylor & Francis Group , 75(3), 309–329.
- Energy, U. S. D. of. (2018). "Engineering Reference: EnergyPlus™ Version 8.9.0 Documentation." U.S. Department of Energy.
- Van Esch, M. M. E., Looman, R. H. J., and De Bruin-Hordijk, G. J. (2012). "The effects of urban and building design parameters on solar access to the urban canyon and the potential for direct passive solar heating strategies." *Energy and Buildings*, 47, 189–200.
- Eumorfopoulou, E., and Aravantinos, D. (1998). "The contribution of a planted roof to the thermal protection of buildings in Greece." *Energy and Buildings*, Elsevier, 27(1), 29–36.
- European Committee for Standardization (CEN). (2007). "CEN - EN 15251 -Indoor environmental input parameters for design and assessment of energy performance of buildings-addressing indoor air quality, thermal environment, lighting and acoustics." CEN (European Committee for Standardization).
- Fan, Y., and Xia, X. (2017). "A multi-objective optimization model for energy-efficiency building envelope retrofitting plan with rooftop PV system installation and maintenance." *Applied Energy*, Elsevier, 189, 327–335.
- Fanger, P. O. (1970). *Thermal comfort. Analysis and applications in environmental*

engineering. Copenhagen: Danish Technical Press., Hoersholm, Denmark.

- Fazlollahi, S., Girardin, L., and Maréchal, F. (2014). “Clustering urban areas for optimizing the design and the operation of district energy systems.” *Computer Aided Chemical Engineering*, Elsevier B.V., 1291–1296.
- Feng, Y. Y., Chen, S. Q., and Zhang, L. X. (2013). “System dynamics modeling for urban energy consumption and CO₂ emissions: a case study of Beijing, China.” *Ecological Modelling*, 252, 44–52.
- Fonseca, J. A., Nguyen, T.-A., Schlueter, A., and Marechal, F. (2016). “City Energy Analyst (CEA): Integrated framework for analysis and optimization of building energy systems in neighborhoods and city districts.” *Energy and Buildings*, Elsevier, 113, 202–226.
- Fonseca, J. A., and Schlueter, A. (2015). “Integrated model for characterization of spatiotemporal building energy consumption patterns in neighborhoods and city districts.” *Applied Energy*, Elsevier, 142, 247–265.
- Fox, J., and Monette, G. (1992). “Generalized collinearity diagnostics.” *Journal of the American Statistical Association*, 87(417), 178–183.
- Freitas, S., Catita, C., Redweik, P., and Brito, M. C. (2015). “Modelling solar potential in the urban environment: State-of-the-art review.” *Renewable and Sustainable Energy Reviews*, Elsevier Ltd.
- Frohner, I., and Bánhidi, L. (2007). “Comfort Ranges Drawn up Based on the PMV Equation as a Tool for Evaluating Thermal Sensation.” *Proceedings of Clima 2007 WellBeing Indoors*, FINVAC, Helsinki, Finland.
- Gahrooei, M. R., Zhang, Y., Ashuri, B., and Augenbroe, G. (2016). “Timing residential photovoltaic investments in the presence of demand uncertainties.” *Sustainable Cities and Society*, 20, 109–123.
- Garrett, R. C., Nar, A., Fisher, T. J., and Maurer, K. (2018). “ggvoronoi: Voronoi Diagrams and Heatmaps with ggplot2.” *The Journal of Open Source Software*, 3(32), 1096.
- Gelman, A., and Rubin, D. B. (1992). “Inference from Iterative Simulation Using Multiple Sequences.” *Statistical Science*, Institute of Mathematical Statistics, 7(4), 457–472.

- Ghazi Wakili, K., Hugi, E., Karvonen, L., Schnewlin, P., and Winnefeld, F. (2015). "Thermal behaviour of autoclaved aerated concrete exposed to fire." *Cement and Concrete Composites*, Elsevier, 62, 52–58.
- Giagkiozis, I., and Fleming, P. J. (2012). *Increasing the Density of Available Pareto Optimal Solutions. Research Report. ACSE Research Report Automatic Control and ACSE RESEARCH REPORT.*
- Goldberg, D. E., Korb, B., and Deb, K. (1989). *Messy Genetic Algorithms: Motivation, Analysis, and First Results. Complex Systems.*
- Gossard, D., Lartigue, B., and Thellier, F. (2013). "Multi-objective optimization of a building envelope for thermal performance using genetic algorithms and artificial neural network." *Energy and Buildings*, Elsevier, 67, 253–260.
- Govindan, K., Madan Shankar, K., and Kannan, D. (2016). "Sustainable material selection for construction industry – A hybrid multi criteria decision making approach." *Renewable and Sustainable Energy Reviews*, 55, 1274–1288.
- Gratia, E., and De Herde, A. (2004). "Natural cooling strategies efficiency in an office building with a double-skin façade." *Energy and Buildings*, Elsevier, 36(11), 1139–1152.
- Grippa, T., Georganos, S., Zarougui, S., Bognounou, P., Diboulo, E., Forget, Y., Lennert, M., Vanhuyse, S., Mboga, N., and Wolff, E. (2018). "Mapping Urban Land Use at Street Block Level Using OpenStreetMap, Remote Sensing Data, and Spatial Metrics." *ISPRS International Journal of Geo-Information*, MDPI AG, 7(7), 246.
- Güçyeter, B., and Günaydın, H. M. (2012). "Optimization of an envelope retrofit strategy for an existing office building." *Energy and Buildings*, Elsevier, 55, 647–659.
- He, X., Miao, S., Shen, S., Li, J., Zhang, B., Zhang, Z., and Chen, X. (2015). "Influence of sky view factor on outdoor thermal environment and physiological equivalent temperature." *International Journal of Biometeorology*, Springer Berlin Heidelberg, 59(3), 285–297.
- Heo, Y., Choudhary, R., and Augenbroe, G. A. (2012). "Calibration of building energy models for retrofit analysis under uncertainty." *Energy and Buildings*, Elsevier, 47, 550–560.

- Herbst, R., Cleveland, J., Rogers, J., Baer, J., Fulton, M., and Grady, H. (2012). *U.S. Energy Efficiency Retrofits: Market Sizing and Financing Models*.
- Hernandez, P., and Kenny, P. (2010). “From net energy to zero energy buildings: Defining life cycle zero energy buildings (LC-ZEB).” *Energy and Buildings*, Elsevier, 42(6), 815–821.
- Hoffman, M. D., and Gelman, A. (2014). “The No-U-Turn Sampler: Adaptively Setting Path Lengths in Hamiltonian Monte Carlo.” *Journal of Machine Learning Research*, 15, 1593–1623.
- Hofierka, J., and Kaňuk, J. (2009). “Assessment of photovoltaic potential in urban areas using open-source solar radiation tools.” *Renewable Energy*, Pergamon, 34(10), 2206–2214.
- Hong, T., Koo, C., Kwak, T., and Park, H. S. (2014). “An economic and environmental assessment for selecting the optimum new renewable energy system for educational facility.” *Renewable and Sustainable Energy Reviews*, 29, 286–300.
- Hwang, R.-L., and Shu, S.-Y. (2011). “Building envelope regulations on thermal comfort in glass facade buildings and energy-saving potential for PMV-based comfort control.” *Building and Environment*, Pergamon, 46(4), 824–834.
- IBA Hamburg. (2013). “IBA Hamburg – BIQ.” IBA, <<http://www.iba-hamburg.de/en/themes-projects/the-building-exhibition-within-the-building-exhibition/smart-material-houses/biq/projekt/biq.html>> (Mar. 27, 2017).
- Ihara, T., Gustavsen, A., and Jelle, B. P. (2015). “Effect of facade components on energy efficiency in office buildings.” *Applied Energy*, Elsevier, 158, 422–432.
- IPCC. (2018). *Global warming of 1.5°C. An IPCC Special Report on the impacts of global warming of 1.5°C above pre-industrial levels and related global greenhouse gas emission pathways*. (V. Masson-Delmotte, P. Zhai, H.-O. Pörtner, D. Roberts, J. Skea, P. R. Shukla, A. Pirani, W. Moufouma-Okia, C. Péan, R. Pidcock, S. Connors, J. B. R. Matthews, Y. Chen, X. Zhou, M. I. Gomis, E. Lonnoy, T. Maycock, M. Tignor, and T. Waterfield, eds.).
- Iwano, J., and Mwashia, A. (2013). “The impact of sustainable building envelope design on building sustainability using Integrated Performance Model.” *International Journal of Sustainable Built Environment*, Elsevier, 2(2), 153–171.

- Jaber, S., and Ajib, S. (2011). "Optimum design of Trombe wall system in mediterranean region." *Solar Energy*, Pergamon, 85(9), 1891–1898.
- Jafari, A., and Valentin, V. (2017). "An optimization framework for building energy retrofits decision-making." *Building and Environment*, Pergamon, 115, 118–129.
- Jafari, A., and Valentin, V. (2018). "Selection of optimization objectives for decision-making in building energy retrofits." *Building and Environment*, Pergamon, 130, 94–103.
- James, T., Goodrich, A., Woodhouse, M., Margolis, R., and Ong, S. (2011). *Building-Integrated Photovoltaics (BIPV) in the Residential Sector: An Analysis of Installed Rooftop System Prices*.
- Jang, C., Kim, J., and Song, T.-H. (2011). "Combined heat transfer of radiation and conduction in stacked radiation shields for vacuum insulation panels." *Energy and Buildings*, Elsevier, 43(12), 3343–3352.
- Javanroodi, K., Mahdavejad, M., and Nik, V. M. (2018). "Impacts of urban morphology on reducing cooling load and increasing ventilation potential in hot-arid climate." *Applied Energy*, Elsevier, 231, 714–746.
- Jelle, B. P., Kalnæs, S. E., and Gao, T. (2015). "Low-emissivity materials for building applications: A state-of-the-art review and future research perspectives." *Energy and Buildings*, Elsevier, 96, 329–356.
- Jeon, J., Lee, J., and Ham, Y. (2018). "Quantifying the impact of building envelope condition on energy use." *Building Research & Information*.
- Johansson, P. (2011). "Assessment of the Risk for Mold Growth in a Wall Retrofitted with Vacuum Insulation Panels." *Proceedings of the Ninth Nordic Symposium on Building Physics*, Tampere, Finland.
- Johnson, G. T., Watson, I. D., Johnson, G. T., and Watson, I. D. (1984). "The Determination of View-Factors in Urban Canyons." *Journal of Climate and Applied Meteorology*, 23(2), 329–335.
- Jordan, D. C., and Kurtz, S. R. (2013). "Photovoltaic Degradation Rates-an Analytical Review." *Progress in Photovoltaics: Research and Applications*, Wiley-Blackwell,

21(1), 12–29.

- Juan, Y.-K., Gao, P., and Wang, J. (2010). “A hybrid decision support system for sustainable office building renovation and energy performance improvement.” *Energy and Buildings*, 42, 290–297.
- Kammen, D. M., and Sunter, D. A. (2016). “City-integrated renewable energy for urban sustainability.” *Science (New York, N.Y.)*, American Association for the Advancement of Science, 352(6288), 922–8.
- Kämpf, J. H., Montavon, M., Bunyesc, J., Bolliger, R., and Robinson, D. (2010). “Optimisation of buildings’ solar irradiation availability.” *Solar Energy*, Pergamon, 84(4), 596–603.
- Kämpf, J. H., and Robinson, D. (2010). “Optimisation of building form for solar energy utilisation using constrained evolutionary algorithms.” *Energy and Buildings*, Elsevier, 42(6), 807–814.
- Kang, T. W., and Hong, C. H. (2015). “A study on software architecture for effective BIM/GIS-based facility management data integration.” *Automation in Construction*, Elsevier, 54, 25–38.
- Khoukhi, M., and Maruyama, S. (2005). “Theoretical approach of a flat plate solar collector with clear and low-iron glass covers taking into account the spectral absorption and emission within glass covers layer.” *Renewable Energy*, Pergamon, 30(8), 1177–1194.
- Kim, K. (2013). “Beyond green: growing algae facade.” *ARCC Conference Repository*.
- Kočí, V., Maděra, J., and Černý, R. (2012). “Exterior thermal insulation systems for AAC building envelopes: Computational analysis aimed at increasing service life.” *Energy and Buildings*, Elsevier, 47, 84–90.
- Koo, C., Park, S., Hong, T., and Park, H. S. (2014). “An estimation model for the heating and cooling demand of a residential building with a different envelope design using the finite element method.” *Applied Energy*, 115, 205–215.
- Koschenz, M., and Lehmann, B. (2004). “Development of a thermally activated ceiling panel with PCM for application in lightweight and retrofitted buildings.” *Energy and*

Buildings, 36, 567–578.

- Kuramochi, T., Höhne, N., Schaeffer, M., Cantzler, J., Hare, B., Deng, Y., Sterl, S., Hagemann, M., Rocha, M., Yanguas-Parra, P. A., Mir, G. U. R., Wong, L., El-Laboudy, T., Wouters, K., Deryng, D., and Blok, K. (2018). “Ten key short-term sectoral benchmarks to limit warming to 1.5°C.” *Climate Policy*, Taylor and Francis Ltd., 18(3), 287–305.
- Kwon, J.-S., Jang, C. H., Jung, H., and Song, T.-H. (2009). “Effective thermal conductivity of various filling materials for vacuum insulation panels.” *International Journal of Heat and Mass Transfer*, Pergamon, 52(23–24), 5525–5532.
- Levinson, R., Akbari, H., Berdahl, P., Wood, K., Skilton, W., and Petersheim, J. (2010). “A novel technique for the production of cool colored concrete tile and asphalt shingle roofing products.” *Solar Energy Materials and Solar Cells*, North-Holland, 94(6), 946–954.
- Liang, Y., Wu, H., Huang, G., Yang, J., and Wang, H. (2017). “Thermal performance and service life of vacuum insulation panels with aerogel composite cores.” *Energy and Buildings*, Elsevier, 154, 606–617.
- Lindberg, R., Binamu, A., and Teikari, M. (2004). “Five-year data of measured weather, energy consumption, and time-dependent temperature variations within different exterior wall structures.” *Energy and Buildings*, Elsevier, 36(6), 495–501.
- Liu, C., Wu, Y., Li, D., Zhou, Y., Wang, Z., and Liu, X. (2017). “Effect of PCM thickness and melting temperature on thermal performance of double glazing units.” *Journal of Building Engineering*, Elsevier, 11, 87–95.
- Liu, S., and Li, Y. (2015). “Heating performance of a solar chimney combined PCM: A numerical case study.” *Energy and Buildings*, Elsevier, 99, 117–130.
- Lloyd, C. D. (2014). “Scale in Spatial Data Analysis: Key Concepts.” *Exploring Spatial Scale in Geography*, John Wiley & Sons, Ltd, Chichester, UK, 9–28.
- Lobaccaro, G., and Frontini, F. (2014). “Solar energy in urban environment: How urban densification affects existing buildings.” *Energy Procedia*, Elsevier Ltd, 1559–1569.
- Löwe, R., Kleidorfer, M., and Arnbjerg-Nielsen, K. (2019). “Data-driven approaches to

- derive parameters for lot-scale urban development models.” *Cities*, Pergamon, 95, 102374.
- Lozano, E. (1990). *Community Design, Culture of Cities: The Crossroad and the Wall*. Cambridge University Press, New York.
- Lu, Y., Shengwei Wang, Yan, C., and Huang, Z. (2017). “Robust optimal design of renewable energy system in nearly/net zero energy buildings under uncertainties.” *Applied Energy*, Elsevier, 187, 62–71.
- Lynch, K. (1995). *City sense and city design: writings and projects of Kevin Lynch*. MIT Press.
- Ma, Q., Fukuda, H., Kobatake, T., Lee, M., Ma, Q., Fukuda, H., Kobatake, T., and Lee, M. (2017). “Study of a Double-Layer Trombe Wall Assisted by a Temperature-Controlled DC Fan for Heating Seasons.” *Sustainability*, Multidisciplinary Digital Publishing Institute, 9(12), 2179.
- Macdonald, I. A. (2002). “Quantifying the effects of uncertainty in building simulation.” University of Strathclyde.
- Magnier, L., and Haghghat, F. (2010). “Multiobjective optimization of building design using TRNSYS simulations, genetic algorithm, and Artificial Neural Network.” *Building and Environment*, Pergamon, 45(3), 739–746.
- Marchi, M., Pulselli, R. M., Marchettini, N., Pulselli, F. M., and Bastianoni, S. (2015). “Carbon dioxide sequestration model of a vertical greenery system.” *Ecological Modelling*, Elsevier, 306, 46–56.
- Mastrapostoli, E., Karlessi, T., Pantazaras, A., Kolokotsa, D., Gobakis, K., and Santamouris, M. (2014). “On the cooling potential of cool roofs in cold climates: Use of cool fluorocarbon coatings to enhance the optical properties and the energy performance of industrial buildings.” *Energy and Buildings*, Elsevier, 69, 417–425.
- Matsui, K. (2018). “An information provision system to promote energy conservation and maintain indoor comfort in smart homes using sensed data by IoT sensors.” *Future Generation Computer Systems*, North-Holland, 82, 388–394.
- Mavromatidis, L. E., Bykalyuk, A., and Lequay, H. (2013). “Development of polynomial

- regression models for composite dynamic envelopes' thermal performance forecasting." *Applied Energy*, Elsevier, 104, 379–391.
- Mertin, S., Hody-Le Caër, V., Joly, M., Mack, I., Oelhafen, P., Scartezzini, J.-L., and Schüler, A. (2014). "Reactively sputtered coatings on architectural glazing for coloured active solar thermal façades." *Energy and Buildings*, Elsevier, 68, 764–770.
- Miettinen, K. (1999). *Nonlinear Multiobjective Optimization*. Springer.
- MIT. (2011). "The Density Atlas." <<http://densityatlas.org/measuring/metrics.shtml>> (Jan. 31, 2018).
- Morganti, M., Salvati, A., Coch, H., and Cecere, C. (2017). "Urban morphology indicators for solar energy analysis." *Energy Procedia*, Elsevier, 134, 807–814.
- Mosavi, M. R., Sadeghian, M., and Saeifi, S. (2011). "Increasing DGPS navigation accuracy using Kalman filter tuned by genetic algorithm." *International Journal of Computer Science Issues*, www.IJCSI.org, 246–252.
- Moussavi Nadoushani, Z. S., Akbarnezhad, A., Ferre Jornet, J., and Xiao, J. (2017). "Multi-criteria selection of façade systems based on sustainability criteria." *Building and Environment*, Pergamon, 121, 67–78.
- Murakami, D., and Yamagata, Y. (2017). "Micro grids clustering for electricity sharing: an approach considering micro urban structure." *Energy Procedia*, Elsevier, 142, 2748–2753.
- Murakami, D., Yamagata, Y., Yoshida, T., and Matsui, T. (2019). "Optimization of local microgrid model for energy sharing considering daily variations in supply and demand." *Energy Procedia*, Elsevier, 158, 4109–4114.
- Nagel, J. B., and Sudret, B. (2016). "A unified framework for multilevel uncertainty quantification in Bayesian inverse problems." *Probabilistic Engineering Mechanics*, Elsevier, 43, 68–84.
- Newman, M. E. J., and Girvan, M. (2004). "Finding and evaluating community structure in networks." *Physical Review E*, American Physical Society, 69(2), 026113.

- Nouvel, R., Mastrucci, A., Leopold, U., Baume, O., Coors, V., and Eicker, U. (2015). "Combining GIS-based statistical and engineering urban heat consumption models: Towards a new framework for multi-scale policy support." *Energy and Buildings*, Elsevier, 107, 204–212.
- Nouvel, R., Zirak, M., Coors, V., and Eicker, U. (2017). "The influence of data quality on urban heating demand modeling using 3D city models." *Computers, Environment and Urban Systems*, Pergamon, 64, 68–80.
- Nunna, H. S. V. S. K., and Srinivasan, D. (2017). "Multiagent-Based Transactive Energy Framework for Distribution Systems With Smart Microgrids." *IEEE Transactions on Industrial Informatics*, 13(5), 2241–2250.
- Nutkiewicz, A., Jain, R. K., and Bardhan, R. (2018). "Energy modeling of urban informal settlement redevelopment: Exploring design parameters for optimal thermal comfort in Dharavi, Mumbai, India." *Applied Energy*, Elsevier, 231, 433–445.
- O'Brien, R. M. (2007). "A caution regarding rules of thumb for variance inflation factors." *Quality and Quantity*, Springer, 41(5), 673–690.
- O'Hegarty, R., Kinnane, O., and McCormack, S. (2014). "A Simplified Procedure for Sizing Solar Thermal Systems; Based on National Assessment Methods in the UK and Ireland." *Energy Procedia*, Elsevier, 62, 647–655.
- De Oliveira, G., Jacomino, M., Ha, D. L., and Ploix, S. (2011). "Optimal power control for smart homes." *IFAC Proceedings Volumes*, Elsevier, 44(1), 9579–9586.
- Pagliaro, M., Ciriminna, R., and Palmisano, G. (2010). "BIPV: merging the photovoltaic with the construction industry." *PROGRESS IN PHOTOVOLTAICS: RESEARCH AND APPLICATIONS*, 18, 61–72.
- Parasonis, J., Keizikas, A., and Kalibatiene, D. (2012). "The relationship between the shape of a building and its energy performance." *Architectural Engineering and Design Management*, Taylor & Francis, 8(4), 246–256.
- Park, J. H., Jeon, J., Lee, J., Wi, S., Yun, B. Y., and Kim, S. (2019). "Comparative analysis of the PCM application according to the building type as retrofit system." *Building and Environment*, Pergamon.

- Park, K. E., Kang, G. H., Kim, H. I., Yu, G. J., and Kim, J. T. (2010). "Analysis of thermal and electrical performance of semi-transparent photovoltaic (PV) module." *Energy*, Pergamon, 35(6), 2681–2687.
- Pasupathy, A., Velraj, R., and Seeniraj, R. V. (2008). "Phase change material-based building architecture for thermal management in residential and commercial establishments." *Renewable and Sustainable Energy Reviews*, 12(1), 39–64.
- Peippo, K., Lund, P. D., and Vartiainen, E. (1999). "Multivariate optimization of design trade-offs for solar low energy buildings." *Energy and Buildings*, Elsevier, 29(2), 189–205.
- Penna, P., Prada, A., Cappelletti, F., and Gasparella, A. (2015). "Multi-objectives optimization of Energy Efficiency Measures in existing buildings." *Energy and Buildings*, Elsevier, 95, 57–69.
- Pérez-Grande, I., Meseguer, J., and Alonso, G. (2005). "Influence of glass properties on the performance of double-glazed facades." *Applied Thermal Engineering*, Pergamon, 25(17–18), 3163–3175.
- Pérez-Lombard, L., Ortiz, J., and Pout, C. (2008). "A review on buildings energy consumption information." *Energy and Buildings*, 40(3), 394–398.
- Perini, K., Ottelé, M., Haas, E. M., and Raiteri, R. (2013). "Vertical greening systems, a process tree for green façades and living walls." *Urban Ecosystems*, Springer US, 16(2), 265–277.
- Premrov, M., Žegarac Leskovar, V., and Mihalič, K. (2016). "Influence of the building shape on the energy performance of timber-glass buildings in different climatic conditions." *Energy*, Pergamon, 108, 201–211.
- Quan, S. J., Economou, A., Grasl, T., and Yang, P. P.-J. (2014). "Computing Energy Performance of Building Density, Shape and Typology in Urban Context." *Energy Procedia*, Elsevier, 61, 1602–1605.
- Quan, S. J., Igou, T. K., Chang, S., Dutt, F., Castro-Lacouture, D., Chen, Y., and Pei-Ju Yang, P. (2017). "Decentralized algal energy system design at various urban densities and scales." *Energy Procedia*, 143(World Engineers Summit – Applied Energy Symposium & Forum: Low Carbon Cities & Urban Energy Joint Conference, WES-CUE 2017, 19–21 July 2017, Singapore), 767–773.

- Quan, S. J., Li, Q., Augenbroe, G., Brown, J., and Yang, P. P.-J. (2015a). “Urban Data and Building Energy Modeling: A GIS-Based Urban Building Energy Modeling System Using the Urban-EPC Engine.” Springer, Cham, 447–469.
- Quan, S. J., Li, Q., Augenbroe, G., Brown, J., and Yang, P. P.-J. (2015b). “A GIS-based Energy Balance Modeling System for Urban Solar Buildings.” *Energy Procedia*, Elsevier, 75, 2946–2952.
- Quan, S. J., Wu, J., Wang, Y., Shi, Z., Yang, T., and Yang, P. P.-J. (2016). “Urban Form and Building Energy Performance in Shanghai Neighborhoods.” *Energy Procedia*, Elsevier, 88, 126–132.
- Rashdi, W. S. S. W. M., and Embi, M. R. (2016). “Analysing Optimum Building form in Relation to Lower Cooling Load.” *Procedia - Social and Behavioral Sciences*, Elsevier, 222, 782–790.
- Reinhart, C. F., and Cerezo Davila, C. (2016). “Urban building energy modeling – A review of a nascent field.” *Building and Environment*, Pergamon, 97, 196–202.
- Reinhart, C. F., Dogan, T., Jakubiec, A., Rakha, T., and Sang, A. (2013). “Umi-An urban simulation environment for building energy use, daylighting and walkability.” *13th Conference of International Building Performance Simulation Association*, Chambéry, France, August 26-28, 476–483.
- Robbins, F. V., and Spillman, C. K. (1980). “Computer modeling of a ventilated Trombe Wall—With actual performance results.” *Solar Energy*, Pergamon, 25(3), 207–213.
- Roberti, F., Oberegger, U. F., Lucchi, E., and Troi, A. (2017). “Energy retrofit and conservation of a historic building using multi-objective optimization and an analytic hierarchy process.” *Energy and Buildings*, Elsevier, 138, 1–10.
- Rodríguez-Álvarez, J. (2016). “Urban Energy Index for Buildings (UEIB): A new method to evaluate the effect of urban form on buildings’ energy demand.” *Landscape and Urban Planning*, Elsevier, 148, 170–187.
- Rodríguez Serrano, A., and Porras Álvarez, S. (2016). “Life Cycle Assessment in Building: A Case Study on the Energy and Emissions Impact Related to the Choice of Housing Typologies and Construction Process in Spain.” *Sustainability*, 8(3), 287.

- Saad Al-Homoud, M. (2001). "Computer-aided building energy analysis techniques." *Building and Environment*, 36, 421–433.
- Salehi, A., Fayaz, R., Bozorgi, M., Asadi, S., Costanzo, V., Imani, N., and Nocera, F. (2019). "Investigation of thermal comfort efficacy of solar chimneys under different climates and operation time periods." *Energy and Buildings*, Elsevier Ltd, 205.
- Sanaieian, H., Tenpierik, M., Linden, K. van den, Mehdizadeh Seraj, F., and Mofidi Shemrani, S. M. (2014). "Review of the impact of urban block form on thermal performance, solar access and ventilation." *Renewable and Sustainable Energy Reviews*, Pergamon, 38, 551–560.
- Shahandeh, H., Jafari, M., Kasiri, N., and Ivakpour, J. (2015). "Economic optimization of heat pump-assisted distillation columns in methanol-water separation." *Energy*, Pergamon, 80, 496–508.
- Shi, W., and Pang, M. Y. C. (2000). "Development of Voronoi-based cellular automata - an integrated dynamic model for Geographical Information Systems." *International Journal of Geographical Information Science*, Taylor & Francis Group , 14(5), 455–474.
- Shi, Z., Fonseca, J. A., and Schlueter, A. (2017). "A review of simulation-based urban form generation and optimization for energy-driven urban design." *Building and Environment*, Elsevier Ltd, 121, 119–129.
- Shi, Z., and Zhang, X. (2011). "Analyzing the effect of the longwave emissivity and solar reflectance of building envelopes on energy-saving in buildings in various climates." *Solar Energy*, Pergamon, 85(1), 28–37.
- Stephan, A., and Athanassiadis, A. (2017). "Quantifying and mapping embodied environmental requirements of urban building stocks." *Building and Environment*, Elsevier Ltd, 114, 187–202.
- Stephan, A., and Crawford, R. H. (2014). "A multi-scale life-cycle energy and greenhouse-gas emissions analysis model for residential buildings." *Architectural Science Review*, Earthscan, James and James, 57(1), 39–48.
- Stewart, I. D., Oke, T. R., Stewart, I. D., and Oke, T. R. (2012). "Local Climate Zones for Urban Temperature Studies." *Bulletin of the American Meteorological Society*, American Meteorological Society , 93(12), 1879–1900.

- Sun, T., Bou-Zeid, E., Wang, Z.-H., Zerba, E., and Ni, G.-H. (2013). “Hydrometeorological determinants of green roof performance via a vertically-resolved model for heat and water transport.” *Building and Environment*, Pergamon, 60, 211–224.
- Synnefa, A., Santamouris, M., and Akbari, H. (2007). “Estimating the effect of using cool coatings on energy loads and thermal comfort in residential buildings in various climatic conditions.” *Energy and Buildings*, Elsevier, 39(11), 1167–1174.
- TEPCO (Tokyo Electric Power Company Holdings). (2016). “Electricity Rate Plans | TEPCO.” <https://www7.tepco.co.jp/ep/rates/electricbill-e.html>, <<https://www7.tepco.co.jp/ep/rates/electricbill-e.html>> (Apr. 22, 2019).
- The European Portal For Energy Efficiency In Buildings. (2015). “The BIQ House: first algae-powered building in the world | Build Up.” *The European Portal For Energy Efficiency In Buildings*, <<http://www.buildup.eu/en/practices/cases/biq-house-first-algae-powered-building-world>> (Mar. 27, 2017).
- Tina, G., Gagliano, S., and Raiti, S. (2006). “Hybrid solar/wind power system probabilistic modelling for long-term performance assessment.” *Solar Energy*, Pergamon, 80(5), 578–588.
- Ton, D. T., and Smith, M. A. (2012). “The U.S. Department of Energy’s Microgrid Initiative.” *Electricity Journal*, Elsevier, 25(8), 84–94.
- U.S. Census Bureau. (2018). “US Census Bureau Construction Spending Survey.” *U.S. Department of Commerce*, <https://www.census.gov/construction/c30/historical_data.html> (Sep. 24, 2018).
- U.S. EIA. (2018a). “Annual Energy Outlook 2018.” *U.S. Energy Information Administration*, <<https://www.eia.gov/outlooks/aeo/>> (Jun. 15, 2018).
- U.S. EIA. (2018b). “U.S. Energy-Related Carbon Dioxide Emissions, 2017.” *U.S. Energy Information Administration*, <<https://www.eia.gov/environment/emissions/carbon/>> (Sep. 27, 2018).
- U.S.DOE. (2011). *Solar Technologies Market Report*.
- UN. (2014). “World’s population increasingly urban with more than half living in urban areas.” *United Nations Department of Economic and Social Affairs*,

<<http://www.un.org/en/development/desa/news/population/world-urbanization-prospects-2014.html>> (Dec. 5, 2018).

- Ünlü, T. (2018). “Planning Practice and the Shaping of the Urban Pattern.” *Teaching Urban Morphology*, V. Oliveira, ed., Springer, 31–49.
- Vanderhaegen, S., and Canters, F. (2017). “Mapping urban form and function at city block level using spatial metrics.” *Landscape and Urban Planning*, Elsevier B.V., 167, 399–409.
- Varun, Bhat, I. K., and Prakash, R. (2009a). “LCA of renewable energy for electricity generation systems—A review.” *Renewable and Sustainable Energy Reviews*, Pergamon, 13(5), 1067–1073.
- Varun, Prakash, R., and Bhat, I. K. (2009b). “Energy, economics and environmental impacts of renewable energy systems.” *Renewable and Sustainable Energy Reviews*, 13(9), 2716–2721.
- Visa, I., Moldovan, M., Comsit, M., Neagoe, M., and Duta, A. (2017). “Facades Integrated Solar-thermal Collectors – Challenges and Solutions.” *Energy Procedia*, Elsevier, 112, 176–185.
- Wang, L., Wong Nyuk, H., and Li, S. (2007). “Facade design optimization for naturally ventilated residential buildings in Singapore.” *Energy and Buildings*, Elsevier, 39(8), 954–961.
- Wei, S., Li, M., Lin, W., and Sun, Y. (2010). “Parametric studies and evaluations of indoor thermal environment in wet season using a field survey and PMV–PPD method.” *Energy and Buildings*, Elsevier, 42(6), 799–806.
- Wilkinson, S., Stoller, P., Ralph, P., Hamdorf, B., Catana, L. N., and Kuzava, G. S. (2017). “Exploring the Feasibility of Algae Building Technology in NSW.” *Procedia Engineering*, Elsevier, 1121–1130.
- Wlkinson, S., Stoller, P., and Ralph, P. (2016). *Feasibility of Algae Building Technology in Sydney. Feasibility of Algae*.
- Wong, N. ., Cheong, D. K. ., Yan, H., Soh, J., Ong, C. ., and Sia, A. (2003). “The effects of rooftop garden on energy consumption of a commercial building in Singapore.”

- Energy and Buildings*, Elsevier, 35(4), 353–364.
- Wong, N. H., Tan, A. Y. K., Tan, P. Y., and Wong, N. C. (2009). “Energy simulation of vertical greenery systems.” *Energy and Buildings*, Elsevier, 41(12), 1401–1408.
- Wong, P. W., Shimoda, Y., Nonaka, M., Inoue, M., and Mizuno, M. (2008). “Semi-transparent PV: Thermal performance, power generation, daylight modelling and energy saving potential in a residential application.” *Renewable Energy*, Pergamon, 33(5), 1024–1036.
- Wood, S. N., Scheipl, F., and Faraway, J. J. (2013). “Straightforward intermediate rank tensor product smoothing in mixed models.” *Statistics and Computing*, Springer US, 23(3), 341–360.
- World Nuclear Association. (2011). *Comparison of Lifecycle Greenhouse Gas Emissions of Various Electricity Generation Sources*.
- Wu, P., Huang, W., Tai, N., and Liang, S. (2018). “A novel design of architecture and control for multiple microgrids with hybrid AC/DC connection.” *Applied Energy*, Elsevier, 210, 1002–1016.
- Yamagata, Y., Murakami, D., Minami, K., Arizumi, N., Kuroda, S., Tanjo, T., and Maruyama, H. (2016). “Electricity Self-Sufficient Community Clustering for Energy Resilience.” *Energies*, 9(7), 543.
- Yamagata, Y., and Seya, H. (2014). “Proposal for a local electricity-sharing system: a case study of Yokohama city, Japan.” *IET Intelligent Transport Systems*, 9(1), 38–49.
- Yang, L., Yan, H., and Lam, J. C. (2014a). “Thermal comfort and building energy consumption implications – A review.” *Applied Energy*, 115, 164–173.
- Yang, P. P.-J. (2012). “Complexity Question in Urban Systems Design.” *Journal of Architectural Engineering Technology*, 1(2).
- Yang, P. P.-J., Quan, S. J., Castro- Lacouture, D., Rudolph, C., and Stuart, B. (2014b). “GIS-based Planning Support System for Waste Stream and Algal Cultivation in Residential Construction.” *Proceedings of the 2014 ASCE Construction Research Congress*, American Society of Civil Engineers, Atlanta, GA, USA, 2385–2394.

- Yang, X., Li, Y., and Yang, L. (2012a). "Predicting and understanding temporal 3D exterior surface temperature distribution in an ideal courtyard." *Building and Environment*, Elsevier Ltd, 57, 38–48.
- Yang, X., Zhao, L., Bruse, M., and Meng, Q. (2012b). "An integrated simulation method for building energy performance assessment in urban environments." *Energy and Buildings*, Elsevier, 54, 243–251.
- ZENRIN CO., L. (2018). "ZENRIN | ZENRIN." <http://www.zenrin.co.jp/english/>, <<https://www.zenrin.co.jp/english/>> (Apr. 22, 2019).
- Zhang, J., Heng, C. K., Malone-Lee, L. C., Hii, D. J. C., Janssen, P., Leung, K. S., and Tan, B. K. (2012). "Evaluating environmental implications of density: A comparative case study on the relationship between density, urban block typology and sky exposure." *Automation in Construction*, 90–101.
- Zhang, S., Huang, P., and Sun, Y. (2016). "A multi-criterion renewable energy system design optimization for net zero energy buildings under uncertainties." *Energy*, 94, 654–665.
- Zhao, H., and Magoulès, F. (2012). "A review on the prediction of building energy consumption." *Renewable and Sustainable Energy Reviews*, Pergamon, 16(6), 3586–3592.